BioMed Research International

The Right Ventricle: From Bench to Bedside

Lead Guest Editor: Ruxandra Jurcut
Guest Editors: Kristina Haugaa and Andre La Gerche

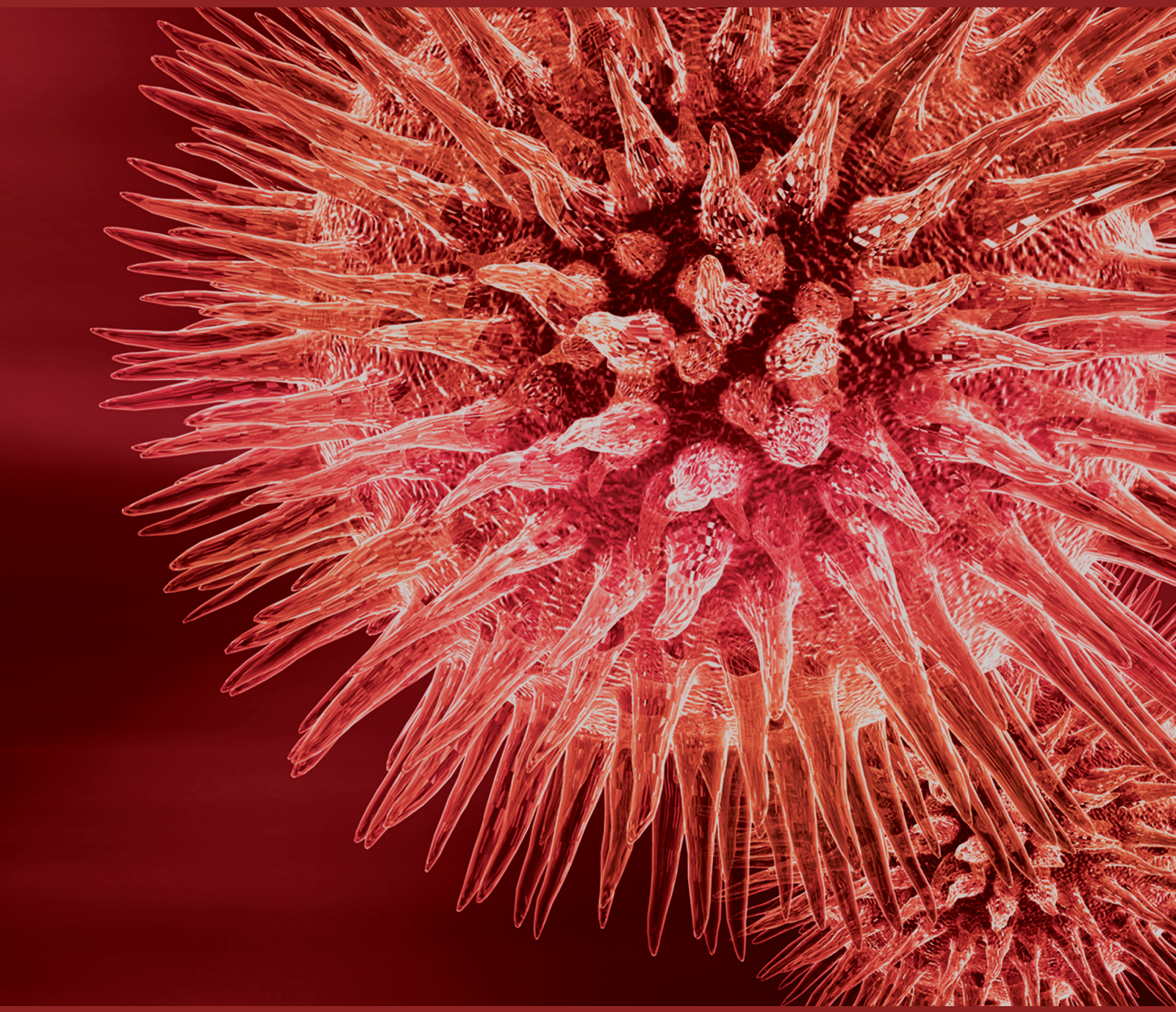

The Right Ventricle: From Bench to Bedside

BioMed Research International

The Right Ventricle: From Bench to Bedside

Lead Guest Editor: Ruxandra Jurcut
Guest Editors: Kristina Haugaa and Andre La Gerche

Contents

Hindawi
BioMed Research International
Volume 2018, Article ID 2868437, 3 pages
https://doi.org/10.1155/2018/2868437

Editorial

The Right Ventricle: From Bench to Bedside

Ruxandra Jurcut,[1] **Kristina Haugaa**,[2,3] **and Andre La Gerche**[4]

[1]*Institute of Emergency for Cardiovascular Diseases "Prof. Dr. C.C. Iliescu", University of Medicine and Pharmacy "Carol Davila", Bucharest, Romania*
[2]*Oslo University Hospital, Center for Cardiological Innovation, Department of Cardiology, Unit for Cardiac Genetic Diseases, Oslo, Norway*
[3]*University of Oslo, Oslo, Norway*
[4]*Clinical Research Department, Baker Heart and Diabetes Institute, Melbourne, VIC, Australia*

Correspondence should be addressed to Ruxandra Jurcut; rjurcut@gmail.com

Received 11 March 2018; Accepted 18 March 2018; Published 14 May 2018

1. Introduction

The right ventricle (RV) remains the cardiac chamber for which scientific data regarding structure, function, adaptation to load, or arrhythmogenic potential is still behind what we know for the left ventricle, despite more recent efforts in this field. RV function is critical in numerous pathologies, related to pressure overload (like pulmonary hypertension but also arterial hypertension), volume overload (left-to-right shunts, tricuspid regurgitation), and myocardial diseases (which can be global, left ventricular, or right ventricular, more specific cardiomyopathies) as well as right ventricular ischemia or infarction. Moreover, the adaptation of the RV to more extreme physiologic situations (e.g., hypoxia at high altitude, high-level exercise) opens windows for understanding its physiology.

Despite data on the prognostic value of RV function, there is still debate on the best parameters that describe it and their clinical relevance. Important developments in right ventricular imaging have occurred during the last years, from myocardial deformation imaging to 3D-echocardiography and from cardiac MRI to right ventriculoarterial coupling studies, which have all contributed to a better understanding of right ventricular pathophysiology.

2. Anatomy and Physiology of the Right Ventricle

The RV is the most anterior cardiac chamber and is situated immediately behind the sternum. With a triangular shape, it has three components: inlet (sinus) portion, apical trabecular section, and outlet (conus) section. The muscular wall of the RV is normally very thin (3–5 mm), adequately serving the ejection of blood in a low impedance pulmonary circulation [1]. The RV free wall has subepicardial myofibers with transverse orientation and longitudinally arranged apex to base subendocardial myofibers [2, 3]. The middle layer of circumferential fibers seen in the left ventricle (LV) is absent in RV [4].

The shape, architecture, and structure of the RV facilitate the understanding of its physiology. Owing to the curvature of the interventricular septum (IVS) in the normal heart, the RV is described as wrapping around the LV. This particular shape, as well as the connection of the two ventricles through the IVS, constitute the interventricular dependence. In consequence, in cross section, the RV has a crescent shape which is formed because of its lower pressures, thinner walls, and greater compliance compared to the LV [5].

RV contraction has a longitudinal "peristaltic" pattern, with a 30–40 ms delay from the onset of contraction of the RV free wall from apex to the outflow tract [6], facilitating the ejection of blood to the outflow tract in the crescent shaped cavity. Under normal loading conditions, there are little short axis thickening, rotation, and twisting [7, 8].

Several studies have tried to understand the mechanisms of adaptation and maladaptation of the RV to volume and pressure overload, respectively. A few years ago, we demonstrated that at similar levels of pressure overload the RV is less dilated and performs better in patients with pulmonary

stenosis as compared with those with pulmonary arterial hypertension (PAH) [9], which was in line with experimental observations. These data suggested that beyond pressure overload effects on the sarcomeric function other pathogenic factors should be taken into account. In the present issue, S. Guimaron et al. discuss the current knowledge and recent advances of RV molecular biology and metabolism from congenital heart disease to chronic PAH, with a common pathway during RV failure of metabolic glycolytic shift and altered angiogenesis.

Moreover, acute RV failure is increasingly seen in the intensive care unit and can cause or aggravate many common critical diseases. It can be due to either acute pressure or volume overload or other aggravating factors leading to a reduction of myocardial contractility owing to ischemia, cardiomyopathy, or arrhythmia [10]. J. C. Grignola and E. Domingo discuss in their paper from the present issue the mechanisms and management of acute RV dysfunction in the intensive care unit.

3. Pulmonary Hypertension and RV Changes

It has been demonstrated that, beyond etiology, a key element for establishing prognosis in patients with PAH is RV function [11]. The RV is especially challenged when it has to adapt to markedly (up to four- to fivefold) increased chronic afterload. According to the law of Laplace, myocardial hypertrophy allows normal wall stress, while initially preserving RV function. Over time, however, this adaptive mechanism is overrun, and contractile dysfunction and RV dilation occur, with subsequent increase in wall stress which stimulates further hypertrophy, leading to a vicious circle of declining RV performance, with ensuing RV failure and eventually death [7]. The evolution of RV failure in this setting is highly variable. Especially in the setting of congenital heart disease, as in Eisenmenger syndrome or pulmonary stenosis, RV performance may only decline slowly, showing that increased afterload is not the only determinant of RV failure [12, 13].

While pulmonary vasodilators appear to have impacted on the natural history of PAH, there have been few investigations assessing the impact of these drugs on RV remodeling. In the study of N. Rai et al. from the present issue, both sildenafil and riociguat prevented the deterioration of RV function, as determined by a decrease in RV dilation and restoration of the RV ejection fraction, while riociguat also prevented RV fibrosis induced by pulmonary artery banding (a model of fixed RV pressure overload). These experimental data need further investigation in the clinical setting.

4. Right Ventricular Dysfunction Secondary to Left Heart Disease

It is well known that the most frequent cause of RV failure in clinical practice is related to pulmonary hypertension due to left heart disease (e.g., systolic and diastolic LV dysfunction or left side valvular diseases) [14]. The prognostic importance of RV failure in this setting has been well demonstrated [15, 16], and data has emerged on the prognostic significance of exercise induced RV dysfunction in valvular heart disease [17]. Moreover, the association of RV dysfunction to left valvulopathies, even if not included in surgical risk scores, is often perceived as a limitation for surgery in these patients [18]. New less aggressive techniques for valvular repair, as the Mitral Clip, can surpass this barrier, and M. Hünlich et al. showed in their paper that Mitral Clip implantation improved pulmonary artery pressure, tricuspid regurgitation, and TAPSE after 12 months, while there was also a decrease in the RVOT diameter.

5. Right Ventricular Myocardial Changes in Specific Diseases

Various systemic or cardiac diseases can directly affect the RV. This has been described for genetic and nonhereditary cardiomyopathies. For example, diseases like hypertrophic cardiomyopathy, amyloidosis, Fabry's cardiomyopathy, and dilated cardiomyopathy can have biventricular involvement which occurs most often late during the disease evolution.

Not only cardiomyopathies but also immune and inflammatory diseases with cardiac tropism can affect the RV as well. Chagas disease is a tropical disease caused by *T. cruzi* protozoan infection, which can be at the root of more than 10% of heart failure cases in endemic regions (like Brazil). As it is often associated with systemic congestion, studies of RV involvement were started years ago, and the review of M. M. D. Romano et al. in this issue has discussed the role of imaging in the diagnosis of RV involvement in Chagas cardiomyopathy. While no specific cardiovascular imaging tools appear to assess myocardial involvement in this infectious disease, there is a place for speckle tracking imaging and cardiac MRI to identify early functional changes during the course of disease.

Systemic sclerosis (SSc) is a disease which can involve the RV in various ways. Being the leading cause of pulmonary arterial hypertension (PAH) among connective tissue diseases, it has been reported to result in increased pressure afterload of the RV in up to 12% of cases, which can subsequently result in right ventricular failure. Moreover, a direct effect of scleroderma on the myocardium consists of increased fibrosis and inflammatory lesions, and autopsy studies identified significant cardiac fibrotic changes in 70–80% of the examined patients [19]. Moreover, Hachulla et al. found that decreased left ventricular (LV) ejection fraction could be demonstrated on cardiac MRI in almost one-quarter of SSc patients. Mid-myocardial LV delayed contrast enhancement in a noncoronary distribution was also observed suggesting fibrosis mediated by an inflammatory process [20]. The paper of R. Cucuruzac et al. in the present issue provides an in-depth discussion of the current knowledge on RV remodeling and function in scleroderma patients.

6. Future Directions

More studies investigating the normal right ventricle structure and function and especially its adaptation to physiological states (e.g., exercise, pregnancy) and disease are warranted. While its relation to prognosis in PAH was

demonstrated, quantitative parameters of RV dysfunction are not yet considered a part of risk stratification for these patients, proving insufficient knowledge of the best parameter to follow.

Ruxandra Jurcut
Kristina Haugaa
Andre La Gerche

References

[1] S. Giusca, R. Jurcut, C. Ginghina, and J.-U. Voigt, "The right ventricle: Anatomy, physiology and functional assessment," *Acta Cardiologica*, vol. 65, no. 1, pp. 67–77, 2010.

[2] S. Y. Ho and P. Nihoyannopoulos, "Anatomy, echocardiography, and normal right ventricular dimensions," *Heart*, vol. 92, supplement 1, pp. i2–i13, 2006.

[3] F. Torrent-Guasp, G. D. Buckberg, C. Clemente, J. L. Cox, H. C. Coghlan, and M. Gharib, "The structure and function of the helical heart and its buttress wrapping. I. The normal macroscopic structure of the heart," *Seminars in Thoracic and Cardiovascular Surgery*, vol. 13, no. 4, pp. 301–319, 2001.

[4] R. H. Anderson, M. Smerup, D. Sanchez-Quintana, M. Loukas, and P. P. Lunkenheimer, "The three-dimensional arrangement of the myocytes in the ventricular walls," *Clinical Anatomy*, vol. 22, no. 1, pp. 64–76, 2009.

[5] K. M. Chin and G. Coghlan, "Characterizing the right ventricle: Advancing our knowledge," *American Journal of Cardiology*, vol. 110, no. 6, 2012.

[6] G. D. Meier, A. A. Bove, W. P. Santamore, and P. R. Lynch, "Contractile function in canine right ventricle," *American Journal of Physiology-Heart and Circulatory Physiology*, vol. 239, no. 6, pp. H794–H804, 1980.

[7] N. F. Voelkel, R. A. Quaife, L. A. Leinwand et al., "Right ventricular function and failure: report of a National Heart, Lung, and Blood Institute working group on cellular and molecular mechanisms of right heart failure," *Circulation*, vol. 114, no. 17, pp. 1883–1891, 2006.

[8] H. A. Leather, R. Ama', C. Missant, S. Rex, F. E. Rademakers, and P. F. Wouters, "Longitudinal but not circumferential deformation reflects global contractile function in the right ventricle with open pericardium," *American Journal of Physiology-Heart and Circulatory Physiology*, vol. 290, no. 6, pp. H2369–H2375, 2006.

[9] R. Jurcut, S. Giusca, R. Ticulescu et al., "Different patterns of adaptation of the right ventricle to pressure overload: A comparison between pulmonary hypertension and pulmonary stenosis," *Journal of the American Society of Echocardiography*, vol. 24, no. 10, pp. 1109–1117, 2011.

[10] V.-P. Harjola, A. Mebazaa, and J. Čelutkiene, "Contemporary management of acute right ventricular failure: a statement from the Heart failure association and the Working Group on pulmonary circulation and right ventricular function of the European Society of Cardiology," *European Journal of Heart Failure*, vol. 18, no. 3, pp. 226–241, 2016.

[11] S. Giusca, R. Jurcut, I. M. Coman et al., "Right ventricular function predicts clinical response to specific vasodilator therapy in patients with pulmonary hypertension," *Journal of Echocardiography*, vol. 30, no. 1, pp. 17–26, 2013.

[12] W. E. Hopkins, "The remarkable right ventricle of patients with Eisenmenger syndrome," *Coronary Artery Disease*, vol. 16, no. 1, pp. 19–25, 2005.

[13] S. Giusca, E. Popa, M. S. Amzulescu et al., "Is Right Ventricular Remodeling in Pulmonary Hypertension Dependent on Etiology? An Echocardiographic Study," *Echocardiography (Mount Kisco, N.Y.)*, vol. 33, no. 4, pp. 546–554, 2016.

[14] J. Magne, P. Pibarot, P. P. Sengupta, E. Donal, R. Rosenhek, and P. Lancellotti, "Pulmonary hypertension in valvular disease: A comprehensive review on pathophysiology to therapy from the HAVEC group," *JACC: Cardiovascular Imaging*, vol. 8, no. 1, pp. 83–99, 2015.

[15] Y. Juilliere, G. Barbier, L. Feldmann, A. Grentzinger, N. Danchin, and F. Cherrier, "Additional predictive value of both left and right ventricular ejection tractions on long-term survival in idiopathic dilated cardiomyopathy," *European Heart Journal*, vol. 18, no. 2, pp. 276–280, 1997.

[16] F. L. Dini, U. Conti, P. Fontanive et al., "Right ventricular dysfunction is a major predictor of outcome in patients with moderate to severe mitral regurgitation and left ventricular dysfunction," *American Heart Journal*, vol. 154, no. 1, pp. 172–179, 2007.

[17] K. Kusunose, Z. B. Popović, H. Motoki, and T. H. Marwick, "Prognostic significance of exercise-induced right ventricular dysfunction in asymptomatic degenerative mitral regurgitation," *Circulation: Cardiovascular Imaging*, vol. 6, no. 2, pp. 167–176, 2013.

[18] R. Rosenhek, B. Iung, P. Tornos et al., "ESC working group on valvular heart disease position paper: Assessing the risk of interventions in patients with valvular heart disease," *European Heart Journal*, vol. 33, no. 7, pp. 822–828, 2012.

[19] W. P. Follansbee, T. R. Miller, and E. I. Curtiss, "A controlled clinicopathologic study of myocardial fibrosis in systemic sclerosis (scleroderma)," *The Journal of Rheumatology*, vol. 17, no. 5, pp. 656–662, 1990.

[20] A.-L. Hachulla, D. Launay, V. Gaxotte et al., "Cardiac magnetic resonance imaging in systemic sclerosis: A cross-sectional observational study of 52 patients," *Annals of the Rheumatic Diseases*, vol. 68, no. 12, pp. 1878–1884, 2009.

Hindawi
BioMed Research International
Volume 2018, Article ID 4528148, 9 pages
https://doi.org/10.1155/2018/4528148

Review Article

Right Ventricle Remodeling and Function in Scleroderma Patients

Roxana Cucuruzac, Iolanda Muntean, Imre Benedek, Andras Mester, Nora Rat, Adriana Mitre, Monica Chitu, and Theodora Benedek

University of Medicine and Pharmacy of Târgu Mureș, Gh. Marinescu Street, No. 38, 540139 Tîrgu Mureș, Romania

Correspondence should be addressed to Iolanda Muntean; iolanda.muntean@gmail.com

Received 1 September 2017; Accepted 12 February 2018; Published 20 March 2018

Academic Editor: Shigeru Kotake

Scleroderma, known also as systemic sclerosis (SSc), is a severe disease associated with high mortality rates, and right ventricular (RV) remodeling and dysfunction, along with pulmonary artery hypertension (PAH), are among the most important internal organ manifestations of this disease. PAH has a higher prevalence in patients with SSc compared to the general population and represents a significant predictor of mortality in SSc. In patients with SSc, the morphological remodeling and alteration of RV function begin even before the setting of PAH and lead to development of a specific adaptive pattern of the RV which is different from the one recorded in patients with IAPH. These alterations cause worse outcomes and increased mortality rates in SSc patients. Early detection of RV dysfunction and remodeling is possible using modern imaging tools currently available and can indicate the initiation of specific therapeutic measures before installation of PAH. The aim of this review is to summarize the current knowledge related to mechanisms involved in the remodeling and functional alteration of the RV in SSc patients.

1. Introduction

Scleroderma, known also as systemic sclerosis (SSc), is a severe disease associated with high mortality rates, and right ventricular (RV) remodeling and dysfunction, along with pulmonary artery hypertension (PAH), are among the most important internal organ manifestations of this disease [1].

The mortality of SSc depends primary on the burden of the internal organ involvement. Pulmonary hypertension (PH), pulmonary fibrosis, and kidney damage are the most frequent causes of death in SSc [2, 3]. Myocardial, pericardial, and pulmonary artery (PA) involvement is observed in 1 out of 4 patients and serve as predictors of mortality in SSc, as approximately 30% of the SSc deaths are attributed to cardiac causes, followed by respiratory causes (17%) [4].

SSc is a complex autoimmune disease characterized by a marked chronic inflammation, which leads to increased connective tissue fibrosis and vascular involvement causing severe damage of internal organs (mainly the heart, lungs, gastrointestinal tract, kidneys, and muscles) and the skin [5].

Activation of the immune system, linked with fibroblast dysfunction, T lymphocyte, macrophage, and mast cell disturbances induce the alteration of the extracellular matrix by secretion of cytokines, chemokines, growth factors, and other potent mediators resulting in excessive collagen deposit in the tissues [6]. The exact etiology and trigger of the disease still remain unknown, but many studies suggest that genetic and environmental factors (silica, solvent, or radiation exposure) play an important role in the pathophysiology of SSc, generating changes in the expression of deoxyribonucleic acid (DNA) and microribonucleic acid (miRNA), which ultimately lead to inadequate activation of the immune system with phenotypic transformation of various cell types [7, 8]. Infiltration of the microvasculature accompanied by endothelial dysfunction and fibrosis initiates platelet activation and thrombosis causing ischemia of the surrounding tissues [9, 10]. It has been suggested that eNOS G894T polymorphism is correlated with an increased risk of SSc and PAH as well [11, 12].

The various clinical form of SSc varies from limited cutaneous systemic sclerosis (lcSSc) or CREST (calcinosis, Raynaud phenomenon, esophageal dysmotility, sclerodactyly, and telangiectasias) syndrome, to diffuse, sometimes fulminant forms with extended involvement of internal organs. The incidence of SSc greatly varies between different geographical regions and ethnic groups, with higher numbers among the African American population [13, 14]. The risk of developing SSc is significantly higher in woman than in men, with a 3–6 : 1 female to male ratio [15].

The aim of this review is to summarize the current knowledge related to mechanisms involved in the remodeling and functional alteration of the RV in SSc patients.

2. Systemic Sclerosis-Related Pulmonary Artery Hypertension (SSc-PAH)

PAH has a higher prevalence in patients with SSc compared to the general population, being more commonly observed in patients with lcSSc form, and represents a significant predictor of mortality in SSc [16, 17]. Current literature data suggests that the prevalence of PAH in this patient category reaches 12% and, despite the introduction of modern optimized treatments, the 3-year survival rate is still 52%, compared to 94% for SSc patients without PAH [18, 19]. At the same time one-year mortality rate of patients with SSc-PAH is around 30% versus 15% in patients with IPAH [20, 21]. Despite the fact that hemodynamic changes are less pronounced in SSc-PAH compared to idiopathic PAH (IPAH), SSc-related PAH is associated with twofold to threefold higher mortality risk, due to the systemic nature and complexity of the disease, added to a limited efficiency of the administered therapy [22, 23].

Argula et al. evaluated the functional changes of the RV during treatment in patients with SSc-PAH and IPAH at 3.8 and 1.95 years of follow-up. While the IPAH group showed significant improvement of the tricuspid annular plane systolic excursion (TAPSE [$p = 0.01$]), no such gain was observed in SSc-PAH patients, who also exhibited a worsening trend in tricuspid regurgitation jet velocity, right atrium (RA), and ventricular size [24].

In a comparative study Tedford et al. evidenced worse RV systolic function and prognosis in patients with SSc-PAH, compared to IPAH patients at similar RV afterload settings, suggesting the presence of an intrinsic systolic dysfunction in SSc patients [1]. The increase of the pulmonary artery pressure is a result of the alteration of the pulmonary microvascular bed triggered by the chronic inflammation, vasoconstriction, endothelial dysfunction, microthromboses, hypoxia, and excessive fibrous deposits at the level of the arterioles, causing increase of the pulmonary resistance [25, 26].

Hassoun et al. performed endomyocardial biopsies of the RV in SSc patients with and without PAH and compared these with samples from preserved ejection fraction heart failure (HFpEF) patients. Unpublished data from this study showed a significant decrease of the capillary density in SSc-PAH samples compared to the HFpEF and SSc without PAH samples. Furthermore, myocardial capillary density was significantly lower in samples from SSc patients with increased right atrial pressure (RAP), compared with lower RAP SSc samples, supporting the theory of structural RV alteration in these patients [27].

3. Right Ventricular Involvement in Scleroderma: A Distinctive Pattern

3.1. Right Ventricular Involvement in Scleroderma Patients without PAH. Cardiac manifestation of SSc includes involvement of the myocardium, pericardium, and the electrical conduction system, which may lead to ischemia, heart failure, pericardial effusion, and arrhythmias. RV failure can represent an important cause of mortality in SSc patients. It was believed that RV involvement is mainly linked to PAH, but recent studies suggest that SSc may have a direct impact on the RV structure and function, as alteration of RV function is more expressed in SSc-associated PAH than in non-SSc-PAH [28, 29]. The extent of cardiac involvement is likely to be underestimated, as autopsy studies identified considerable fibrotic changes of the myocardium in 70% of the examined patients [30]. Focal recurrent ischemia because of microvascular thrombosis, vasospasm thickening of the vascular wall, and fibrous deposits lead to irreversible functional and structural modifications of the myocardium [31, 32]. It is hard to differentiate the primary heart involvement from secondary development of these alterations due to PAH and kidney injuries. These changes may remain silent for long time (thus frequently underdiagnosed), but when clinically manifested it is described to represent an important negative prognostic factor [33].

Several studies tried to characterize RV involvement that occurs in SSc patients before development of PAH. Proper echocardiographic assessment of the RV function and volume estimation has been bound by its crescent shape, presence of intense trabeculations, and different contraction pattern, but novel techniques overcame these limitations [34]. Pigatto et al. evaluated the RV function of 45 SSc patients without any signs or symptoms of heart disease of PAH using three-dimensional echocardiography (3DE) and two-dimensional speckle-tracking echocardiography (2DSTE) and compared these findings with the similar parameters of 43 healthy subjects. A significant increase in RV size was observed in SSc patients with higher end-systolic volume [ESV, ($p < 0.0001$)], end-diastolic volume [EDV, ($p = 0.049$)], and reduced ejection fraction ($p < 0.0001$) determined by 3DE. Doppler measurements showed increased systolic pulmonary artery pressure (sPAP) and pulmonary vascular resistance (tPVR) in SSc patients compared to the control group. These changes were more pronounced in patients with lcSSc form [35].

Durmus et al. used 2DSTE for the assessment of RV function in patients with SSc without PAH. Significantly higher sPAP (within normal limits) was recorded in SSc patients ($p = 0.002$), accompanied by decreased RV systolic function with significantly lower TAPSE and tissue Doppler maximum systolic myocardial velocity (RVS′), but no correlation was

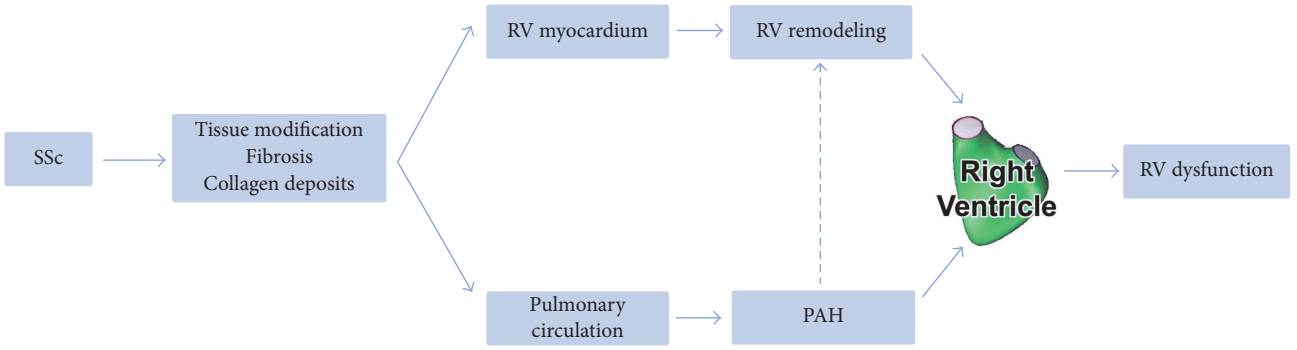

Figure 1: The complex interrelation between the mechanisms involved in development of RV dysfunction and remodeling.

observed between these parameters. Right ventricle global longitudinal strain (RVGLS) was also significantly lower in SSc patients compared to the control group ($p < 0.001$). An inverse correlation was observed between duration of the disease and TAPSE and RVGLS [36]. These findings consolidate the earlier results published by Schattke et al. who reported significantly decreased TAPSE and RVS′ determined by 2DSTE in SSc patients without PAH and identified isovolumetric acceleration (IVA) as the best predictor of early RV systolic impairment in this patient category [37].

Another early predictor of RV systolic dysfunction in SSc patients determined by 2DSTE may be represented by elevated longitudinal strain rates of the RV, which may serve as an adaptive response to even subtle elevation of the sPAP [38]. Furthermore these early systolic dysfunctions of the RV and RA may presage the sPAP elevation; thus it is important to detect them for the optimization of the further treatment of SSc patients, as recent trials show support for an early aggressive therapy [39–42].

3.2. The Distinctive Pattern of RV Remodeling and Function in Scleroderma Patients. Functional and structural alterations of the RV develop even before the setting of PAH in SSc patients, suggesting a remodeling pattern different from the one usually recorded in IPAH. Poor response to optimal therapy was observed in SSc-PAH, ultimately leading to RV failure and death, generating higher mortality rates compared to IPAH patients [1, 43, 44]. These findings led to the emergence of a novel theory about a different adaptive functional and structural remodeling of the RV in SSc patients. The complex interrelation between the mechanisms involved in development of RV dysfunction and remodeling is summarized in Figure 1. Different clinical studies tried to characterize the clinical condition of patients with SSc with or without PAH and to identify predictors of RV involvement and dysfunction. The main clinical studies and their findings are presented in Table 1.

In an autopsy study Overbeek et al. analyzed the histological samples of the RV from SSc-PAH and IPAH patients and compared them with samples taken from healthy controls. Significantly more inflammatory cells were observed in interstitium of the RV from SSc-PAH patients compared to IPAH patients and controls; however the quantity of fibrosis did not show significant differences between the groups, suggesting that the underlying mechanism of RV dysfunction may have multiple factors [45].

Kelemen et al. assessed the RV remodeling of SSc-PAH and IPAH patients using cardiac magnetic resonance imaging (cMRI). No significant differences were recorded in terms of RV mass, RV-EDV, RV ejection fraction, stroke volume, or TAPSE between the two groups [46]. It has been demonstrated that SSc-PAH patients exhibit significantly less pronounced increase of the RV mass (assessed by right ventricular modeling index (RVMI) and volume mass index (VMI)), in response to increased RV load (assessed by PVR and (mean) mPAP) compared to IPAH patients, evidencing a different adaptive hypertrophy mechanism of these patients [46]. However, the benefits and disadvantages gained from RV hypertrophy in this patient category are still under debate [47]. In a recently published article Ramjug et al. did not confirm the aforementioned findings, as no significant differences of RV mass were recorded between SSc-PAH and IPAH patients at increased RV load. Nevertheless, they found a notable correlation between the VMI and PVR in SSc-PAH through the entire range of PVR, which may be a predictor for survival, as earlier studies suggested [48, 49].

The functional reserve of RV may also play an important role in the adaptive remodeling of the RV in SSc. Hsu et al. assessed RV function and morphology during exercise (or atrial pacing) testing in 15 SSc-PAH and 9 IPAH patients with comparable resting RV parameters. The RV contractility of the IPAH group was significantly increased during exercise, while the SSc-PAH group did not display improved contractility leading to important increase of RV-EDV and RV-ESV. The authors attribute these changes to decreased calcium cycling in the myocytes of SSc-PAH group ($p = 0.03$). The abnormal RV-PA coupling and diminished force-frequency responsiveness (FFR) of these patients during exercise, along with reduced contractile and diastolic reserve, plead for the depletion of RV functional reserve of SSc-PAH patients. These results highlight the importance of intrinsic RV dysfunction, which ultimately leads to RV failure in SSc-PAH patients [50].

Kovacs et al. determined the pulmonary exercise hemodynamics of SSc patients with a 4-year follow-up period, observing significant increase of mPAP ($p = 0.02$) and PVR

Table 1: Main clinical studies addressing Ssc in patients with or without PAH.

Imaging method	Author (year)	Number of patients	Clinical setting	Analyzed parameter	SSc	Controls	p
Echocardiography	Pigatto et al. (2015) [35]	$n = 88$	SSc versus healthy subjects	sPAP (mmHg)	33 ± 14.0	22 ± 5.0	<0.0001
				TAPSE (mm)	23 ± 3.0	26 ± 2.0	<0.0001
				PVR (WU)	1.9 ± 0.6	1.4 ± 0.3	0.001
				global RVLS (%)	−24.8 ± 4.0	−25.6 ± 3	n.s.
	Mukherjee et al. (2016) [58]	$n = 178$	SSc versus healthy subjects	sPAP (mmHg)	31.4 ± 13.3	22.6 ± 4.4	0.0001
				TAPSE (mm)	21.6 ± 4.7	22.5 ± 4.0	0.307
				PVR (WU)	1.48 ± 0.45	1.24 ± 0.26	0.002
				global RVLS (%)	−17.7 ± 5.9	−20.4 ± 2.4	0.005
	Durmus et al. (2015) [36]	$n = 80$	SSc versus healthy subjects	sPAP (mmHg)	24.2 ± 5.7	19.8 ± 6.2	0.002
				TAPSE (mm)	21.1 ± 3.2	24.3 ± 3.4	<0.001
				global RVLS (%)	−18.5 ± 4.9	−21.8 ± 2.4	<0.001
cMRI	Hachulla et al. (2009) [69]	$n = 52$	SSc-PAH versus SSc without PAH	RV hypertophy, n (%)	2 (17)	0 (0)	0.04
				RV dilation, n (%)	4 (33)	7 (17)	0.25
				Mean RV EF (%)	54 (13)	50 (11)	0.20
				Mean RV EDV index (ml/mm2)	75 (9)	79 (23)	0.67
				Delayed contrast enhancement, n (%)	1 (8)	10 (26)	0.42
	Tzelepis et al. (2007) [70]	$n = 36$	Abnormal versus normal 24-h ECG in SSc	Delayed contrast enhancement, n (%)	15 (78.9)	9 (52.9)	0.098
				Number of enhancing segments, n	5.4 ± 4.8	2.5 ± 2.9	0.035
				Enhancement at RV insertion points, n (%)	4 (21.1)	2 (11.8)	0.66
	Kelemen et al. (2015) [46]	$n = 53$	SSc-PAH versus IPAH	RV mass (g)	58.8	65.9	0.47
				RV EDV index (ml/mm2)	88.1	90.1	0.83
				RV EF (%)	46.0	41.6	0.29
Scintigraphy	Papagoras et al. (2014) [65]	$n = 35$	SSc patients	Reversible myocardial perfusion defects, n of pts (%)	21 (60)	-	-

sPAP: systolic pulmonary artery pressure; TAPSE: tricuspid annular plane systolic excursion; PVR: pulmonary vascular resistance; RVLS: right ventricle longitudinal strain; EF: ejection fraction; EDV: end diastolic volume.

($p = 0.002$) during exercise, with no changes in resting mPAP values. These findings illustrate the progressive nature of the disease and point out that alterations of exercise hemodynamic parameters precede the routinely determined resting values. The aforementioned changes might be related to the distinctive morphological and functional remodeling pattern of the RV in SSc patients [51].

4. Imaging Tools for Characterization of the RV in Scleroderma

Different imaging technologies are currently available for characterization of RF function and morphology, the most used ones being represented by echocardiography, scintigraphy, and cardiac magnetic resonance imaging (cMRI) (Table 1).

4.1. Echocardiography. Given the high prevalence of RV impairment in scleroderma patients, current guidelines recommend early echocardiographic screening of SSc patients at risk for PAH. Immediate initiation of optimal therapy and prevention of right heart failure can improve the prognosis and survival of patients with SSc-PAH [26]. Transthoracic echocardiography (TTE) is a widely available imaging method used for a proper functional and morphological assessment of the RV; however, a considerable number of patients remain undiagnosed until late stages of heart failure, presumably because of the complex geometry of the RV. Conventional 2D echocardiography along with Doppler technology is able to evaluate RV diameters, areas, and volumes, as well as pressures, velocities, and gradients across the cardiac chambers and valves [52].

Different echocardiographic biomarkers have been proposed for characterization of RV function and can serve for evaluation of ventricular dysfunction in patients with SSc. TAPSE is an easily determinable parameter which is considered the most accurate in the assessment of the global RV contractility (albeit it is influenced by load and structure). It correlates with the parameters obtained from right heart catheterization and was proved as a prognostic factor in SSc-PAH [53, 54]. Another useful parameter for the assessment of RV and global ventricular function is represented by the Tei index, or myocardial performance index (expressed as isovolumetric contraction time and isovolumetric relaxation time divided ejection time), which uses pulsed wave Doppler velocities of ventricular inflow and outflow to calculate ventricular performance. Several studies validated its correlation with lower survival rates in SSc patients [55–57]. Tissue Doppler imaging (TDI) has the advantage to determine myocardial velocities, allowing detection of systolic and diastolic deformations (defined as strain); therefore it is able to assess segmental and global RV function. The major drawback of this method is the dependence of the Doppler beam angle [34, 39].

Novel echocardiographic modalities based on speckle tracking technology allow a better identification of subclinical heart failure. The technique is a software-based method that allows the calculation of tissue velocity and deformations of the myocardium derived from 2D images, tracking pixels (speckles) of a certain myocardial sector along the cardiac cycle. It can detect the changes in length of the tracked segment during systole and diastole with calculation of strain and strain rate (SR) parameters. These parameters offer an accurate, operator, and angle-independent view of the segmental and global (systolic and diastolic) function of the ventricles. Multiple studies suggest that RV longitudinal strain values and patterns are helpful in the assessment of RV function in SSc and PAH patients and correlate well with the prognosis of this patient category [57–61].

4.2. Scintigraphy. The evaluation of the right ventricular function with nuclear imaging and scintigraphy can determine myocardial damage caused by SSc in early stages by identification of small perfusion defects. A ten-year survival study conducted by Steen et al. showed that SSc patients that presented perfusion defects upon scintigraphy examination with thallium presented a higher rate of cardiac disease and mortality [62]. Furthermore, 99 m Technetium ventriculography performed on 42 patients without PAH revealed a significantly lower RV ejection fraction compared to controls, both at baseline and at 2 hours from administration of 40 mg of oral Nicardipine [63]. Additionally, patients with SSc may present the so-called "myocardial Raynaud's phenomenon" that leads to transient ischemic episodes induced during the cold pressor test. Lekakis et al. performed dipyridamole-thallium-201 scintigraphy during cold pressor testing and found that scleroderma patients presented transient myocardial ischemia induced by cold and that subjects with Raynaud's phenomenon of under 5 years did not present any defects [64]. A combined echocardiography and scintigraphy research study by Papagoras et al. reported that 60% of patients presented reversible myocardial perfusion defects in spite of the lack of clinically active heart disease, even in younger patients [65].

Although scintigraphy has been proven to be a sensitive method for detection of early perfusion defects in systemic sclerosis patients with no cardiac symptomatology, further studies are needed to elucidate its role in establishing prognosis and therapeutic management, which may be a hard task, since nuclear imaging methods present high costs and are not widely available.

4.3. Cardiac MRI. cMRI is a noninvasive imaging modality that faced a tremendous development in the last decade, being able to provide high quality images on the anatomy and function of the heart [66–68]. cMRI has been shown to offer a significant aid in the diagnosis of several inflammatory processes affecting the myocardium as well as in fibrosis detection and quantification in a great number of pathologies, including SSc [69–73]. cMRI currently is the gold standard method for evaluation of RV parameters, and several studies have focused on the role of cardiac magnetic resonance for assessing right and left ventricular function, the extent and pattern of myocardial fibrosis, and perfusion abnormalities in SSc subjects [69, 70, 74]. Bezante et al. aimed to research the myocardial effects of SSc by cMRI imaging in 50 patients with scarce or no clinical signs of heart failure. The study

showed that both the right and left ventricular ejection fractions were reduced compared to controls ($p < 0.001$ and $p < 0.009$, resp.), and the RV ejection fraction matched for body surface area was significantly reduced in subjects with diffuse compared to limited cutaneous SSc [74]. Tzelepis et al. sought to evaluate the distribution and pattern of the fibrotic involvement of the myocardium on 41 patients with SSc with the use of Delayed-Enhancement cMRI (DE-CMR) with gadolinium [70]. Their results revealed that 66% of the enrolled patients presented late enhancement, predominantly in the middle region of the myocardium wall, with a sparing of the endo- and epicardial regions, predominantly in the middle and basal areas of the left ventricle, with a noncoronary distribution. As for the right ventricular involvement, 17% of patients presented globular, intermittent enhanced areas in the RV insertion points, independent of the presence of PAH, upon echocardiographic assessment [70].

Hachulla et al. found that 75% of SSc patients presented cMRI abnormalities in their study population and that 21% of patients presented an altered RV ejection fraction, while 17% showed RV dilation in the absence of PAH. Moreover, they observed the thinning of the left ventricular myocardium that affected primarily patients with diffuse cutaneous SSc and those with no PAH, suggesting that this might be caused by disease's chronic effect on the microvasculature of the heart, being similar to the thinning that occurs during the ventricular remodeling process secondary to infarction [69].

Magnetic resonance imaging of the heart is also a useful tool in evaluating the effects of various therapies in patients with PAH, as well as for prognosis implications. Allanore et al. have evaluated the effect of bosentan on the perfusion and function of the myocardium by performing cMRI and Tissue Doppler Echocardiography on 18 SSc patients with no PA and no symptoms of impaired cardiac function. The study found that cMRI perfusion index and the echocardiography parameters were improved after 4 weeks of bosentan administration [75]. This shows that an improved myocardial function and perfusion can be revealed in SSc patients by highly sensitive imaging methods such as cMRI, which is a valuable noninvasive, nonirradiating, and highly reproducible imaging method useful in this patient population.

5. Conclusions

In patients with SSc, the morphological remodeling and alteration of RV function begin even before the setting of PAH and lead to development of a specific adaptive pattern of the RV which is different from the one recorded in patients with IAPH. These alterations cause worse outcomes and increased mortality rates in SSc patients. Early detection of RV dysfunction and remodeling is possible using modern imaging tools currently available and can indicate the initiation of specific therapeutic measures before installation of PAH.

Conflicts of Interest

The authors declare that there are no conflicts of interest regarding the publication of this article.

References

[1] R. J. Tedford, J. O. Mudd, R. E. Girgis et al., "Right ventricular dysfunction in systemic sclerosis-associated pulmonary arterial hypertension," *Circulation: Heart Failure*, vol. 6, no. 5, pp. 953–963, 2013.

[2] L. Chung, H. W. Farber, R. Benza et al., "Unique Predictors of Mortality in Patients With Pulmonary Arterial Hypertension Associated With Systemic Sclerosis in the REVEAL Registry," *CHEST*, vol. 146, no. 6, pp. 1494–1504, 2014.

[3] T. A. Winstone, D. Assayag, P. G. Wilcox et al., "Predictors of mortality and progression in scleroderma-associated interstitial lung disease: A systematic review," *CHEST*, vol. 146, no. 2, pp. 422–436, 2014.

[4] M. Elhai, C. Meune, M. Boubaya et al., "Mapping and predicting mortality from systemic sclerosis," *Annals of the Rheumatic Diseases*, 2017.

[5] K. Romanowska-Próchnicka, M. Walczyk, and M. Olesińska, "Recognizing systemic sclerosis: Comparative analysis of various sets of classification criteria," *Reumatología Clínica*, vol. 54, no. 6, pp. 296–305, 2016.

[6] L. I. Sakkas, "New developments in the pathogenesis of systemic sclerosis," *Autoimmunity*, vol. 38, no. 2, pp. 113–116, 2005.

[7] S. Barsotti, C. Stagnaro, A. d'Ascanio, and A. Della Rossa, "One year in review 2016: Systemic sclerosis," *Clinical and Experimental Rheumatology*, vol. 34, pp. 3–13, 2016.

[8] A. J. Gilbane, C. P. Denton, and A. M. Holmes, "Scleroderma pathogenesis: A pivotal role for fibroblasts as effector cells," *Arthritis Research & Therapy*, vol. 15, no. 3, article no. 215, 2013.

[9] M. Matucci-Cerinic, B. Kahaleh, and F. M. Wigley, "Review: evidence that systemic sclerosis is a vascular disease," *Arthritis & Rheumatology*, vol. 65, no. 8, pp. 1953–1962, 2013.

[10] S. A. Jimenez, "Role of endothelial to mesenchymal transition in the pathogenesis of the vascular alterations in systemic sclerosis," *ISRN Rheumatology*, vol. 2013, Article ID 835948, 15 pages, 2013.

[11] C. Fatini, F. Gensini, E. Sticchi et al., "High prevalence of polymorphisms of angiotensin-converting enzyme (I/D) and endothelial nitric oxide synthase (Glu298Asp) in patients with systemic sclerosis," *American Journal of Medicine*, vol. 112, no. 7, pp. 540–544, 2002.

[12] R. Togănel, I. Muntean, C. Duicu, A. Făgărăşan, L. Gozar, and C. Bănescu, "The role of eNOS and AGT gene polymorphisms in secondary pulmonary arterial hypertension in Romanian children with congenital heart disease," *Revista Romana de Medicina de Laborator*, vol. 21, no. 3-4, pp. 267–274, 2013.

[13] J. Barnes and M. D. Mayes, "Epidemiology of systemic sclerosis: Incidence, prevalence, survival, risk factors, malignancy, and environmental triggers," *Current Opinion in Rheumatology*, vol. 24, no. 2, pp. 165–170, 2012.

[14] A. C. Gelber, R. L. Manno, A. A. Shah et al., "Race and association with disease manifestations and mortality in scleroderma : A 20-year experience at the johns hopkins scleroderma center and review of the literature," *Medicine (United States)*, vol. 92, no. 4, pp. 191–205, 2013.

[15] C. Nguyen, A. Bérezné, T. Baubet et al., "Association of gender with clinical expression, quality of life, disability, and depression and anxiety in patients with systemic sclerosis," *PLoS ONE*, vol. 6, no. 3, Article ID e17551, 2011.

[16] J. Le Pavec, M. Humbert, L. Mouthon, and P. M. Hassoun, "Systemic sclerosis-associated pulmonary arterial hypertension,"

American Journal of Respiratory and Critical Care Medicine, vol. 181, no. 12, pp. 1285–1293, 2010.

[17] C. J. Mullin and S. C. Mathai, "New insights into the recognition, classification and management of systemic sclerosis-associated pulmonary hypertension," *Current Opinion in Rheumatology*, vol. 29, no. 6, pp. 561–567, 2017.

[18] G. Lefèvre, L. Dauchet, E. Hachulla et al., "Survival and prognostic factors in systemic sclerosis–associated pulmonary hypertension: a systematic review and meta-analysis," *Arthritis & Rheumatology*, vol. 65, no. 9, pp. 2412–2423, 2013.

[19] A. Tyndall, "Systemic sclerosis in Europe: first report from the EULAR Scleroderma Trials And Research (EUSTAR) group database," *Annals of the Rheumatic Diseases*, vol. 64, no. 7, pp. 1107-1107, 2005.

[20] M. Hinchcliff, A. Fischer, E. Schiopu, and V. D. Steen, "Pulmonary hypertension assessment and recognition of outcomes in scleroderma (PHAROS): Baseline characteristics and description of study population," *The Journal of Rheumatology*, vol. 38, no. 10, pp. 2172–2179, 2011.

[21] G. Simonneau, M. Gatzoulis, and I. Adatia, "Updated clinical classification of pulmonary hypertension," *Journal of the American College of Cardiology*, vol. 62, no. 25, supplement, 2013.

[22] M. R. Fisher, S. C. Mathai, H. C. Champion et al., "Clinical differences between idiopathic and scleroderma-related pulmonary hypertension," *Arthritis & Rheumatology*, vol. 54, no. 9, pp. 3043–3050, 2006.

[23] A. Campo, S. C. Mathai, J. Le Pavec et al., "Hemodynamic predictors of survival in scleroderma-related pulmonary arterial hypertension," *American Journal of Respiratory and Critical Care Medicine*, vol. 182, no. 2, pp. 252–260, 2010.

[24] R. G. Argula, A. Karwa, A. Lauer et al., "Differences in right ventricular functional changes during treatment between systemic sclerosis-associated pulmonary arterial hypertension and idiopathic pulmonary arterial hypertension," *Annals of the American Thoracic Society*, vol. 14, no. 5, pp. 682–689, 2017.

[25] V. McLaughlin, R. N. Channick, H.-A. Ghofrani et al., "Bosentan added to sildenafil therapy in patients with pulmonary arterial hypertension," *European Respiratory Journal*, vol. 46, no. 2, pp. 405–413, 2015.

[26] N. Galiè, M. Humbert, J. L. Vachiery et al., "2015 ESC/ERS Guidelines for the diagnosis and treatment of pulmonary hypertension: The Joint Task Force for the Diagnosis and Treatment of Pulmonary Hypertension of the European Society of Cardiology (ESC) and the European Respiratory Society (ERS): Endorsed by: Association for European Paediatric and Congenital Cardiology (AEPC), International Society for Heart and Lung Transplantation (ISHLT)," *European Heart Journal*, vol. 37, no. 1, pp. 67–119, 2016.

[27] P. M. Hassoun, "The right ventricle in scleroderma (2013 Grover conference series)," *Pulmonary Circulation*, vol. 5, no. 1, pp. 3–14, 2015.

[28] S. C. Mathai, M. Bueso, L. K. Hummers et al., "Disproportionate elevation of N-terminal pro-brain natriuretic peptide in scleroderma-related pulmonary hypertension," *European Respiratory Journal*, vol. 35, no. 1, pp. 95–104, 2010.

[29] M. J. Overbeek, J.-W. Lankhaar, N. Westerhof et al., "Right ventricular contractility in systemic sclerosis-associated and idiopathic pulmonary arterial hypertension," *European Respiratory Journal*, vol. 31, no. 6, pp. 1160–1166, 2008.

[30] W. P. Follansbee, T. R. Miller, E. I. Curtiss et al., "A controlled clinicopathologic study of myocardial fibrosis in systemic sclerosis (scleroderma)," *The Journal of Rheumatology*, vol. 17, no. 5, pp. 656–662, 1990.

[31] C. Meune, O. Vignaux, A. Kahan, and Y. Allanore, "Heart involvement in systemic sclerosis: evolving concept and diagnostic methodologies," *Archives of Cardiovascular Diseases*, vol. 103, no. 1, pp. 46–52, 2010.

[32] F. Fernandes, F. J. A. Ramires, E. Arteaga, B. M. Ianni, E. S. D. O. Bonfá, and C. Mady, "Cardiac remodeling in patients with systemic sclerosis with no signs or symptoms of heart failure: An endomyocardial biopsy study," *Journal of Cardiac Failure*, vol. 9, no. 4, pp. 311–317, 2003.

[33] S. Lambova, "Cardiac manifestations in systemic sclerosis," *World Journal of Cardiology*, vol. 6, no. 9, p. 993, 2014.

[34] J. Kjærgaard, "Assessment of right ventricular systolic function by tissue Doppler echocardiography.," *Danish Medical Journal*, vol. 59, no. 3, p. B4409, 2012.

[35] E. Pigatto, D. Peluso, E. Zanatta et al., "Evaluation of right ventricular function performed by 3d-echocardiography in scleroderma patients," *Reumatismo*, vol. 66, no. 4, pp. 259–263, 2015.

[36] E. Durmus, M. Sunbul, K. Tigen et al., "Right ventricular and atrial functions in systemic sclerosis patients without pulmonary hypertension: Speckle-tracking echocardiographic study," *Herz*, vol. 40, no. 4, pp. 709–715, 2015.

[37] S. Schattke, F. Knebel, A. Grohmann et al., "Early right ventricular systolic dysfunction in patients with systemic sclerosis without pulmonary hypertension: A Doppler Tissue and Speckle Tracking echocardiography study," *Cardiovascular Ultrasound*, vol. 8, no. 1, article no. 3, 2010.

[38] C. Matias, L. P. D. Isla, M. Vasconcelos et al., "Speckle-tracking-derived strain and strain-rate analysis: A technique for the evaluation of early alterations in right ventricle systolic function in patients with systemic sclerosis and normal pulmonary artery pressure," *Journal of Cardiovascular Medicine*, vol. 10, no. 2, pp. 129–134, 2009.

[39] M. D'Alto, G. Cuomo, E. Romeo et al., "Tissue Doppler imaging in systemic sclerosis: A 3-year longitudinal study," *Seminars in Arthritis and Rheumatism*, vol. 43, no. 5, pp. 673–680, 2014.

[40] P. M. Hassoun, R. T. Zamanian, R. Damico et al., "Ambrisentan and tadalafil up-front combination therapy in scleroderma-associated pulmonary arterial hypertension," *American Journal of Respiratory and Critical Care Medicine*, vol. 192, no. 9, pp. 1102–1110, 2015.

[41] G. Kovacs and H. Olschewski, "Borderline pulmonary pressures in scleroderma—a pre-pulmonary arterial hypertension condition?" *Arthritis Research & Therapy*, vol. 17, no. 1, p. 123, 2015.

[42] A. D'Andrea, M. D'Alto, M. Di Maio et al., "Right atrial morphology and function in patients with systemic sclerosis compared to healthy controls: a two-dimensional strain study," *Clinical Rheumatology*, vol. 35, no. 7, pp. 1733–1742, 2016.

[43] M. Rubenfire, M. D. Huffman, S. Krishnan, J. R. Seibold, E. Schiopu, and V. V. McLaughlin, "Survival in systemic sclerosis with pulmonary arterial hypertension has not improved in the modern era," *CHEST*, vol. 144, no. 4, pp. 1282–1290, 2013.

[44] M. R. Fisher, S. C. Mathai, H. C. Champion et al., "Clinical differences between idiopathic and scleroderma-related pulmonary hypertension," *Arthritis & Rheumatology*, vol. 54, no. 9, pp. 3043–3050, 2006.

[45] M. J. Overbeek, K. T. B. Mouchaers, H. M. Niessen et al., "Characteristics of interstitial fibrosis and inflammatory cell

infiltration in right ventricles of systemic sclerosis-associated pulmonary arterial hypertension," *International Journal of Rheumatology*, vol. 2010, Article ID 604615, 2010.

[46] B. W. Kelemen, S. C. Mathai, R. J. Tedford et al., "Right ventricular remodeling in idiopathic and scleroderma-associated pulmonary arterial hypertension: Two distinct phenotypes," *Pulmonary Circulation*, vol. 5, no. 2, pp. 327–334, 2015.

[47] A. Harrison, N. Hatton, and J. J. Ryan, "The right ventricle under pressure: Evaluating the adaptive and maladaptive changes in the right ventricle in pulmonary arterial hypertension using echocardiography (2013 Grover conference series)," *Pulmonary Circulation*, vol. 5, no. 1, pp. 29–47, 2015.

[48] S. Ramjug, N. Hussain, J. Hurdman et al., "Idiopathic and Systemic Sclerosis-Associated Pulmonary Arterial Hypertension: A Comparison of Demographic, Hemodynamic, and MRI Characteristics and Outcomes," *CHEST*, vol. 152, no. 1, pp. 92–102, 2017.

[49] D. Hagger, R. Condliffe, N. Woodhouse et al., "Ventricular mass index correlates with pulmonary artery pressure and predicts survival in suspected systemic sclerosis-associated pulmonary arterial hypertension," *Rheumatology*, vol. 48, no. 9, pp. 1137–1142, 2009.

[50] S. Hsu, B. A. Houston, E. Tampakakis et al., "Right ventricular functional reserve in pulmonary arterial hypertension," *Circulation*, vol. 133, no. 24, pp. 2413–2422, 2016.

[51] G. Kovacs, A. Avian, N. Wutte et al., "Changes in pulmonary exercise haemodynamics in scleroderma: A 4-year prospective study," *European Respiratory Journal*, vol. 50, no. 1, Article ID 1601708, 2017.

[52] E. Hachulla, D. Launay, A. Yaici et al., "Pulmonary arterial hypertension associated with systemic sclerosis in patients with functional class II dyspnoea: mild symptoms but severe outcome.," *Rheumatology*, vol. 49, no. 5, pp. 940–944, 2010.

[53] P. R. Forfia, M. R. Fisher, S. C. Mathai et al., "Tricuspid annular displacement predicts survival in pulmonary hypertension," *American Journal of Respiratory and Critical Care Medicine*, vol. 174, no. 9, pp. 1034–1041, 2006.

[54] S. C. Mathai, C. T. Sibley, P. R. Forfia et al., "Tricuspid annular plane systolic excursion is a robust outcome measure in systemic sclerosis-associated pulmonary arterial hypertension," *The Journal of Rheumatology*, vol. 38, no. 11, pp. 2410–2418, 2011.

[55] C. Tei, "New non-invasive index for combined systolic and diastolic ventricular function," *Journal of Cardiology*, vol. 26, no. 2, pp. 135-136, 1995.

[56] S. Frea, M. Capriolo, W. G. Marra et al., "Echo doppler predictors of pulmonary artery hypertension in patients with systemic sclerosis," *Journal of Echocardiography*, vol. 28, no. 8, pp. 860–869, 2011.

[57] H. Blessberger and T. Binder, "Two dimensional speckle tracking echocardiography: Basic principles," *Heart*, vol. 96, no. 9, pp. 716–722, 2010.

[58] M. Mukherjee, S. Chung, V. K. Ton et al., "Unique abnormalities in right ventricular longitudinal strain in systemic sclerosis patients," *Circulation: Cardiovascular Imaging*, vol. 9, article e003792, no. 6, 2016.

[59] A. Meris, F. Faletra, C. Conca et al., "Timing and magnitude of regional right ventricular function: A speckle tracking-derived strain study of normal subjects and patients with right ventricular dysfunction," *Journal of the American Society of Echocardiography*, vol. 23, no. 8, pp. 823–831, 2010.

[60] L. G. Rudski, W. W. Lai, J. Afilalo et al., "Guidelines for the echocardiographic assessment of the right heart in adults: a report from the American Society of Echocardiography endorsed by the European Association of Echocardiography, a registered branch of the European Society of Cardiology, and the Canadian Society of Echocardiography," *Journal of the American Society of Echocardiography*, vol. 23, no. 7, pp. 685–713, 2010.

[61] I. Muntean, T. Benedek, M. Melinte, C. Suteu, and R. Togãnel, "Deformation pattern and predictive value of right ventricular longitudinal strain in children with pulmonary arterial hypertension," *Cardiovascular Ultrasound*, vol. 14, no. 1, article no. 27, 2016.

[62] V. D. Steen, W. P. Follansbee, C. G. Conte, and T. A. Medsger Jr., "Thallium perfusion defects predict subsequent cardiac dysfunction in patients with systemic sclerosis," *Arthritis & Rheumatology*, vol. 39, no. 4, pp. 677–681, 1996.

[63] C. Meune, Y. Allanore, J.-Y. Devaux et al., "High prevalence of right ventricular systolic dysfunction in early systemic sclerosis," *The Journal of Rheumatology*, vol. 31, no. 10, pp. 1941–1945, 2004.

[64] J. Lekakis, M. Mavrikakis, and M. Emmanuel, "Cold-induced coronary Raynaud's phenomenon in patients with systemic sclerosis," *Clinical and Experimental Rheumatology*, vol. 16, no. 2, pp. 135–140, 1998.

[65] C. Papagoras, K. Achenbach, N. Tsifetaki, S. Tsiouris, A. Fotopoulos, and A. A. Drosos, "Heart involvement in systemic sclerosis: A combined echocardiographic and scintigraphic study," *Clinical Rheumatology*, vol. 33, no. 8, pp. 1105–1111, 2014.

[66] R. C. Hendel, M. R. Patel, C. M. Kramer et al., "ACCF/ACR/SCCT/SCMR/ASNC/NASCI/SCAI/SIR 2006 appropriateness criteria for cardiac computed tomography and cardiac magnetic resonance imaging: a report of the American College of Cardiology Foundation Quality Strategic Directions Committee Appropriateness Criteria Working Group, American College of Radiology, Society of Cardiovascular Computed Tomography, Society for Cardiovascular Magnetic Resonance, American Society of Nuclear Cardiology, North American Society for Cardiac Imaging, Society for Cardiovascular Angiography and Interventions, and Society of Interventional Radiology," *Journal of the American College of Cardiology*, vol. 48, pp. 1475–1497, 2006.

[67] J. P. Ridgway, "Cardiovascular magnetic resonance physics for clinicians: Part i," *Journal of Cardiovascular Magnetic Resonance*, vol. 12, no. 1, article no. 71, 2010.

[68] J. D. Biglands, A. Radjenovic, and J. P. Ridgway, "Cardiovascular magnetic resonance physics for clinicians: Part II," *Journal of Cardiovascular Magnetic Resonance*, vol. 14, no. 1, article no. 66, 2012.

[69] A.-L. Hachulla, D. Launay, V. Gaxotte et al., "Cardiac magnetic resonance imaging in systemic sclerosis: A cross-sectional observational study of 52 patients," *Annals of the Rheumatic Diseases*, vol. 68, no. 12, pp. 1878–1884, 2009.

[70] G. E. Tzelepis, N. L. Kelekis, S. C. Plastiras et al., "Pattern and distribution of myocardial fibrosis in systemic sclerosis: A delayed enhanced magnetic resonance imaging study," *Arthritis & Rheumatology*, vol. 56, no. 11, pp. 3827–3836, 2007.

[71] O. Vignaux, Y. Allanore, C. Meune et al., "Evaluation of the effect of nifedipine upon myocardial perfusion and contractility using cardiac magnetic resonance imaging and tissue Doppler echocardiography in systemic sclerosis," *Annals of the Rheumatic Diseases*, vol. 64, no. 9, pp. 1268–1273, 2005.

[72] M. A. Olimulder, J. van Es, and M. A. Galjee, "The importance of cardiac MRI as a diagnostic tool in viral myocarditis-induced

cardiomyopathy," *Netherlands Heart Journal*, vol. 17, no. 12, pp. 481–486, 2009.

[73] B. Heydari, M. Jerosch-Herold, and R. Y. Kwong, "Assessment of Myocardial Ischemia with Cardiovascular Magnetic Resonance," *Progress in Cardiovascular Diseases*, vol. 54, no. 3, pp. 191–203, 2011.

[74] G. P. Bezante, D. Rollando, M. Sessarego et al., "Cardiac magnetic resonance imaging detects subclinical right ventricular impairment in systemic sclerosis," *The Journal of Rheumatology*, vol. 34, pp. 2431–2437, 2007.

[75] Y. Allanore, C. Meune, O. Vignaux, S. Weber, P. Legmann, and A. Kahan, "Bosentan increases myocardial perfusion and function in systemic sclerosis: A magnetic resonance imaging and Tissue-Doppler echography study," *The Journal of Rheumatology*, vol. 33, no. 12, pp. 2464–2469, 2006.

Hindawi
BioMed Research International
Volume 2018, Article ID 6817832, 6 pages
https://doi.org/10.1155/2018/6817832

Research Article

Acute and Long-Term Hemodynamic Effects of MitraClip Implantation on a Preexisting Secondary Right Heart Failure

M. Hünlich,[1] E. Lubos,[2] B. E. Beuthner,[1] M. Puls,[1] A. Bleckmann,[3] T. Beißbarth,[3] T. Tichelbäcker,[1] V. Rudolph,[4] S. Baldus,[4] U. Schäfer,[2] H. Treede,[5] R. S. Von Bardeleben,[6] S. Blankenberg,[2] and W. Schillinger[1]

[1]*Herzzentrum, Abt. Kardiologie und Pneumologie, Universitätsklinikum Göttingen, Göttingen, Germany*
[2]*Klinik und Poliklinik für Allgemeine und Interventionelle Kardiologie, Universitäres Herzzentrum Hamburg GmbH, Hamburg, Germany*
[3]*Institut für Medizinische Statistik, Universitätsmedizin Göttingen, Göttingen, Germany*
[4]*Klinik für Kardiologie, Angiologie, Pneumologie und Internistische Intensivmedizin, Herzzentrum der Universität zu Köln, Köln, Germany*
[5]*Universitätsklinik und Poliklinik für Herzchirurgie, Martin-Luther-Universität, Halle-Wittenberg, Halle, Germany*
[6]*II. Medizinische Klinik und Poliklinik, Universitätsmedizin der Johannes-Gutenberg-Universität, Mainz, Germany*

Correspondence should be addressed to M. Hünlich; huenlich@med.uni-goettingen.de

Received 6 July 2017; Revised 14 January 2018; Accepted 23 January 2018; Published 14 March 2018

Academic Editor: Ruxandra Jurcut

Positive results of MitraClip in terms of improvement in clinical and left ventricular parameters have been described in detail. However, long-term effects on secondary pulmonary hypertension were not investigated in a larger patient cohort to date. 70 patients with severe mitral regurgitation, additional pulmonary hypertension, and right heart failure as a result of left heart disease were treated in the heart centers Hamburg and Göttingen. Immediately after successful MitraClip implantation, a reduction of the RVOT diameter from 3.52 cm to 3.44 cm was observed reaching a statistically significant value of 3.39 cm after 12 months. In contrast, there was a significant reduction in the velocity of the tricuspid regurgitation (TR) from 4.17 m/s to 3.11 m/s, the gradient of the TR from 48.5 mmHg to 39.3 mmHg, and the systolic pulmonary artery pressure (PAPsyst) from 58.6 mmHg to 50.0 mmHg. This decline continued in the following months (V_{max} TR 3.09 m/s, peak TR 38.6 mmHg, and PAPsyst 47.4 mmHg). The tricuspid annular plane systolic excursion (TAPSE) increased from 16.5 mm to 18.9 mm after 12 months. MitraClip implantation improves pulmonary artery pressure, tricuspid regurgitation, and TAPSE after 12 months. At the same time, there is a decrease in the RVOT diameter without significant changes in other right ventricular and right atrial dimensions.

1. Introduction

Mitral regurgitation is the second most common cause of heart valve failure in Europe [1] and leads to a continuous backflow of blood into the pulmonary vessels.

While an acute pressure increase in the pulmonary veins leads to pulmonary edema, chronic congestion often ends in reactive pulmonary vasoconstriction with consecutive secondary pulmonary hypertension. Alongside the degree of mitral regurgitation, other factors, such as severe impaired left ventricular ejection fraction, may also have an impact on secondary pulmonary hypertension [2–4].

Previous published data demonstrate an important prognostic effect on perioperative course of right ventricular function and hemodynamics in patients with impaired left ventricular ejection fraction and pulmonary venous hypertension [5, 6]. Echocardiography provides a noninvasive standard method for determination of right ventricular functional parameters. Due to its complex geometry, the ejection fraction of the right ventricle cannot be easily quantified by echo. In daily routine, the end-diastolic and end-systolic volumes in the apical four-chamber view are determined and from this, the right ventricular ejection fraction is usually calculated, though it can easily lead to misinterpretation

of both ejection fraction and RV volumes [7]. In contrast, a very good correlation with the right ventricular ejection fraction is possible from the determination of the movement of the tricuspid valve ring. Unlike the left ventricle, the right ventricle consists primarily of longitudinal muscle fibers, leading to a marked basoapical movement of the tricuspid valve ring (TAPSE) during systole. Movement restrictions of less than 17 mm are regarded as pathological [8]. In addition, the systolic and mean pulmonary artery pressure can be determined, which correlate very well with invasively measured values [9].

Patients with chronic heart failure due to ischemic or dilated cardiomyopathy often undergo surgical revascularization or cardiac valve surgery to improve the left ventricular function. In large surgical cohorts, an influence of the secondary right heart failure solely by correction of mitral valve insufficiency was often associated with inconstant outcomes and increased mortality and morbidity [10–12].

Positive results of a MitraClip implantation in terms of an improvement in clinical and left ventricular parameters have been described in detail in the current literature [13, 14]. Pulmonary hypertension and/or right heart failure are an important and frequently encountered clinical scenario in patients with severe mitral regurgitation [15, 16]. However, long-term effects of a minimally invasive Mitral Valve Repair using MitraClip on secondary pulmonary hypertension were not investigated in a larger patient cohort to date.

2. Methods

Patients with severe mitral regurgitation have been treated in the heart centers of Hamburg and Göttingen since 2009, using the MitraClip procedure. Anonymized clinical and epidemiological data were scientifically evaluated after written informed consent by the patient. The current study was done in accordance with national and international guidelines and the Declaration of Helsinki after approval by the local ethical committees.

2.1. Inclusion and Exclusion Criteria. Between 2009 and 2015, 70 patients with severe mitral regurgitation were treated in both cardiac centers, using MitraClip where additional pulmonary hypertension was present due to left heart disease. In addition, clinical signs of right heart failure, for example, edema or aszites, had to exist. Patients with pulmonary hypertension or right heart failure from other causes such as chronic thromboembolism (CTEPH) or unclear or multifactorial mechanisms were excluded from the current analysis.

2.2. Specific Inclusion/Exclusion Criteria. To estimate the pulmonary artery pressure, the presence of a measureable tricuspid regurgitation was necessary. Additionally, evaluable echocardiographic data for each patient had to be available, prior the MitraClip implantation, before hospital discharge after successful implantation, and again after twelve months.

2.3. Echocardiography. All transthoracic echocardiography readings were made during clinical routine and digitally stored, so that subsequent measurements and evaluations were possible. A retrospective echocardiographic analysis took place in accordance with the recommendations of the American and European scientific societies [17, 18]. Particular attention was being paid to the right ventricular parameters by two independent investigators to whom patient names and time point of examination (before the MitraClip implantation, before discharge after successful MitraClip implantation, or twelve months after the implantation) were not revealed. Given the variation of particular RV und TV measurements on echocardiography, an inter- and intraobserver variability analysis was performed which revealed no significant difference.

RV dimensions and tricuspid valve parameters were quantified from the apical four-chamber view. LVOT diameters were measured in the parasternal outflow view and inferior vena cava diameters in the subcostal view.

The estimation of systolic pulmonary artery pressure (PAPsyst) was carried out by a continuous-wave Doppler determination of the maximum velocity of the tricuspid regurgitation (V_{max}) and this value was used in the modified Bernoulli equation (PAPsyst $= 4 * V_{max}$ + medium right atrial pressure). For the right atrial pressure (RAP), a value of 5 mmHg at complete collapse of the inferior vena cava was applied as well as a value of 10 mmHg at a partial collapse and a value of 15 mmHg in the absence of collapse [19]. Mean pulmonary artery pressure (MPAP) was calculated by tricuspid regurgitation jet velocity-time integral (TR VTI) and RAP using the following formula: mPAP = mean ΔP + RAP [20]. In accordance with current ESC and AHA/ACC guidelines, a pulmonary hypertension was assumed with a mean pulmonary pressure value greater than 25 mmHg at rest [17, 18, 21]. In addition, PAPsyst values > 50 mmHg were used as cut-off since Barbieri et al. showed an increased mortality of patients with severe mitral regurgitation [11].

2.4. Statistical Analysis. Statistical analysis was performed with the Statistical Computing Software R (version 2.15.1; https://www.r-project.org). Differences in echocardiographic measurements were calculated using Wilcoxon paired signed-rank test. A value of $P < 0.05$ was considered statistically significant.

3. Results

3.1. Baseline Characteristics. The demographic and clinical characteristics of the patients at the inclusion date are summarized in Table 1. The average age was 72.5 years, with a proportion of 66% male patients. The secondary mitral regurgitation predominated with 71%. All patients had symptomatic heart failure predominantly in NYHA stages III and IV (94%). At the same time, multiple comorbidities existed in the patients studied, in particular impaired renal function (66%) and atrial fibrillation (64%). However, coronary heart disease (36%) and diabetes mellitus (27%) were often observed, too. The comorbidities mentioned above contributed to the very high mean logistic Euro score of 30% and STS score of 10%. The average distance walked in the six-minute walk test was determined to be 213 meters.

Table 1: Demographic and clinical characteristics of all patients at baseline.

Mean age (yrs)	72,5 ± 9
Male	66%
NYHA functional class II	4 (6%)
NYHA functional class III	43 (61%)
NYHA functional class IV	23 (33%)
Kidney disease	66%
Atrial fibrillation	64%
Coronary artery disease	36%
Diabetes mellitus	27%
6-minute walk distance (m)	213 ± 54
Log EuroScore	30 ± 12
STS score	10 ± 4
Mitral regurgitation etiology	
Degenerative	20 (29%)
Functional	50 (71%)

3.2. Diameter and Area of the RA, RV, and the Vena Cava Inferior. The exact echocardiographic readings are summarized in the first part of Table 2.

Both the basal and the middle and longitudinal diameters of the RV and the diameter of the RA compared to baseline did not change significantly in the follow-up period. The area measurements of the RA and RV and the width of the vena cava inferior also remained unchanged over 12 months. Immediately after successful MitraClip implantation, a reduction of the RVOT diameter of 3.52 cm to 3.44 cm was observed in contrast to the above parameters. However, this decrease was not yet significant at the time of discharge. In the further course of time, the diameter decreased further, reaching a statistically significant value of 3.39 cm after 12 months (Figure 1).

3.3. Echocardiographic Changes to the TV. The exact echocardiographic measurements are summarized in the second part of Table 2.

The systolic and diastolic distance measurements of the TV annulus and the determination of the TR-Regurgitation area compared to the other time points remained unchanged within the observation period. Immediately after successful intervention, the vena contracta of the TR diminished from 0.88 cm to 0.82 cm, according to the RVOT. But a statistically significant value of 0.77 cm was reached after 12 months. In contrast, immediately after the intervention, there was a significant reduction in the maximum velocity of the TR from 4.17 m/s to 3.11 m/s, of the maximum gradient of the TR from 48.5 mmHg to 39.3 mmHg, and of the systolic pulmonary artery pressure from 58.6 mmHg to 50.0 mmHg. This decline continued in the following months (V_{max} TR to 3.09 m/s, peak TR to 38.6 mmHg, and PAPsyst to 47.4 mmHg), yet without becoming significant again compared to the values determined at discharge (Figure 2). Though, the significance in comparison to the results before implantation was continued. The TAPSE measurements revealed a similar picture. Immediately after the intervention, a significant increase

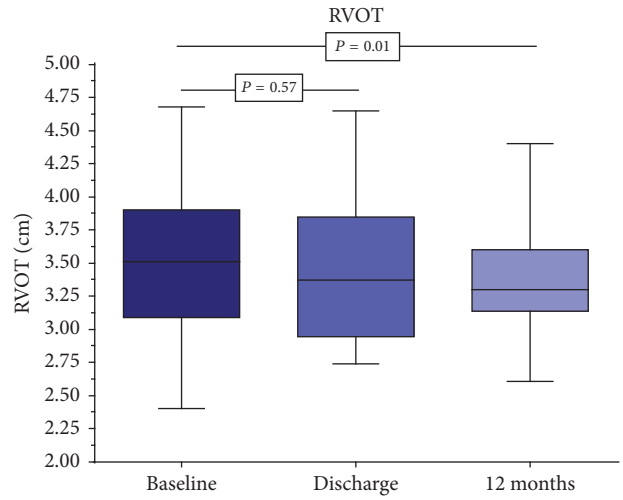

Figure 1: Significant decrease of right ventricular outflow tract (RVOT) diameter from 3.52 cm to 3.39 cm after twelve months.

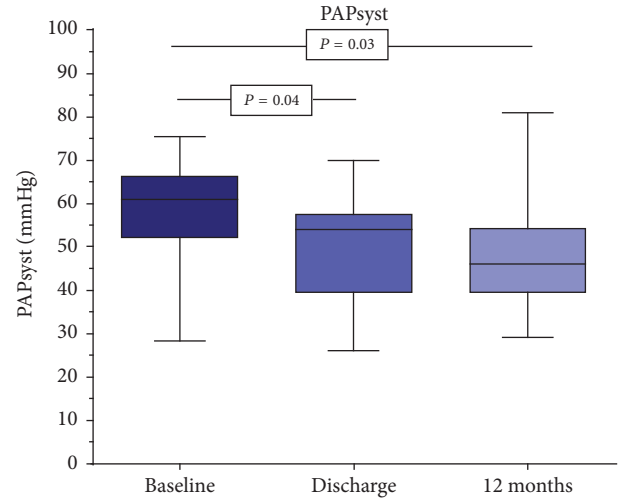

Figure 2: Decrease in systolic pulmonary artery pressure from 59 mmHg to 47 mmHg after twelve months.

from 16.5 mm to 18.1 mm was observed and to 18.9 mm after 12 months (Figure 3). However, statistically after one year, no difference existed between the measurements at the time of discharge and the representation of the patients after 12 months.

4. Discussion

Our results demonstrate that a significant reduction in systolic pulmonary artery pressure and the flow velocity of the tricuspid regurgitation follows immediately after successful MitraClip implantation. A Swiss research group observed a comparable immediate effect on the pulmonary artery pressure [22]. Both the pulmonary artery pressure and the flow reduced further during the 12-month follow-up observations. However, there was no longer any significant difference compared to the examination before dismissal. In addition, in

Table 2: All measured echocardiographic parameters are shown as median and interquartile range in brackets.

Variable	Baseline	Discharge	*P* value	12 months	*P* value
RVD1 (cm)	4.27 (3.84; 4.59)	4.47 (3.91; 4.63)	0.16	4.48 (3.94; 4.59)	0.20
RVD2 (cm)	2.40 (2.07; 2.78)	2.58 (2.21; 2.99)	0.14	2.45 (2.20; 2.71)	0.38
RVD3 (cm)	6.03 (5.38; 6.70)	6.08 (5.47; 6.66)	0.89	5.97 (5.30; 6.55)	0.36
RV area (cm^2)	19.8 (15.8; 23.4)	22.7 (17.0; 23.4)	0.39	19.7 (15.1; 22.1)	0.58
RAD (cm)	4.44 (3.88; 4.90)	4.45 (3.91; 4.80)	0.90	4.45 (4.00; 4.71)	0.71
RA area (cm^2)	25.0 (21.2; 28.3)	25.6 (20.7; 28.8)	0.35	24.9 (20.9; 27.8)	0.37
IVC diameter (cm)	1.84 (1.55; 2.12)	1.86 (1.39; 2.21)	0.68	1.99 (1.74; 2.30)	0.16
RVOT (cm)	3.52 (3.09; 3.90)	3.44 (2.95; 3.85)	0.57	3.39 (3.13; 3.60)	0.01
TADes (cm)	3.13 (2.81; 3.38)	3.11 (2.85; 3.41)	0.75	3.21 (2.99; 3.50)	0.31
TADed (cm)	3.95 (3.59; 4.30)	4.04 (3.78; 4.34)	0.15	4.03 (3.60; 4.30)	0.70
Vena contracta (cm)	0.88 (0.65; 1.02)	0.82 (0.59; 0.89)	0.06	0.77 (0.61; 0.93)	0.01
Vmax TR (m/s)	4.17 (3.51; 4.73)	3.11 (2.78; 3.42)	0.001	3.09 (2.77; 3.27)	0.001
Peak TR (mmHg)	48.5 (41.2; 56.0)	39.3 (30.8; 46.4)	0.001	38.6 (30.7; 42.5)	0.001
PAPsyst (mmHg)	58.6 (52.1; 66.3)	50.0 (39.5; 57.5)	0.04	47.4 (39.5; 54.3)	0.03
TR area (cm^2)	9.2 (4.9; 11.4)	9.0 (4.6; 11.3)	0.54	8.5 (5.0; 10.3)	0.69
TAPSE (mm)	16.5 (13.0; 20.1)	18.1 (15.0; 21.0)	0.002	18.9 (17.0; 21.3)	0.001

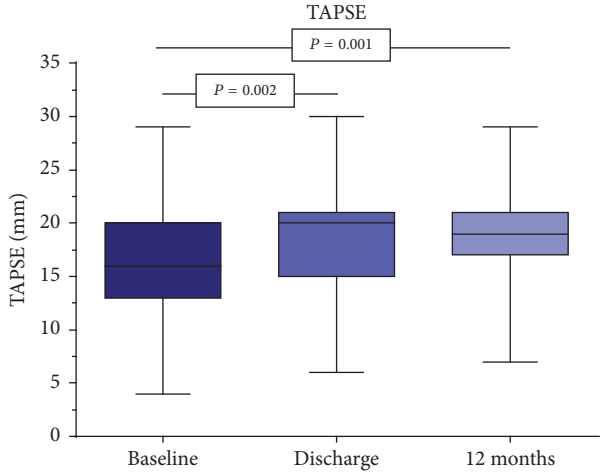

Figure 3: Increase of tricuspid annular plane systolic excursion (TAPSE) from 16.5 mm to 18.9 mm after 12 months.

our patient cohort, a significant increase of TAPSE occurred as a sign of improvement of the right ventricular contractility after successful MitraClip implantation. Giannini et al. could indicate a similar development in their group of patients in pulmonary artery pressure and TAPSE within a six-month observation period [23]. The pronounced reduction in pulmonary arterial pressure and the tricuspid regurgitation velocity and the increase in TAPSE, respectively, immediately after MitraClip implantation therefore most likely depend on smaller left ventricular or atrial regurgitation volumes after successful minimally invasive repair of the mitral valve and simultaneously reduced pressure load on the pulmonary circulation. Pulmonary vascular remodeling processes or adaptations requiring significantly more time appear to play no significant role in our patient group. These positive acute right ventricular changes are not concordant with the results of the EVEREST study [24]. No significant changes in either systolic or diastolic pulmonary artery pressure were observed immediately after MitraClip implantation there. This discrepancy can best be explained by a different composition of the patient cohort and study conditions. While in the EVEREST study primarily patients with a primary (degenerative) mitral regurgitation and very strict inclusion criteria regarding left ventricular function and left ventricular diameter and the valve morphology were enrolled [24–27], our cohort of patients consisted mainly of patients with secondary mitral regurgitation and a severely impaired left ventricular function with high NYHA classes. In addition, the hemodynamic measurements in the EVERST study were still collected during the general anesthesia necessary for the MitraClip implantation, so that here, in contrast to our patients who were examined after intervention in the waking state, there may be a possible reason for the different results. Patients with chronic reduced systolic LV ejection fraction who have abnormal TAPSE at baseline but reverse their RV dysfunction during follow-up by pharmacological optimization have better survival than patients with either worsened TAPSE or persistently abnormal TAPSE [28]. To what extent an improvement in TAPSE achieved by successful minimal invasive Mitral Valve Repair using MitraClip may lead to better long-term survival in our patient cohort as well is not known to date but is currently being analyzed. Preliminary data of our patients demonstrate similar results. In addition to the significant reductions or improvements experienced directly after the MitraClip intervention, comparably significant decreases in both the width of the vena contracta of the Tricuspid valve insufficiency and the diameter of the RVOT are brought about. A statistical significance of this reduction will only be reached after 12 months, so that the slower reduction is not immediately explicable with the decrease of pulmonary volume overload alone. In this case, it may have occurred during the postop observation time as a conversion/renaturation in the pulmonary circulation and

a positive remodeling of the right ventricle, which needs more time to develop fully. These observations relate to the results of two working groups, which showed no significant changes in RV diameter in a follow-up period of six months [23, 29]. With respect to a reduction of the width of the vena contracta, hemodynamic relief of the right ventricle and the diameter of the RVOT after six months appears to be so insufficient as to be statistically significant.

However, in contrast to the above parameters, no significant decrease of the remaining right ventricular and atrial diameters could be documented in our patient cohort, even in the extended follow-up period of twelve months. The width of the tricuspid valve ring and the diameter of the inferior vena cava did not change in our group either. The reason for this is not clear. To what extent an even longer follow-up period of two or more years would result in significant changes remains speculative and should be investigated by further multicenter long-term studies.

5. Conclusion

Mitral Valve Repair by MitraClip improves the pulmonary artery pressure and tricuspid regurgitation in preexisting secondary pulmonary hypertension after 12 months. At the same time, there is a decrease in the diameter of the right ventricular outflow tract without significant changes in other right ventricular and right atrial dimensions. The TAPSE as a sign of right ventricular function also improves significantly within the follow-up period.

Abbreviations

RV:	Right ventricle
LV:	Left ventricle
RA:	Right atrium
TV:	Tricuspid valve
IVC:	Inferior vena cava
TR:	Tricuspid regurgitation
PAPsyst:	Systolic pulmonary artery pressure
TAPSE:	Tricuspid annular plane systolic excursion
RVOT:	Right ventricular outflow tract
RD1:	Basal RV diameter
RD2:	Mid RV diameter
RD3:	RV base apex length
RAD:	Right atrium diameter
V_{max} TR:	Maximum velocity tricuspid regurgitation
Peak TR:	Peak pressure tricuspid regurgitation
TADes:	End-systolic tricuspid annular diameter
TADed:	End-diastolic tricuspid annular diameter.

Conflicts of Interest

The authors declare that they have no conflicts of interest.

References

[1] B. Iung, G. Baron, E. G. Butchart et al., "A prospective survey of patients with valvular heart disease in Europe: The Euro Heart Survey on valvular heart disease," *European Heart Journal*, vol. 24, no. 13, pp. 1231–1243, 2003.

[2] E. L. Hardegree, A. Sachdev, E. R. Fenstad et al., "Impaired left ventricular mechanics in pulmonary arterial hypertension identification of a cohort at high risk," *Circulation: Heart Failure*, vol. 6, no. 4, pp. 748–755, 2013.

[3] T. Le Tourneau, G. Deswarte, N. Lamblin et al., "Right ventricular systolic function in organic mitral regurgitation impact of biventricular impairment," *Circulation*, vol. 127, no. 15, pp. 1597–1608, 2013.

[4] B. A. Carabello, "The myocardium in mitral regurgitation: A tale of 2 ventricles," *Circulation*, vol. 127, no. 15, pp. 1567-1568, 2013.

[5] A. Chrustowicz, A. Gackowski, N. El-Massri, J. Sadowski, and W. Piwowarska, "Preoperative right ventricular function in patients with organic mitral regurgitation," *Journal of Echocardiography*, vol. 27, no. 3, pp. 282–285, 2010.

[6] R. O. Bonow, "Chronic mitral regurgitation and aortic regurgitation: have indications for surgery changed?" *Journal of the American College of Cardiology*, vol. 61, no. 7, pp. 693–701, 2013.

[7] S. A. Zakeri, R. Panayotova, A. N. Borg, C. A. Miller, and M. Schmitt, "Cardiovascular magnetic resonance validation of fractional changes in annulo-apical angles and tricuspid annular plane systolic excursion for rapid assessment of right ventricular systolic function," *Journal of Magnetic Resonance Imaging*, vol. 40, no. 1, pp. 133–139, 2014.

[8] R. M. Lang, L. P. Badano, V. Mor-Avi et al., "Recommendations for cardiac chamber quantification by echocardiography in adults: an update from the American Society of Echocardiography and the European Association of Cardiovascular Imaging," *European Heart Journal—Cardiovascular Imaging*, vol. 16, no. 3, pp. 233–271, 2015.

[9] S. Ghio, P. L. Temporelli, C. Klersy et al., "Prognostic relevance of a non-invasive evaluation of right ventricular function and pulmonary artery pressure in patients with chronic heart failure.," *European Journal of Heart Failure*, vol. 15, no. 4, pp. 408–414, 2013.

[10] T. Murashita, Y. Okada, H. Kanemitsu et al., "The impact of preoperative and postoperative pulmonary hypertension on long-term surgical outcome after mitral valve repair for degenerative mitral regurgitation," *Annals of Thoracic and Cardiovascular Surgery*, vol. 21, no. 1, pp. 53–58, 2014.

[11] A. Barbieri, F. Bursi, F. Grigioni et al., "Prognostic and therapeutic implications of pulmonary hypertension complicating degenerative mitral regurgitation due to flail leaflet: A Multicenter Long-term International Study," *European Heart Journal*, vol. 32, no. 6, pp. 751–759, 2011.

[12] Y. Ye, R. Desai, L. M. Vargas Abello et al., "Effects of right ventricular morphology and function on outcomes of patients with degenerative mitral valve disease," *The Journal of Thoracic and Cardiovascular Surgery*, vol. 148, no. 5, pp. 2012–2020.e8, 2014.

[13] M. Puls, T. Tichelbäcker, A. Bleckmann et al., "Failure of acute procedural success predicts adverse outcome after percutaneous edge-to-edge mitral valve repair with MitraClip," *EuroIntervention*, vol. 9, no. 12, pp. 1407–1417, 2014.

[14] W. Schillinger, T. Athanasiou, N. Weicken et al., "Erratum: Impact of the learning curve on outcomes after percutaneous mitral valve repair with MitraClip ® and lessons learned after the rst 75 consecutive patients (European Journal of Heart Failure (2011) 13 (1331-1339))," *European Journal of Heart Failure*, vol. 14, no. 6, p. 679, 2012.

[15] M. Enriquez-Sarano, A. Rossi, J. B. Seward, K. R. Bailey, and A. J. Tajik, "Determinants of pulmonary hypertension in left ventricular dysfunction," *Journal of the American College of Cardiology*, vol. 29, no. 1, pp. 153–159, 1997.

[16] F. L. Dini, U. Conti, P. Fontanive et al., "Right ventricular dysfunction is a major predictor of outcome in patients with moderate to severe mitral regurgitation and left ventricular dysfunction," *American Heart Journal*, vol. 154, no. 1, pp. 172–179, 2007.

[17] A. Vahanian, H. Baumgartner, J. Bax et al., "Guidelines on the management of valvular heart disease: the task force on the management of valvular heart disease of the European society of cardiology," *European Heart Journal*, vol. 28, no. 2, pp. 230–268, 2007.

[18] American College of Cardiology/American Heart Association Task Force on Practice Guidelines, Society of Cardiovascular Anesthesiologists, and Society for Cardiovascular Angiography and Interventions, "ACC/AHA 2006 guidelines for the management of patients with valvular heart disease: a report of the American College of Cardiology/American Heart Association Task Force on Practice Guidelines (writing committee to revise the 1998 Guidelines for the Management of Patients With Valvular Heart Disease): developed in collaboration with the Society of Cardiovascular Anesthesiologists: endorsed by the Society for Cardiovascular Angiography and Interventions and the Society of Thoracic Surgeons," *Circulation*, vol. 114, no. 5, pp. e84–e231, 2006.

[19] B. J. Kircher, R. B. Himelman, and N. B. Schiller, "Noninvasive estimation of right atrial pressure from the inspiratory collapse of the inferior vena cava," *American Journal of Cardiology*, vol. 66, no. 4, pp. 493–496, 1990.

[20] J. F. Aduen, R. Castello, M. M. Lozano et al., "An Alternative Echocardiographic Method to Estimate Mean Pulmonary Artery Pressure: Diagnostic and Clinical Implications," *Journal of the American Society of Echocardiography*, vol. 22, no. 7, pp. 814–819, 2009.

[21] N. Galie, M. M. Hoeper, and M. Humbert, "Guidelines for the diagnosis and treatment of pulmonary hypertension: the Task Force for the Diagnosis and Treatment of Pulmonary Hypertension of the European Society of Cardiology (ESC) and the European Respiratory Society (ERS), endorsed by the International Society of Heart and Lung Transplantation (ISHLT)," *European Heart Journal*, vol. 30, no. 20, pp. 2493–2537, 2009.

[22] O. Gaemperli, M. Moccetti, D. Surder et al., "Acute haemodynamic changes after percutaneous mitral valve repair: relation to mid-term outcomes," *Heart*, vol. 98, no. 2, pp. 126–132, 2012.

[23] C. Giannini, A. S. Petronio, M. De Carlo et al., "Integrated reverse left and right ventricular remodelling after MitraClip implantation in functional mitral regurgitation: An echocardiographic study," *European Heart Journal—Cardiovascular Imaging*, vol. 15, no. 1, pp. 95–103, 2014.

[24] R. J. Siegel, S. Biner, and A. M. Rafique, "The acute hemodynamic effects of MitraClip therapy," *Journal of the American College of Cardiology*, vol. 57, no. 16, pp. 1658–1665, 2011.

[25] T. Feldman, S. Kar, M. Rinaldi et al., "Percutaneous mitral repair with the MitraClip system: safety and midterm durability in the initial EVEREST (Endovascular Valve Edge-to-Edge REpair Study) cohort," *Journal of the American College of Cardiology*, vol. 54, no. 8, pp. 686–694, 2009.

[26] T. Feldman, H. S. Wasserman, H. C. Herrmann et al., "Percutaneous mitral valve repair using the edge-to-edge technique: Six-month results of the EVEREST phase I clinical trial," *Journal of the American College of Cardiology*, vol. 46, no. 11, pp. 2134–2140, 2005.

[27] T. Feldman, E. Foster, D. G. Glower et al., "Percutaneous repair or surgery for mitral regurgitation," *The New England Journal of Medicine*, vol. 364, no. 15, pp. 1395–1406, 2011.

[28] F. L. Dini, E. Carluccio, A. Simioniuc et al., "Right ventricular recovery during follow-up is associated with improved survival in patients with chronic heart failure with reduced ejection fraction," *European Journal of Heart Failure*, vol. 18, no. 12, pp. 1462–1471, 2016.

[29] A. C. M. J. Van Riel, K. Boerlage-Van Dijk, R. H. A. C. M. De Bruin-Bon et al., "Percutaneous mitral valve repair preserves right ventricular function," *Journal of the American Society of Echocardiography*, vol. 27, no. 10, pp. 1098–1106, 2014.

Hindawi
BioMed Research International
Volume 2018, Article ID 1981568, 10 pages
https://doi.org/10.1155/2018/1981568

Review Article

Current Knowledge and Recent Advances of Right Ventricular Molecular Biology and Metabolism from Congenital Heart Disease to Chronic Pulmonary Hypertension

Samantha Guimaron,[1] Julien Guihaire,[1,2] Myriam Amsallem,[1] François Haddad,[1,3] Elie Fadel,[1,4] and Olaf Mercier[1,4]

[1]*Research and Innovation Unit, RHU BioArt Lung 2020, Marie Lannelongue Hospital, Paris-Sud University, Le Plessis-Robinson, France*
[2]*Cardiac Surgery, Marie Lannelongue Hospital, Paris-Sud University, Le Plessis-Robinson, France*
[3]*Division of Cardiovascular Medicine, Stanford Cardiovascular Institute, Stanford University School of Medicine, Stanford, CA, USA*
[4]*Thoracic and Vascular Surgery and Heart and Lung Transplantation, Marie Lannelongue Hospital, Paris-Sud University, Le Plessis-Robinson, France*

Correspondence should be addressed to Julien Guihaire; julienguihaire@gmail.com

Received 1 September 2017; Accepted 20 December 2017; Published 17 January 2018

Academic Editor: Utako Yokoyama

Studies about pulmonary hypertension and congenital heart diseases have introduced the concept of right ventricular remodeling leading these pathologies to a similar outcome: right ventricular failure. However right ventricular remodeling is also a physiological process that enables the normal fetal right ventricle to adapt at birth and gain its adult phenotype. The healthy mature right ventricle is exposed to low pulmonary vascular resistances and is compliant. However, in the setting of chronic pressure overload, as in pulmonary hypertension, or volume overload, as in congenital heart diseases, the right ventricle reverts back to a fetal phenotype to sustain its function. Mechanisms include angiogenic changes and concomitant increased metabolic activity to maintain energy production. Eventually, the remodeled right ventricle cannot resist the increased afterload, leading to right ventricular failure. After comparing the fetal and adult healthy right ventricles, we sought to review the main metabolic and cellular changes occurring in the setting of PH and CHD. Their association with RV function and potential impact on clinical practice will also be discussed.

1. Introduction

Recent emphasis on pulmonary hypertension (PH) has underscored the need for a better knowledge of the right ventricle mainly because studies have shown that left ventricular (LV) failure pathophysiology cannot be extrapolated to the right ventricle [1, 2]. Right ventricular (RV) physiology in health and disease has been gained thanks to studies in patients with pulmonary hypertension (PH) [3] and congenital heart disease (CHD) [4–6]. Even if PH is still defined as dramatic changes in pulmonary hemodynamics with mean pulmonary arterial pressure (mPAP) $\geq$ 25 mmHg at rest [7], right ventricular (RV) function is known as the major factor of functional capacity and prognosis in PH. PH is a global entity regrouping many subsets with different etiologies. Regardless of PH etiology, chronic pressure overload results in RV remodeling and adaptation and eventually leads to dysfunction and death in absence of lung transplantation. In a study investigating the immediate prognosis of RV failure in PH patients, the overall mortality was 14% but rose to 46% for patients requiring inotropic support and 49% for patients in the intensive care unit [8]. On the other hand, the mortality associated with LV failure requiring inotropic support is usually lower than 15% [9, 10]. Similarly, Humbert et al. reported survival rates of 85,7% at 1 year, 69,6% at 2 years, and 54,9% at 3 years, in patients with WHO group I PH admitted for RV failure [11].

Right heart failure in patients with PH is the result of insufficient blood delivery to the heart and/or increased

systemic venous pressure secondary to elevated RV afterload represented by pulmonary arterial pressure or pulmonary vascular load [12]. The chronic RV pressure overload state results in myocardial remodeling, mainly characterized by a compensated hypertrophy. At the early stage, this adaptive right ventricle already presents with impaired bioenergetics, altered immunological response, and increased adrenergic response. This phenotype resembles the fetal RV phenotype; however, these adaptive mechanisms may lead to systolic dysfunction and cavities enlargement, representing the maladaptive right ventricle [13]. Clinical symptoms of peripheral edema, distended jugular veins, dyspnea, and syncope are consequences of increased filling pressures, diastolic dysfunction, and decreased cardiac output [3, 14, 15]. The transition from adaptive to maladaptive phenotype remains poorly understood and clinically unpredictable. Authors have been dividing this evolution into these 2 phenotypes, but there is a growing evidence for continuum between them: the adaptive right ventricle accumulates molecular and metabolic abnormalities until a point where it cannot overcome the persistent pressure overload and therefore becomes maladaptive.

Pulmonary arterial hypertension (PAH) associated with CHD belongs to group 1 of the WHO clinical classification of PH [7]. The evolution of this subset is characterized by dysfunction of the endothelial cells and hypertrophy and proliferation of the smooth muscle cells in the pulmonary circulation. Consequent obstruction of small arteries then occurs because of a narrowing of their diameter and plexiform lesions, the hallmark lesion of PAH. In this condition, pulmonary vascular resistances (PVR) progressively increase [16]. One of the difficulties to better appraise the natural history of RV failure is the variability of RV adaptation among patients exposed to chronic PH according to the etiology of PH. As an example, patients with PH related to untreated congenital cardiac defect or persistent ductus arteriosus may have a reversal of the left-to-right shunt, known as Eisenmenger syndrome. They tend to keep better RV function for a longer period and higher survival rate compared to patients with idiopathic PAH for a similar level of PVR and their survival is better [17–19]. Among the reasons to explain these different outcomes, the long-lasting fetal hypertrophied RV phenotype may prevent RV dilation and therefore its bowing towards the left ventricle. Second, persistent right to left shunts through septal defects enable tolerance of suprasystemic pulmonary hypertension [16].

The present review sought to summarize the current knowledge of RV metabolism and molecular physiology as studied in CHD and adult PH, in order to better understand RV failure associated with these diseases. After a brief overview of the fetal and adult right ventricle in health, we will review insights from experimental studies about pathophysiological evolution of RV remodeling in CHD and adult PH. Finally, we will develop the potential role of RV molecular biology and metabolism in the diagnosis, prognosis, and therapeutic approaches of RV dysfunction in PH. Inflammatory pattern of RV remodeling will be not described here as it has been recently well reviewed elsewhere [20, 21].

2. Right Ventricle in Health: From the Fetal Right Ventricle to the Adult Phenotype

2.1. Physiological Transition from the Fetal to the Adult Right Ventricle. The human heart originates from 3 main sources of cells: the first heart field, the second heart field and the neural crest cells. The first heart field gives the primitive left ventricle, a small part of the atria, and the atrioventricular canal myocardium resulting in the primary heart tube. The second heart field gives the complete right ventricle including the RV side of the ventricular septum and the RV outflow tract or pulmonary trunk. Finally, the neural crest cells participate in the constitution of the cardiac conduction system, as well as the RV outflow tract [22]. In utero, the right ventricle is not completely connected to the pulmonary circulation as it remains exposed to a high afterload and is not compliant. At this stage, the right ventricle plays the role of a systemic ventricle because of high PVR and low systemic vascular resistance in the placental circulation [22]. At birth, with the first breaths, fetal lung fluid is evacuated, partial O_2 pressure increases, both creating an air-liquid interface, and ventilation occurs. These events result in increased shear stress in the pulmonary circulation leading to vasodilation secondary to the release of vasodilators, such as prostacyclin and nitric oxide, and decreased secretion of vasoconstrictors, such as endothelin-1. Since the placental circulation in utero is under high PVR and low systemic vascular resistance, clamping the umbilical cord at birth will therefore separate the newborn from the low resistance placental circulation, leading to a decrease in PVR and increase in systemic vascular tone. Concomitantly, patent ductus arteriosus progressively closes leading the right ventricle to eject only in the pulmonary arterial tree. As a result of these events occurring at birth, RV wall thickness progressively decreases and LV mass increases [22, 23]. This physiological transition occurs with important molecular, structural, and functional changes. Eventually, the right ventricle becomes more compliant and gains its adult phenotype, with normal relation and interdependence to the left ventricle.

2.2. Features of the Normal Fetal Right Ventricle. The fetal right ventricle is exposed to a low oxygen environment. Carbohydrates substrates are preferentially used to produce energy from the glycolytic pathway such as glucose, lactate, and pyruvate. The major signaling pathway expressed is the hypoxia inducible factor 1α (HIF1α) and vascular endothelial growth factor (VEGF) pathway, promoting angiogenesis. It is associated with upregulated glycolysis. Both of these mechanisms lead the fetal right ventricle to better tolerate hypoxia compared to the adult right ventricle [19, 22–24]. Moreover, because of patent ductus arteriosus, the fetal right ventricle is more sensitive to systemic vascular resistances than to PVR. Fisher et al. studied regional blood flow in fetal ($n = 16$), newborn ($n = 12$), and adult ($n = 9$) sheep, using radionuclide-labeled microsphere imaging [25]. He observed in all fetal lambs that regional blood flow was significantly higher in the right ventricular free wall compared to the left ventricular free wall, respectively, 213 ± 13 ml/min versus 162 ± 12 ml/min ($p < 0.001$). Similarly, the right side of the

Table 1: Main characteristics of healthy phenotypes of fetal and adult right ventricles.

Characteristics	Fetal phenotype	Adult phenotype
Environment		
Oxygen environment	Low	High
Main blood circulation	Placental circulation	Systemic circulation
Ductus arteriosus	Opened	Closed
PVR	High	Low
Main vascularized heart regions	Right ventricular free wall, Right side of the IVS	Left ventricular free wall, Left side of the IVS
Systemic ventricle	Right ventricle	Left ventricle
Genetics		
Gene pattern expression	β-MHC	α-MHC
Metabolic features		
Mitochondrial function	Normal/adapted	Normal/adapted
mROS production	Adapted to heart activity	Adapted to heart activity
Energetic substrates	Carbohydrates	Fatty acids
Hypoxia-induced factors (i) HIF1α (ii) VEGF	Expressed	Not expressed
Ca^{2+} homeostasis	Immature	Mature
Cellular features		
Myocytes diameter	5–7 μm	15–25 μm
Myocytes/nonmyocytes ratio	30%	70%
Sarcomeres	Disoriented	Parallel
Capillary density	Preserved	Preserved
Fibrosis	Absent	Absent

PVR: pulmonary vascular resistance; MHC: myosin heavy chain; mROS: mitochondrial reactive oxygen species; HIF-1α: hypoxia inducible factor 1 alpha; VEGF: vascular endothelial growth factor; Ca^{2+}: calcium.

interventricular septum had a higher blood flow compared to the left side, respectively, 190 ± 13 ml/min versus 147 ± 12 ml/min ($p < 0.05$) [25]. Finally, microscopic features of the fetal right ventricle include small myocytes ranging from 5 to 7 μm, a predominance of 70% of noncontractile mass represented of nuclei, cell membranes and mitochondria (30% of cardiomyocytes) [4], and disoriented sarcomeres with immature calcium homeostasis (Ca^{2+} pumps and transporters) and therefore immature contractility with genetic expression of β-myosin heavy chain (β-MHC) [24, 26, 27].

2.3. Features of the Normal Adult Right Ventricle. The adult right ventricle is exposed to a high oxygen environment with the adapted metabolic pathway including fatty acids oxidation, which produces more ATP than glycolysis [24]. Depending on injury or stress, there is an adaptation of metabolic substrates from fatty acids to glucose oxidation known as the Randle cycle. The HIF1α-angiogenesis signaling pathway and the glycolytic phenotype are no longer expressed in these conditions. In fact there are adult isoforms of enzymes such as pyruvate dehydrogenase kinase (PDK), especially the cardiac specific PDK4, which are responsible for glycolysis inhibition and promotion of glucose oxidation [21, 28]. In their study [25], Fisher et al. reported that, after birth, regional blood flow was higher in the left ventricular free wall compared to the right ventricular free wall, respectively, 204 ± 18 ml/min versus 140 ± 15 ml/min ($p < 0.01$). They explained this reversal in blood flow delivery by a change in oxygen requirements occurring after birth. In fact, because of the dramatic fall of PVR after birth, and therefore the decrease in right ventricular afterload, there is a major decrease in oxygen requirements for the right ventricle, with increased oxygen needs for the left ventricle being exposed to high systemic pressure [25]. Considering cellular features, myocytes are larger (from 15 to 25 μm), sarcomeres are parallel, Ca^{2+} homeostasis is mature, and β-MHC gene is expressed [26], leading to a more efficient contractility [4, 27]. Table 1 summarizes the main differences between the normal fetal right ventricle and the normal adult right ventricle.

3. The Parallel between RV Remodeling in Pulmonary Hypertension and Congenital Heart Disease

3.1. Insights of Right Heart Failure in CHD. In conditions such as tetralogy of Fallot, surgically and congenitally corrected transposition of the great vessels, Ebstein anomaly, or late Fontan circulation, RV dysfunction is frequent because the right ventricle is chronically exposed to pressure overload. In the early phases, the right ventricle responds to increased

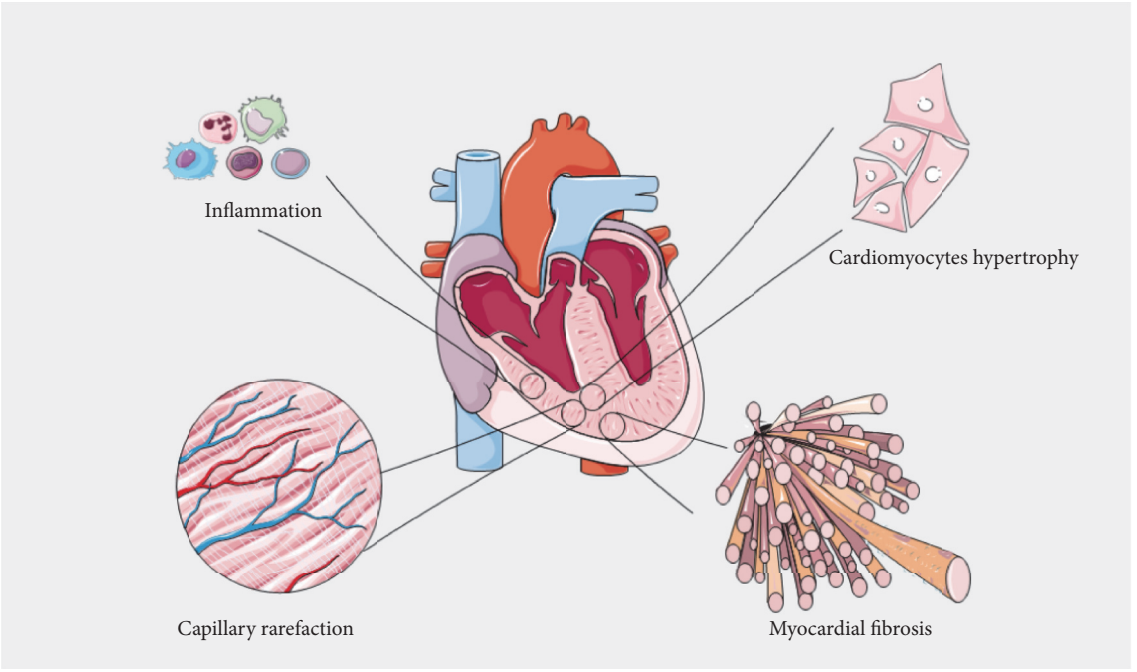

Figure 1: Main histological patterns of right ventricular remodeling in the setting of chronic pressure overload. Inflammation involving mononuclear cells and cardiomyocytes hypertrophy are observed at the early stage. Reduced capillary density and myocardial fibrosis are associated with right ventricular maladaptive phenotype.

wall stress with RV hypertrophy. It carries the role of a systemic ventricle characterized by coarse trabeculation, hypertrophied muscular band, and an abnormal septal tricuspid leaflet [29]. It increases its mitochondrial activity and carbohydrates use for energy production. Long-term evolution is characterized by substrates deprivation and energy loss. In addition, tricuspid regurgitation (congenitally corrected transposition of the great vessels and Ebstein anomaly), pulmonary regurgitation (Tetralogy of Fallot and RV dilation), and arrhythmias may occur [5]. Reasons for these evolution are multiple [29]. First of all, the right ventricle is characterized by a longitudinal contractile pattern compared to the circumferential pattern of the left ventricle (both radial and longitudinal). That makes the right ventricle unable to have a twisting and torsion component necessary to deal with high pressure overload. Second, RV tissue samples obtained in surgical CHD have shown decreased angiogenesis and marked fibrosis associated with arrhythmia, decreased RV ejection fraction, and increased RV wall stress [29, 30]. Third, studies showed that the hypertrophied right ventricle, because of its increased mass, has an impaired coronary flow and is therefore exposed to ischemia [19, 29, 30]. Finally, metabolic events include accumulation of mitochondrial reactive oxygen species (mROS) and of p53 protein responsible for HIF-1α signaling pathway inhibition and ventricular dilation as reported by Sano et al. in a mice model of transverse aortic constriction. At 14 days, maximum hypertrophy was reached, followed by loss of microvessels, ventricular dilation, and failure. When these mice were p53 knocked out, ventricular hypertrophy was sustained with high number of microvessels [31]. Another molecular feature has been described by Wu et al. on RV tissues from children with tetralogy of Fallot, hypoxia and hypertrophy (HH group), pulmonary stenosis, hypertrophy (H group), and small isolated ventricular septal defect compared to a control group. They reported that contractile dysfunction was linked to increased mROS associated with the decreased mRNA expression of a Ca^{2+}-regulatory protein responsible for calcium homeostasis, as known as sarcoplasmic reticulum Ca^{2+}-ATPase 2a (SERCA2a) [27].

3.2. Insights into Right Heart Failure in PH. Numerous experimental studies of RV remodeling in the setting of PH have been conducted in rodents including the fawn-hooded rat model [32] and then in the pulmonary arterial banding model, the hypoxia-induced PH [33], the angioproliferative PH, and the monocrotaline models [19]. The main histological features of RV tissular remodeling are summarized in Figure 1. Two phenotypes are usually described: "adaptive" versus "maladaptive" RV remodeling, or "compensated" RV hypertrophy (cRDVH) versus "decompensated" RV hypertrophy (dRDVH). That has been well described by Sutendra et al. especially by comparing baseline animals versus cRVH and dRVH in the same animals over time [19, 28, 34].

cRHV is characterized by numerous normal shaped hyperpolarized mitochondria, with low but continuous production of mROS, which does not allow p53 protein expression. This state is associated with high expression of HIF-1α pathway, increased levels of glucose transporter Glut-1, PDK4 enzyme, and therefore glucose uptake. These changes are responsible for a switch from a mitochondria-based glucose oxidation to a glycolytic status, as well as increased

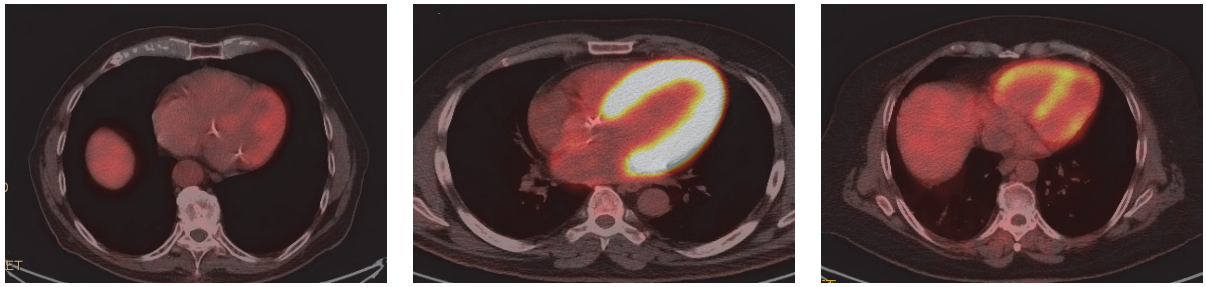

Control (a) Aortic valve sclerosis (b) CTEPH (c)

Figure 2: 18-Fluorodeoxyglucose Positron Emission Tomography in a control healthy patient (a), in a patient with aortic valve sclerosis (b), and in a chronic thromboembolic pulmonary hypertension patient (CTEPH) (c). Images show 4 chambers views. Control imaging shows no right ventricular uptake, but presence of left ventricular uptake. Picture (b) shows increased glucose uptake localized on the left ventricular free wall and on the interventricular septum in a patient with marked hypertrophy of the left ventricle due to aortic sclerosis.

angiogenesis/VEGF expression [19]. Progressively accumulation of mROS leads to reduced number of mitochondria, sometimes clustered together, and usually with abnormal shapes and sizes [33, 35]. Finally, energy supply is insufficient with substrates deprivation and therefore dRHV. Activation of p53 protein and inhibition of HIF1α are key elements resulting in decreased angiogenesis and are associated with decreased PDK expression and glucose uptake leading to a reversed glycolytic shift. This last element was reflected by ^{18}Fluorodeoxyglucose Positron Emission Tomography (^{18}FDG-PET) showing increased glucose uptake in cRVH and reverse uptake in dRVH. In summary, a protective glycolytic shift appears to be associated with cRVH and reversed in dRVH because of excessive oxidative stress, substrates starvation, and mitochondrial loss of function [19, 34].

Concomitant of metabolic features, impaired angiogenesis is crucial in the pathology. Because of increased RV wall stress, myocardial oxygen consumption increases and therefore leads to loss of microvessels and reduced right coronary artery perfusion pressure (below 50 mmHg). This leads to an increased RV mass without compensatory angiogenesis and therefore results in ischemia [14, 36, 37]. Gómez et al. studied RV ischemia in patients with primary PH using stress technetium 99 m myocardial scintigraphy. RV ischemia was significantly correlated to increased RV end-diastolic pressure and increased right atrial pressure [14]. Bogaard et al. compared an isolated RV pressure overloaded rodent model (pulmonary arterial banding) versus a model with progressive pressure overload due to angioproliferative PH secondary to hypoxia and VEGF receptors blockage. In the context of angioproliferative PH, RV failure occurred with apoptosis, fibrosis, decreased VEGF gene and protein expressions, and decreased RV capillary density [36]. Finally, Tian et al. recently showed that RV ischemia causes mitochondrial-mediated fission that was responsible for diastolic dysfunction. When inhibiting mitochondrial fission, they showed a preserved RV function [38]. It is important to acknowledge that molecular and metabolic changes are a continuous process, starting as early as cRVH or "adaptive" RV remodeling. The precise role of the glycolytic shift, either protective or detrimental, remains a matter of debate and requires further investigations. Table 2 summarizes characteristics of RV remodeling in CHD and PH. Figure 3 depicts evolution of RV failure in CHD and PH.

Recent emphasis has been observed about the concept of right ventricular-pulmonary arterial (RV-PA) coupling as a relevant marker of cardiac performance and energetics for the right ventricle. It represents the maximal efficiency between stroke work and myocardial oxygen consumption. RV-PA coupling can be assessed using pressure-volume loops as the ratio between RV end-systolic elastance (Ees) and pulmonary arterial elastance (Ea) [2, 39]. Ventricular-arterial uncoupling is defined as Ees/Ea ratio below 1. At the early stage of PH, RV-PA coupling may be decreased, despite preserved RV function and increased contractility. When the elevated afterload is too high, RV stroke volume and RV ejection fraction decrease. Uncoupling therefore occurs, followed by RV dilation and failure [2, 40, 41]. Because pressure-volume loops assessment is invasive and time-consuming and may be dangerous for PH patients because of the need for transient but repeated occlusions of the inferior vena cava, this remains dedicated to experimental studies.

4. Clinical Perspectives

4.1. What Do RV Metabolic and Molecular Features Add to the Diagnosis of PH Related RV Dysfunction? The glycolytic shift associated with RV remodeling is characterized by an upregulation of glucose uptake, shown by the increased uptake of ^{18}FDG-PET [19, 37, 42, 43]. Figure 2 illustrates the hypermetabolism of hypertrophied RV observed in PH patients. Glucose uptake has been correlated with invasive PVR, mean pulmonary artery pressure, right atrial pressure, and RV wall stress [24, 44]. In addition, Lundgrin et al. showed the correlation between 18-FDG uptake and echocardiographic markers of systolic dysfunction (i.e., altered TAPSE, dilated RV, and RV fraction area change) and HIF-1α activation [45].

Brittain et al. hypothesized that alterations of FA metabolism were due to a decrease in FA oxidation. They focused on FA in blood samples, RV tissue samples, and their

Table 2: Common features of functional and dysfunctional remodeled right ventricles in congenital heart disease and pulmonary hypertension.

Characteristics	Functional remodeled right ventricle	Dysfunctional remodeled right ventricle
Morphology		
Chambers size	Normal	Dilated (i.e., RV/LV > 0,6)
Free wall thickness	Thick (>5 mm)	Thin
IVS motion	Normal	End-diastolic bowing in the left ventricle
Pericardial effusion	Absent or minimal	Moderate to important
CHD common features	Coarse trabeculation Hypertrophied and muscular moderator band Abnormal tricuspid septal leaflet insertion (mitral valve proximity)	
Function		
RVEF	Preserved	Decreased
Contractility	Hypercontractility	Decreased
Cardiac index	Preserved	Decreased Bad prognosis < 2 l/min/m^2
RV-arterial coupling	Preserved	Uncoupling
Rhythm	Mostly preserved	Arrhythmias
CHD common features	Tricupid and pulmonary regurgitations prior to dilation	
Metabolic features		
Mitochondria	Adapted sizes and shapes	Small, abnormal shapes, clustered
Mitochondrial function	Increased	Decreased
mROS production	Continuous and Low	High accumulation
Signaling pathway	Down-regulation of p53 Up-regulation of HIF1α-VEGF pathway	Up-regulation of p53 Inhibition of HIF1α-VEGF pathway
Energetic substrates	Carbohydrates > fatty acids High use of PDK4, Glut1 = glycolytic shift	Total substrates deprivation Energy starvation = reversed glycolytic shift
Cellular and Tissular features		
Myocytes	Hypertrophied	?
Capillary density	Increased	Rarefaction
Ischemia	Present With role of CHD-associated coronary malformations	Present
Fibrosis	Absent	Present

IVS: inter entricular septum; RVEF: right ventricular ejection fraction; CHD: congenital heart disease; RV-arterial coupling: right ventricular arterial coupling; mROS: mitochondrial reactive oxygen species; p53: p53 protein; HIF-1α: hypoxia inducible factor 1 alpha; VEGF: vascular endothelial growth factor; PDK4: pyruvate dehydrogenase kinase 4; Glut1: glucose transporter 1.

association with proton magnetic resonance spectroscopy. They observed increased levels of FA in the blood stream and in RV tissue samples. These findings were associated with cardiac steatosis and lipotoxicity on spectroscopy [46]. Studies investigating oxidative stress showed the key role of continuous mROS accumulation over time in the evolution of the pathology [19].

4.2. What Do RV Metabolic and Molecular Features Add to the Prognosis of PH Related RV Dysfunction? The glycolytic shift observed in animal models of PH might be a marker for RV remodeling. Authors have studied PET imaging in PH patients in order to find a prognostic value of the observed metabolic changes. As previously mentioned, correlations between glucose uptake seen using 18FDG-PET imaging and hemodynamic have been reported, as well as association with echocardiographic findings and functional parameters such as the 6-minute walking test and NYHA status [47–49]. Moreover, there is evidence for the additional value of metabolic imaging for long-term follow-up of PH patients under treatment. Changes in FDG uptake over time seem to be related to varying expression of proangiogenic factors and different degrees of HIF-1α activation [45, 50]. Recently, Li et al. studied 45 patients with idiopathic PAH using PET imaging during fasting and glucose-loading conditions. They reported that increased RV to LV 18-FDG uptake ratio significantly predicted mortality [51]. These clinical findings therefore agree on the fact that PET imaging enables strong association between metabolism, mass, and RV function. Finally, in an ongoing clinical trial conducted by our team,

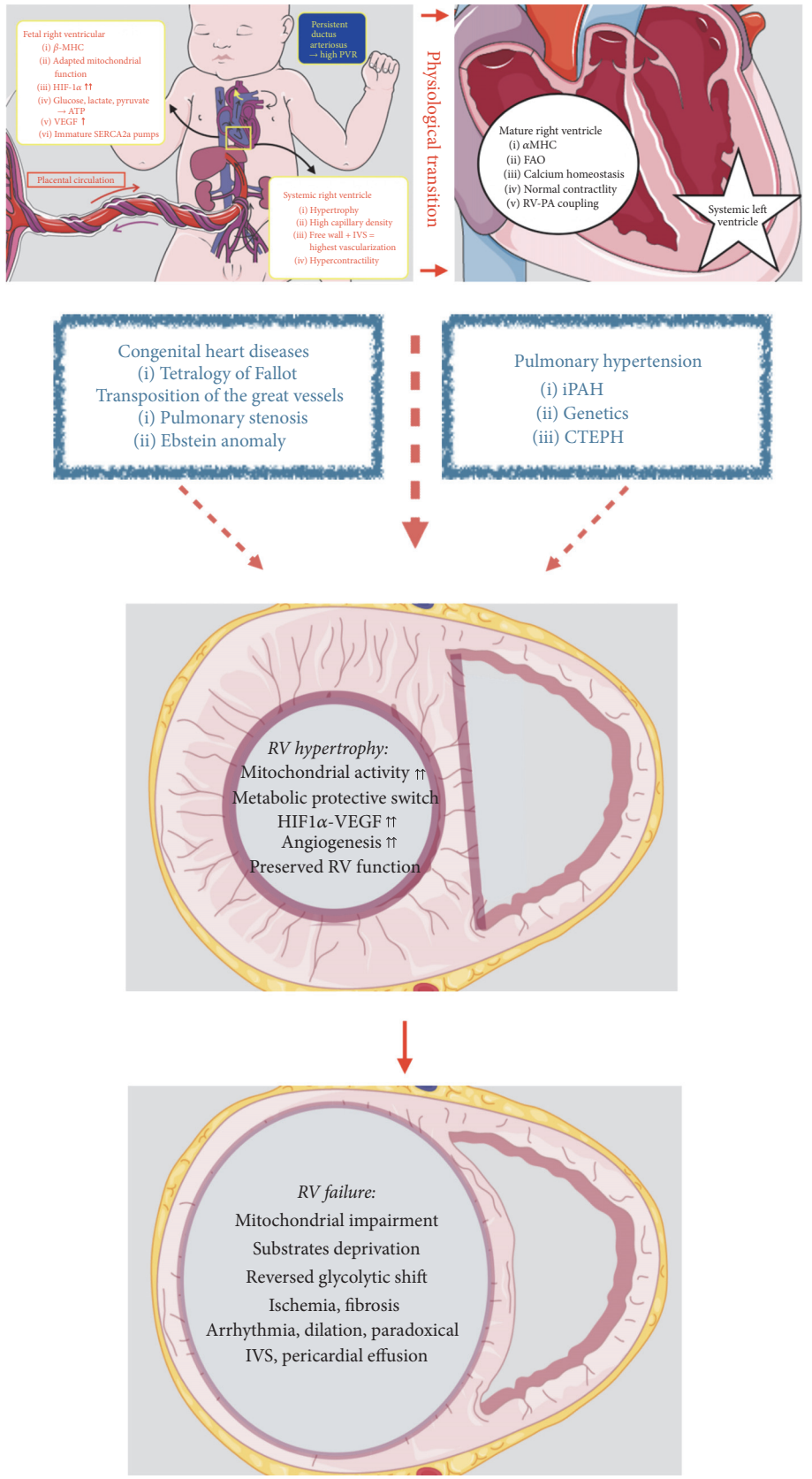

Figure 3: Right ventricular remodeling in congenital heart disease and pulmonary hypertension. βMHC: β-myosin heavy chain; HIF1α: hypoxia inducible factor 1α; VEGF: vascular endothelial growth factor; SERCA2a: sarcoplasmic/endoplasmic reticulum Ca2+ ATPase 2a; IVS: interventricular septum; αMHC: α-myosin heavy chain; FAO: fatty acids oxidation; RV-PA coupling: right ventricular-pulmonary arterial coupling; PVR: pulmonary vascular resistances; RV: right ventricular; iPAH: idiopathic pulmonary arterial hypertension; CTEPH: chronic thromboembolic pulmonary hypertension.

we have been able to see significant correlations between decreased capillary density in human RV tissues and altered RV function (assessed by CMR and echocardiography) in the setting of chronic thromboembolic PH, as well as correlations with PET imaging.

4.3. What Do RV Metabolic and Molecular Features Add to Therapeutic Strategies of PH Related RV Dysfunction? Phosphodiesterase-5, endothelin inhibitors, and prostaglandin D2 (PGD2) agonists have been shown to reduce RV pressure overload in patients with PH. However, their effects on the right ventricle are poorly explored. Authors hypothesized that myocardial substrates usage (such as glucose oxidation) can be modulated with pharmacologic inhibitors [24, 52]. Piao et al. studied the effect of PDK inhibitor, dichloroacetate, in two rat models of RV hypertrophy: monocrotaline-induced PH and pulmonary artery banding without PH. In the first model, dichloroacetate increased glucose oxidation and cardiac stroke work. Long-term use showed improved RV function. In RV compensated hypertrophy induced by pulmonary artery banding, the glycolytic shift could be reversed with dichloroacetate as well. These effects of dichloroacetate were greater in monocrotaline-induced RV hypertrophy associated with PH. Dichloroacetate might therefore correct vascular changes and RV remodeling [42]. These findings suggest that glycolysis is not detrimental for the overload right ventricle. Similarly, the same authors showed that long-term use of dichloroacetate inhibited FOXO1, a transcriptional regulatory factor of PDK. Consequent downregulation of PDK 4 (an isoform of PDK) restored glucose oxidation and improved bioenergetics and RV function [53].

The link between RV remodeling and fatty acid oxidation (the main energy source in healthy adult myocardium) still remains unclear. Fang et al. used partial inhibitors of FA oxidation such as ranolazine and trimetazidine in experimental pulmonary artery banding. They reported abnormal levels of FA oxidation with reduced RV function at baseline. Under ranolazine and trimetazidine treatment, they reported decreased FA oxidation and restored glucose oxidation resulting in increased cardiac output and improved exercise capacity [54]. Another metabolic-oriented therapy, as described earlier, which might be targeting mROS production with p53 protein inhibition might be an alternative [27]. Finally, beneficial effects might be possible by modulating mi-RNA expression in the heart in CHD or in the pulmonary arteries in PAH [6].

5. Conclusion

RV adaptation to pressure overload is a key determinant of survival in patients with PH and CHD. RV failure occurring in these conditions has similar features such as glycolytic shift and altered angiogenesis. A relationship between metabolic changes and RV function is strongly supported by recent experimental findings. Translational approaches of RV metabolism as well as noninvasive assessment of RV-PA coupling are needed to better discriminate the RV phenotype in the setting of chronic pressure overload. Pharmacological support to modulate RV energetics and to restore RV capillary density might be promising approaches to improve the condition of PH patients.

Conflicts of Interest

The authors declare that there are no conflicts of interest regarding the publication of this paper.

Acknowledgments

This work was supported by a public grant overseen by the French National Research Agency (ANR) as part of the second Investissements d'Avenir Program (Reference ANR-15-RHUS-0002).

References

[1] J. Guihaire, H. Bogaard, E. Flécher et al., "Experimental models of right heart failure: a window for translational research in pulmonary hypertension," *Seminars in Respiratory and Critical Care Medicine*, vol. 34, no. 5, pp. 689–699, 2013.

[2] J. Guihaire, P. E. Noly, S. Schrepfer, and O. Mercier, "Advancing knowledge of right ventricular pathophysiology in chronic pressure overload: Insights from experimental studies," *Archives of Cardiovascular Diseases*, vol. 108, no. 10, pp. 519–529, 2015.

[3] N. F. Voelkel, R. A. Quaife, L. A. Leinwand et al., "Right ventricular function and failure: report of a National Heart, Lung, and Blood Institute working group on cellular and molecular mechanisms of right heart failure," *Circulation*, vol. 114, no. 17, pp. 1883–1891, 2006.

[4] W. F. Friedman, "The intrinsic physiologic properties of the developing heart," *Progress in Cardiovascular Diseases*, vol. 15, no. 1, pp. 87–111, 1972.

[5] L. Lopez, M. S. Cohen, R. H. Anderson et al., "Unnatural history of the right ventricle in patients with congenitally malformed hearts," *Cardiology in the Young*, vol. 20, supplement 3, pp. 107–112, 2010.

[6] D. Iacobazzi, M.-S. Suleiman, M. Ghorbel, S. J. George, M. Caputo, and R. M. Tulloh, "Cellular and molecular basis of RV hypertrophy in congenital heart disease," *Heart*, vol. 102, no. 1, pp. 12–17, 2016.

[7] N. Galie, M. Humbert, J. L. Vachiery et al., "2015 ESC/ERS Guidelines for the diagnosis and treatment of pulmonary hypertension: the joint task force for the diagnosis and treatment of pulmonary hypertension of the european society of cardiology (ESC) and the european respiratory society (ERS)," in *European Heart Journal*, Association for European Paediatric and Congenital Cardiology (AEPC) and International Society for Heart and Lung Transplantation (ISHLT), Eds., vol. 37, pp. 67–119, 2016.

[8] B. Sztrymf, R. Souza, L. Bertoletti et al., "Prognostic factors of acute heart failure in patients with pulmonary arterial hypertension," *European Respiratory Journal*, vol. 35, no. 6, pp. 1286–1293, 2010.

[9] W. T. Abraham, K. F. Adams, G. C. Fonarow et al., "In-hospital mortality in patients with acute decompensated heart failure requiring intravenous vasoactive medications: an analysis from the acute decompensated heart failure national registry (ADHERE)," *Journal of the American College of Cardiology*, vol. 46, no. 1, pp. 57–64, 2005.

[10] J. J. Ryan and S. L. Archer, "The right ventricle in pulmonary arterial hypertension: disorders of metabolism, angiogenesis

and adrenergic signaling in right ventricular failure," *Circulation Research*, vol. 115, no. 1, pp. 176–188, 2014.

[11] M. Humbert, O. Sitbon, A. Chaouat et al., "Survival in patients with idiopathic, familial, and anorexigen-associated pulmonary arterial hypertension in the modern management era," *Circulation*, vol. 122, no. 2, pp. 156–163, 2010.

[12] A. Vonk-Noordegraaf, F. Haddad, K. M. Chin et al., "Right heart adaptation to pulmonary arterial hypertension: physiology and pathobiology," *Journal of the American College of Cardiology*, vol. 62, no. 25, pp. D22–D33, 2013.

[13] M. Amsallem, T. Kuznetsova, K. Hanneman, A. Denault, and F. Haddad, "Right heart imaging in patients with heart failure: a tale of two ventricles," *Current Opinion in Cardiology*, vol. 31, no. 5, pp. 469–482, 2016.

[14] A. Gómez, D. Bialostozky, A. Zajarias et al., "Right ventricular ischemia in patients with primary pulmonary hypertension," *Journal of the American College of Cardiology*, vol. 38, no. 4, pp. 1137–1142, 2001.

[15] A. Vonk Noordegraaf and N. Galiè, "The role of the right ventricle in pulmonary arterial hypertension," *European Respiratory Review*, vol. 20, no. 122, pp. 243–253, 2011.

[16] J. Guihaire, F. Haddad, O. Mercier, D. J. Murphy, J. C. Wu, and E. Fadel, "The right heart in congenital heart disease, mechanisms and recent advances," *Journal of Clinical & Experimental Cardiology*, vol. 1, no. 8, pp. 1–11, 2012.

[17] W. E. Hopkins, L. L. Ochoa, G. W. Richardson, and E. P. Trulock, "Comparison of the hemodynamics and survival of adults with severe primary pulmonary hypertension or Eisenmenger syndrome," *The Journal of Heart and Lung Transplantation*, vol. 15, no. 1 I, pp. 100–105, 1996.

[18] B. Rondelet, C. Dewachter, F. Kerbaul et al., "Prolonged overcirculation-induced pulmonary arterial hypertension as a cause of right ventricular failure," *European Heart Journal*, vol. 33, no. 8, pp. 1017–1026, 2012.

[19] G. Sutendra, P. Dromparis, R. Paulin et al., "A metabolic remodeling in right ventricular hypertrophy is associated with decreased angiogenesis and a transition from a compensated to a decompensated state in pulmonary hypertension," *Journal of Molecular Medicine*, vol. 91, no. 11, pp. 1315–1327, 2013.

[20] N. F. Voelkel, J. Gomez-Arroyo, A. Abbate, H. J. Bogaard, and M. R. Nicolls, "Pathobiology of pulmonary arterial hypertension and right ventricular failure," *European Respiratory Journal*, vol. 40, no. 6, pp. 1555–1565, 2012.

[21] J. J. Ryan and S. L. Archer, "Emerging concepts in the molecular basis of pulmonary arterial hypertension. Part I: metabolic plasticity and mitochondrial dynamics in the pulmonary circulation and right ventricle in pulmonary arterial hypertension," *Circulation*, vol. 131, no. 19, pp. 1691–1702, 2015.

[22] N. F. Voelkel, "The right ventricle in health and diseas," *Respiratory Medicine*, 2015.

[23] R. G. Kelly, "Building the right ventricle," *Circulation Research*, vol. 100, no. 7, pp. 943–945, 2007.

[24] S. E. Altin and P. C. Schulze, "Metabolism of the right ventricle and the response to hypertrophy and failure," *Progress in Cardiovascular Diseases*, vol. 55, no. 2, pp. 229–233, 2012.

[25] D. J. Fisher, M. A. Heymann, and A. M. Rudolph, "Regional myocardial blood flow and oxygen delivery in fetal, newborn, and adult sheep," *American Journal of Physiology-Heart and Circulatory Physiology*, vol. 243, no. 5, pp. H729–H731, 1982.

[26] B. D. Lowes, W. Minobe, W. T. Abraham et al., "Changes in gene expression in the intact human heart: downregulation of α-myosin heavy chain in hypertrophied, failing ventricular myocardium," *The Journal of Clinical Investigation*, vol. 100, no. 9, pp. 2315–2324, 1997.

[27] Y. Wu, W. Feng, H. Zhang et al., "Ca 2+-regulatory proteins in cardiomyocytes from the right ventricle in children with congenital heart disease," *Journal of Translational Medicine*, vol. 10, no. 1, article 67, 2012.

[28] P. Dromparis, G. Sutendra, and E. D. Michelakis, "The role of mitochondria in pulmonary vascular remodeling," *Journal of Molecular Medicine*, vol. 88, no. 10, pp. 1003–1010, 2010.

[29] S. Shah, T. Gupta, and R. Ahmad, "Managing heart failure in transposition of the great arteries," *The Ochsner Journal*, vol. 15, no. 3, pp. 290–296, 2015.

[30] E. Di Pietro, M. C. De Angelis, F. Esposito et al., "An imbalance between protective and detrimental molecular pathways is associated with right ventricular dysfunction in congenital heart diseases with outflow obstruction," *International Journal of Cardiology*, vol. 172, no. 3, pp. e519–e521, 2014.

[31] M. Sano, T. Minamino, H. Toko et al., "p53-induced inhibition of Hif-1 causes cardiac dysfunction during pressure overload," *Nature*, vol. 446, 2007.

[32] S. Bonnet, E. D. Michelakis, C. J. Porter et al., "An Abnormal mitochondrial-hypoxia inducible factor-1α-Kv channel pathway disrupts oxygen sensing and triggers pulmonary arterial hypertension in fawn hooded rats: Similarities to human pulmonary arterial hypertension," *Circulation*, vol. 113, no. 22, pp. 2630–2641, 2006.

[33] J. Gomez-Arroyo, S. Mizuno, K. Szczepanek et al., "Metabolic gene remodeling and mitochondrial dysfunction in failing right ventricular hypertrophy secondary to pulmonary arterial hypertension," *Circulation: Heart Failure*, vol. 6, no. 1, pp. 136–144, 2013.

[34] G. Sutendra, P. Dromparis, A. Kinnaird et al., "Mitochondrial activation by inhibition of PDKII suppresses HIF1a signaling and angiogenesis in cancer," *Oncogene*, vol. 32, no. 13, pp. 1638–1650, 2013.

[35] H. J. Bogaard, K. Abe, A. V. Noordegmaf, and N. F. Voelkel, "The right ventricle under pressure: cellular and molecular mechanisms of right-heart failure in pulmonary hypertension," *CHEST*, vol. 135, no. 3, pp. 794–804, 2009.

[36] H. J. Bogaard, R. Natarajan, S. C. Henderson et al., "Chronic pulmonary artery pressure elevation is insufficient to explain right heart failure," *Circulation*, vol. 120, no. 20, pp. 1951–1960, 2009.

[37] S. L. Archer, Y. Fang, J. J. Ryan, and L. Piao, "Metabolism and bioenergetics in the right ventricle and pulmonary vasculature in pulmonary hypertension," *Pulmonary Circulation*, vol. 3, no. 1, pp. 144–152, 2013.

[38] L. Tian, M. Neuber-Hess, J. Mewburn et al., "Ischemia-induced Drp1 and Fis1-mediated mitochondrial fission and right ventricular dysfunction in pulmonary hypertension," *Journal of Molecular Medicine*, vol. 95, no. 4, pp. 381–393, 2017.

[39] K. Sagawa, "The end-systolic pressure-volume relation of the ventricle: definition, modifications and clinical use," *Circulation*, vol. 63, no. 6 I, pp. 1223–1227, 1981.

[40] B. A. Maron, R. T. Zamanian, and A. B. Waxman, "Pulmonary hypertension," *Basic Science to Clinical Medicine*, pp. 1–371, 2015.

[41] D. Boulate, O. Mercier, J. Guihaire et al., "Pulmonary circulatory—right ventricular uncoupling: new insights into pulmonary hypertension pathophysiology," *Pulmonary Hypertension: Basic Science to Clinical Medicine*, 2016.

[42] L. Piao, Y.-H. Fang, V. J. J. Cadete et al., "The inhibition of pyruvate dehydrogenase kinase improves impaired cardiac function and electrical remodeling in two models of right ventricular hypertrophy: resuscitating the hibernating right ventricle," *Journal of Molecular Medicine*, vol. 88, no. 1, pp. 47–60, 2010.

[43] G. Hagan, M. Southwood, C. Treacy et al., "(18)FDG PET imaging can quantify increased cellular metabolism in pulmonary arterial hypertension: A proof-of-principle study," *Pulmonary Circulation*, vol. 1, no. 4, pp. 448–455, 2011.

[44] M. Oikawa, Y. Kagaya, H. Otani et al., "Increased [18F]fluorodeoxyglucose accumulation in right ventricular free wall in patients with pulmonary hypertension and the effect of epoprostenol," *Journal of the American College of Cardiology*, vol. 45, no. 11, pp. 1849–1855, 2005.

[45] E. L. Lundgrin, M. M. Park, J. Sharp et al., "Fasting 2-deoxy-2-[18F]fluoro-D-glucose positron emission tomography to detect metabolic changes in pulmonary arterial hypertension hearts over 1 year," *Annals of the American Thoracic Society*, vol. 10, no. 1, pp. 1–9, 2013.

[46] E. L. Brittain, M. Talati, J. P. Fessel et al., "Fatty acid metabolic defects and right ventricular lipotoxicity in human pulmonary arterial hypertension," *Circulation*, vol. 133, no. 20, pp. 1936–1944, 2016.

[47] S. Bokhari, A. Raina, E. B. Rosenweig et al., "PET imaging may provide a novel biomarker and understanding of right ventricular dysfunction in patients with idiopathic pulmonary arterial hypertension," *Circulation: Cardiovascular Imaging*, vol. 4, no. 6, pp. 641–647, 2011.

[48] M. M. Can, C. Kaymaz, I. H. Tanboga et al., "Increased right ventricular glucose metabolism in patients with pulmonary arterial hypertension," *Clinical Nuclear Medicine*, vol. 36, no. 9, pp. 743–748, 2011.

[49] S. Tatebe, Y. Fukumoto, M. Oikawa-Wakayama et al., "Enhanced [18F]fluorodeoxyglucose accumulation in the right ventricular free wall predicts long-term prognosis of patients with pulmonary hypertension: a preliminary observational study," *European Heart Journal—Cardiovascular Imaging*, vol. 15, no. 6, pp. 666–672, 2014.

[50] G. Marsboom, C. Wietholt, C. R. Haney et al., "Lung ^{18}F-fluorodeoxyglucose positron emission tomography for diagnosis and monitoring of pulmonary arterial hypertension," *American Journal of Respiratory and Critical Care Medicine*, vol. 185, no. 6, pp. 670–679, 2012.

[51] W. Li, L. Wang, C.-M. Xiong et al., "The prognostic value of 18F-FDG uptake ratio between the right and left ventricles in idiopathic pulmonary arterial hypertension," *Clinical Nuclear Medicine*, vol. 40, no. 11, pp. 859–863, 2015.

[52] R. M. Tuder, L. A. Davis, and B. B. Graham, "Targeting energetic metabolism: a new frontier in the pathogenesis and treatment of pulmonary hypertension," *American Journal of Respiratory and Critical Care Medicine*, vol. 185, no. 3, pp. 260–266, 2012.

[53] L. Piao, V. K. Sidhu, Y.-H. Fang et al., "FOXO1-mediated upregulation of pyruvate dehydrogenase kinase-4 (PDK4) decreases glucose oxidation and impairs right ventricular function in pulmonary hypertension: therapeutic benefits of dichloroacetate.," *Journal of Molecular Medicine*, vol. 91, no. 3, pp. 333–346, 2013.

[54] Y.-H. Fang, L. Piao, Z. Hong et al., "Therapeutic inhibition of fatty acid oxidation in right ventricular hypertrophy: exploiting Randle's cycle," *Journal of Molecular Medicine*, vol. 90, no. 1, pp. 31–43, 2012.

Hindawi
BioMed Research International
Volume 2018, Article ID 3293584, 9 pages
https://doi.org/10.1155/2018/3293584

Research Article

Effect of Riociguat and Sildenafil on Right Heart Remodeling and Function in Pressure Overload Induced Model of Pulmonary Arterial Banding

Nabham Rai,[1,2] **Swathi Veeroju**,[1,2] **Yves Schymura**,[3] **Wiebke Janssen**,[1,2,4] **Astrid Wietelmann**,[3] **Baktybek Kojonazarov**,[1,2] **Norbert Weissmann**,[1,2] **Johannes-Peter Stasch**,[4,5] **Hossein Ardeschir Ghofrani**,[1,2] **Werner Seeger**,[3] **Ralph Theo Schermuly**,[1,2] **and Tatyana Novoyatleva**[1,2]

[1] *Universities of Giessen and Marburg Lung Centre (UGMLC), Aulweg 130, 35392 Giessen, Germany*
[2] *German Center for Lung Research (DZL), 35392 Giessen, Germany*
[3] *Max-Planck-Institute for Heart and Lung Research, Ludwigstrasse 43, 61231 Bad Nauheim, Germany*
[4] *Bayer Pharma AG, Aprather Weg 18a, 42096 Wuppertal, Germany*
[5] *Institute of Pharmacy, Martin Luther University of Halle-Wittenberg, Wolfgang-Langenbeck-Strasse 4, 06120 Halle (Saale), Germany*

Correspondence should be addressed to Ralph Theo Schermuly; ralph.schermuly@innere.med.uni-giessen.de

Received 7 July 2017; Revised 4 November 2017; Accepted 16 November 2017; Published 3 January 2018

Academic Editor: Ruxandra Jurcut

Pulmonary arterial hypertension (PAH) is a progressive disorder characterized by remodeling of the pulmonary vasculature and a rise in right ventricular (RV) afterload. The increased RV afterload leads to right ventricular failure (RVF) which is the reason for the high morbidity and mortality in PAH patients. The objective was to evaluate the therapeutic efficacy and antiremodeling potential of the phosphodiesterase type 5 (PDE5) inhibitor sildenafil and the soluble guanylate cyclase stimulator riociguat in a model of pressure overload RV hypertrophy induced by pulmonary artery banding (PAB). Mice subjected to PAB, one week after surgery, were treated with either sildenafil (100 mg/kg/d, $n = 5$), riociguat (30 mg/kg/d, $n = 5$), or vehicle ($n = 5$) for 14 days. RV function and remodeling were assessed by right heart catheterization, magnetic resonance imaging (MRI), and histomorphometry. Both sildenafil and riociguat prevented the deterioration of RV function, as determined by a decrease in RV dilation and restoration of the RV ejection fraction (EF). Although both compounds did not decrease right heart mass and cellular hypertrophy, riociguat prevented RV fibrosis induced by PAB. Both compounds diminished TGF-beta1 induced collagen synthesis of RV cardiac fibroblasts *in vitro*. Treatment with either riociguat or sildenafil prevented the progression of pressure overload-induced RVF, representing a novel therapeutic approach.

1. Introduction

Pulmonary arterial hypertension (PAH) involves complex and multifactorial changes in pulmonary vasculature resulting in an increase in pulmonary vascular resistance (PVR) and pulmonary arterial pressure (PAP) [1, 2]. The changes in PVR and PAP lead to an increased right ventricular afterload followed by right ventricular hypertrophy (RVH). Right ventricular afterload serves as a major determinant of the functional state and prognosis of PAH. RVH can initially compensate for the increased afterload and maintain cardiac output, while sustained pressure overload leads to RV ischemia and decompensation of the RV, finally culminating in right heart failure [3]. The mortality rate due to right heart failure in patients with PAH remains high and the capability of the right heart to cope with these changes is a critical factor in the survival of PAH patients [4]. Furthermore, the long-term prognosis in PAH remains poor despite recent improvements in diagnosis and treatment [5, 6].

The Nitric Oxide- (NO-) cyclic guanosine monophosphate (cGMP) pathway plays a major role in the cardiovascular system [7, 8]. NO activates soluble guanylate cyclase

(sGC) to generate the second messenger cGMP, which is in turn degraded and thereby deactivated by phosphodiesterases (PDEs), like PDE 5. Importantly, modulation of NO-sGC-cGMP signaling has been associated with multiple downstream effects on pulmonary vascular remodeling, maladaptive cardiac hypertrophy and inflammation [9]. Likewise does an interruption in cGMP production lead to increased fibrosis and cardiac hypertrophy followed by heart failure [10]. Thus, the restoration of the NO-sGC-cGMP signaling pathway in patients with heart failure (HF) provides a challenge both for preclinical and clinical studies [11].

The sGC stimulator riociguat (BAY 63-2521) and the PDE5 inhibitor sildenafil, well-known modulators of the cGMP pathway, are clinically approved for the treatment of pulmonary arterial hypertension (PAH) [12, 13]. Riociguat enhances cGMP levels both in a NO-dependent and in an independent manner and has demonstrated direct beneficial effects on exercise capacity and secondary efficacy end points in PAH patients [14]. On the other side, PDE inhibitors have been established as targets for pulmonary vasodilation for a long time [15]. Sildenafil improves exercise capacity, WHO functional class, and hemodynamic parameters in patients with symptomatic PAH [16]. Sildenafil exerts direct beneficial effects on RV function in patients with PH [17, 18]. Furthermore, various acute as well as chronic studies in patients with reduced EF demonstrate that sildenafil improved exercise capacity and quality of life in patients with systolic heart failure and secondary PH [19].

In monocrotaline- (MCT-) induced PH, sildenafil caused a restoration of RV function [20–23]. In experimental model of RVH, pulmonary artery banding (PAB) sildenafil led at one side to an improvement of RV diastolic function with a reduction of fibrosis [24] but on the other side resulted in a lack of any beneficial effects on RV remodeling and function at constant pressure overload conditions [22]. In experimental models of PH, riociguat partially reversed PH, RV hypertrophy, and pulmonary vascular remodeling [25]. Our group has previously shown the positive effects of both riociguat and sildenafil on reduction of RV pressure and RVH with concomitant augmentation of RV function in SUGEN (SU5416) associated with chronic hypoxia (SUHx) model of PH [23]. Since the effect of riociguat on RVH by PAB has not been investigated before, the main objective of the current study was to explore the impact of riociguat in comparison to sildenafil on RV remodeling upon pressure overload induced RVH independent from the changes in afterload.

2. Material and Methods

2.1. Animal Model. All animal *in vivo* procedures were approved by the local Animal Ethics Committee Authorities (approval number B2/244). Adult male C57Bl/6J mice ($n = 5$ per each group, 21–24 g body weight) obtained from Harlan Laboratories, Inc., Netherlands, were subjected to continuous pressure overload by surgical banding of the pulmonary artery or sham operation under the influence of isoflurane (1.5–2.5% v/v). Analgesic buprenorphine hydrochloride (0.05 mg/kg, Vetergesic, Braun) was given prior to the operation. Respiration of mice was controlled with a rodent ventilator (MiniVent Type 845, Hugo Sachs Elektronik KG, March, Germany). The left thorax was opened to gain access to the pulmonary artery. The pulmonary artery was bluntly dissected from the aorta and constricted to 350 μm using titanium clips (HemoclipR, Weck, Germany) and a modified adjustable clip applier (Hemoclip®, Weck, Germany). The thorax was closed and the skin was sewn with a Vicryl suture (Vicryl® Plus 5-0, Ethicon, Germany). The sham group underwent the same surgical procedure without a titanium clip being attached.

2.2. Drug Treatment. Sildenafil-citrate was administered to mice at a dose of 100 mg/kg/d in drinking water. Riociguat was dissolved in 1% methylcellulose and administered orally to mice at a dose of 30 mg/kg/d. Treatment for both compounds started 7 days after the surgery and continued for 14 days. Twenty days after PAB the animals were subjected to hemodynamic measurements and organ harvesting. All the mice survived until day 21 after PAB.

2.3. Cardiac Magnetic Resonance Imaging. To characterize the morphological and functional changes, RV structure and function were determined by Cardiac Magnetic Resonance Imaging (MRI) at day 21 after surgery. MRI measurements were performed with a 7.0 T Bruker PharmaScan, equipped with a 300 mT/m gradient system with a custom-built circularly polarized birdcage resonator and the IntraGate™ self-gating tool (Bruker, Ettlingen, Germany). Gradient echo method (repetition time = 6.2 ms; echo time = 1.6 ms; field of view = 2.20 × 2.20 cm; slice thickness = 1.0 mm; matrix = 128 × 128; repetitions = 100; resolution 0.0172 cm/pixel) has been implemented for the measurements. MRI data were analysed using MASS® 4 Mice digital imaging software (Medis) where total volume (V_t) was measured as sum of partial volumes (S_N) using Simpson's rule ($V_t = S_1 + S_2 + S_3 + \cdots + S_{N-1} + S_N$). Images were obtained as contiguous axial slices (9-10) for both the ventricles. The end diastolic and end systolic frame were considered to be the slice with the largest and smallest ventricular volume, respectively. End diastolic and end systolic volumes were calculated using single sliced volumes. Stroke volume (SV) is the amount of blood which is pumped out from the heart with every heartbeat and is derived from SV = EDV − ESV. Ejection fraction (EF) is the relative amount of blood which is pumped out of the heart with every heartbeat and is calculated from EF = SV/EDV. MRI data were analysed using Qmass digital imaging software (Medis). Isoflurane (2.0% v/v) anesthesia was delivered to mice in an oxygen/medical air (0.5/0.5 L/min) mixture during the measurement. All MRI measurements were performed blinded.

2.4. Haemodynamic Measurements and Tissue Processing. Fourteen days after treatment, mice were anesthetized using isoflurane (1.5% v/v). The body temperature of mice was maintained at 37°C using a controlled heating pad. With the use of catheter (SPR-671, FMI, Foehr Medical Instruments GmbH, Seeheim/Ober-Beerbach, Germany) heart rate, systemic blood pressure, and right ventricular (RV) pressure were measured. Systemic arterial pressure (SBPsys) was

measured by right carotid artery catheterizing. PowerLab 8/30 System with the Chart 7.0 Software (ADInstruments GmbH, Spechbach, Germany) was used for all the measurements. After all haemodynamic measurements had been performed, the blood was drained out of mice and the heart was isolated. The RV was dissected from both the left ventricle and the septum (LV + S) and the ratio of RV to LV + S was estimated.

2.5. Histology. Murine RVs were fixed in 4% paraformaldehyde (PFA) and processed for histomorphometrical analyses. The RVs were embedded in paraffin blocks and three μm sections were cut. To assess the extent of fibrosis, Picrosirius red staining was performed. The collagen content was calculated as the ratio (%) of the area occupied by collagen to the total area of the section and given in percentage. FITC-labeled wheat germ agglutinin (WGA) staining was performed to label the skeletal and cardiac sarcolemma and to measure the size of the cardiomyocytes. For cardiomyocyte size assessment transverse RV sections were utilized and evaluated using fluorescence microscopy (Leica DM6000 B, Leica Microsystems GmbH, Wetzlar, Germany). Only cardiomyocytes with the nucleus visible were counted.

2.6. Collagen Assay. RV cardiac fibroblasts (CFs) were isolated from adult mouse hearts, as described previously [26]. Serum-starved for 24 hours, CFs were stimulated with TGF-beta1 at 10 ng/ml for the following 72 hours. Sildenafil and riociguat were added prior to stimulation with TGF-beta1 at indicated concentrations. L-Ascorbic acid (0.25 mM) was added to the medium daily. Cells were lysed in RIPA buffer and total collagen content (type 1–5) was assessed using a Sircol soluble collagen assay kit (Biocolor Ltd.).

2.7. Western Blot. For total protein extraction RV CFs were lysed in RIPA buffer (Thermo Fisher Scientific). Protein extracts were resolved on 4–12% Bis-Tris Gels (Invitrogen) and blotted onto nitrocellulose membranes. Membranes were blocked with 5% nonfat dry milk in TBS/T for one hour at RT, followed by incubation with primary antibodies at 4°C overnight. The following primary antibodies were utilized: rabbit monoclonal anti p-SMAD2 (S465/467), rabbit monoclonal SMAD2 (D43B4), rabbit monoclonal p-SMAD3 (S423/425), rabbit monoclonal SMAD3 (C67H9), and rabbit polyclonal Pan-actin (1 : 1000) (all from Cell Signaling). Antigen-antibody complexes were visualized using horseradish peroxidase-conjugated secondary antibodies (Amersham) and ECL Plus Western Blotting Detection System (GE Healthcare).

2.8. Statistics. Data were analysed with GraphPad Prism (version 5.0c, GraphPad Software Inc.). All values are given as mean ± SD. Differences between groups were assessed using one-way ANOVA and repeated measures ANOVA with Bonferroni post hoc test for multiple comparisons. P values of <0.05 were regarded as statistically significant.

3. Results

3.1. Sildenafil and Riociguat Prevent Deterioration of Right Ventricular (RV) Function in the PAB Model of RV Hypertrophy. PAB resulted in an increase of right ventricular (RV) systolic pressure in Placebo-, sildenafil-, and riociguat-treated mice to the same extent, depicting the accuracy of the surgery to reproduce the extent of constriction of the pulmonary artery (PA) to a predefined magnitude (RVPsys: 24.7 ± 3.081 mmHg for sham versus 58.7 ± 6.534 mmHg for Placebo, 58.23 ± 9.42 mmHg and 60.03 ± 7.42 mmHg for riociguat and sildenafil, resp., $P < 0.001$) (Figure 1(a)). Treatment with either sildenafil or riociguat had no effect on systemic arterial pressure (SBPsys: 80.27 ± 11.45 mmHg for Placebo versus 77.97 ± 12.11 mmHg and 82.36 ± 13.17 mmHg for sildenafil and riociguat, resp., $P > 0.05$) (Figure 1(b)). RV end diastolic volume (RV EDV) was increased in the Placebo group, as compared to sham (RV EDV: 46.3 ± 10.0 μl versus 79.6 ± 13.6 μl, $P < 0.001$), and this effect was significantly diminished by the treatment with either sildenafil or riociguat (59.9 ± 7.2 μl for sildenafil, $P < 0.5$ and 44.0 ± 8.3 μl for riociguat, $P < 0.001$) (Figure 1(c)). Similarly, the banding led to an increase of RV end systolic volume (RV ESV) in Placebo-treated animals (RV ESV: 13.0 ± 5.1 μl versus 54.7 ± 17.1 μl, $P < 0.00001$), and there was a significant decrease in animals treated with sildenafil or riociguat (for sildenafil 33.9 ± 7.7 μl, $P < 0.5$, and for riociguat 24.7 ± 10.1 μl, $P < 0.01$, both versus Placebo) (Figure 1(d)). The decrease in RV dilation and ESV translated into an improved performance of the RV with slightly increased stroke volume (SV) for both sildenafil- and riociguat-treated animals (SV: 33.3 ± 5.1 μl for sham versus 24.2 ± 7.3 μl for Placebo, versus 25.9 ± 3.6 μl for sildenafil, $P < 0.05$ and 28.5 ± 7.3 μl for riociguat; $P > 0.5$) (Figure 1(e)) and a significant increase in RV ejection fraction (RV EF: 72.8 ± 5.7% for sham versus 30 ± 9.5% for Placebo versus 44.9 ± 4.9%, $P < 0.5$ for sildenafil and 57.6 ± 8.6%, $P < 0.001$ for riociguat) (Figure 1(f)).

3.2. Riociguat but Not Sildenafil Prevented RV Fibrosis in the PAB Model of RVH. PAB increased RV hypertrophy with an increase in RV mass (RV/body weight (BW): 0.86 ± 0.08 for sham versus Placebo 1.8 ± 0.4 mg/g, $P < 0.001$). RV mass was not affected by drug treatment (RV/BW: 1.8 ± 0.4 mg/g for Placebo versus 1.7 ± 0.2 mg/g and 1.9 ± 0.2 mg/g for sildenafil and riociguat, resp.; $P > 0.05$) (Figure 1(g)). Similarly, the RV/LV + S ratio was not affected after treatment (RV/LV + S: Placebo 0.5 ± 0.1 versus 0.5 ± 0.08 for sildenafil and 0.5 ± 0.08 for riociguat; $P > 0.05$) (Figure 1(h)). PAB resulted in an increase in cardiomyocyte size (14.15 ± 1.58 μm for sham versus 20.70 ± 1.14 μm for Placebo, $P < 0.0001$), although treatment with both compounds had no effect on cardiomyocyte size (19.70 ± 1.76 μm and 19.76 ± 1.11 μm for sildenafil and riociguat, resp.; both $P > 0.05$) (Figures 2(a) and 2(b)). PAB leads to RV fibrosis with an increase in collagen content (0.74±0.23% for sham versus 5.61±1.02% for Placebo, $P < 0.0001$). Although sildenafil treatment had no effect on fibrosis (5.6±1.02% for Placebo versus 5.4±0.77% for Sildenafil), riociguat administration resulted in a reduction of collagen content to nearly half of the percentage of the

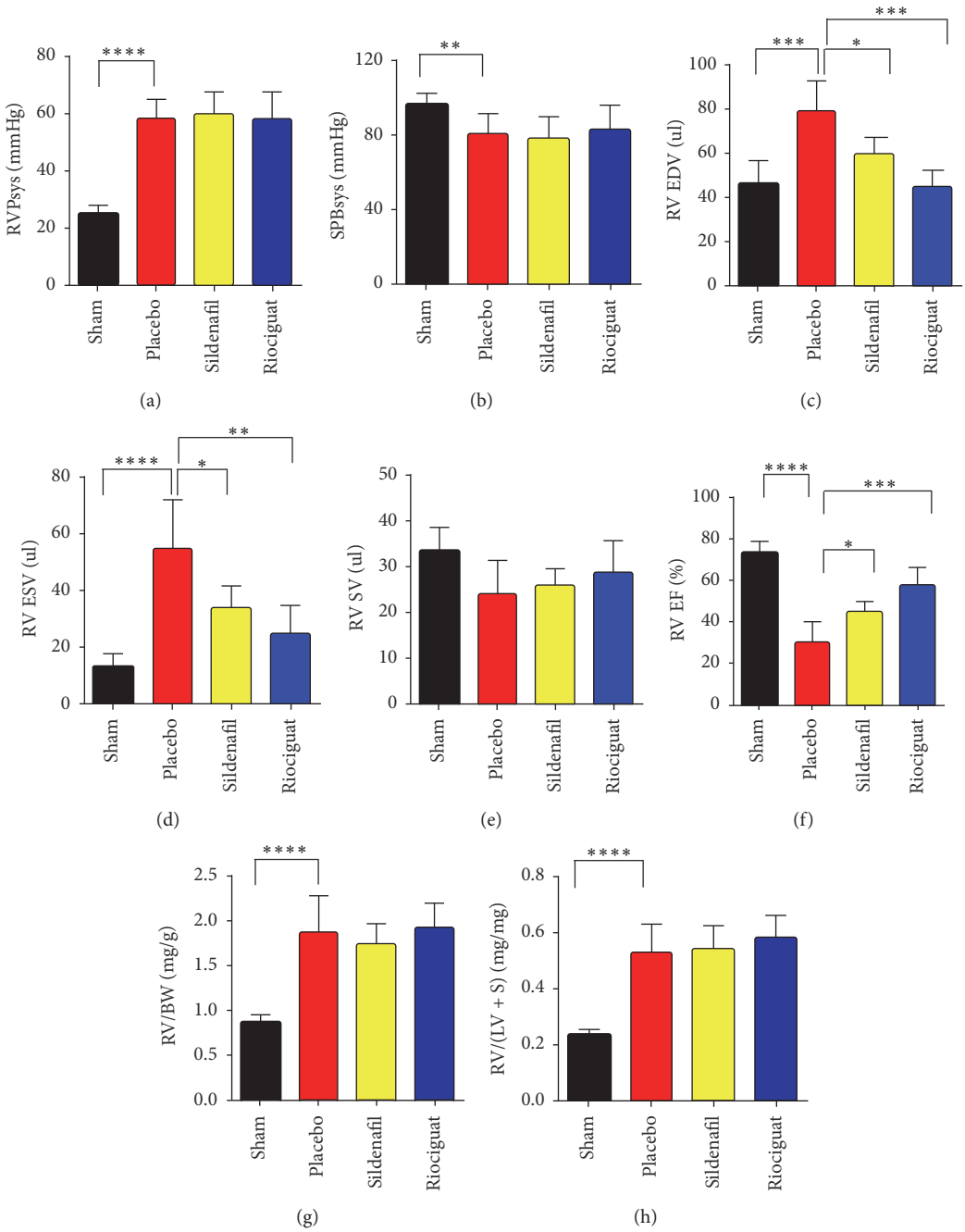

Figure 1: *Effect of sildenafil and riociguat on RV function in pressure overload model.* Hemodynamic and MRI assessment on pulmonary artery banding (PAB) mice treated with sildenafil and riociguat. (a) Right ventricular systolic pressure (RVSPsys, mmHg). (b) Systemic blood pressure (SPBsys, mmHg). (c) Ratio of right ventricular (RV) weight to body weight (RV/BW, mg/g). (d) Ratio of RV weight to LV + septum weight (RV/LV + S, mg/mg). (e) Right ventricular end diastolic volume (RVED, μl). (f) Right ventricular end systolic volume (RVES, μl). (g) Right ventricular stroke volume (μl). (h) Right ventricular ejection fraction (%). Values are means ± SD. $^{*}P < 0.05$, $^{**}P < 0.01$, $^{***}P < 0.001$, $^{****}P < 0.0001$, and $n = 5$ mice per group.

Placebo group (5.6 ± 1.02% for Placebo versus 3.1 ± 1.07% for riociguat; $P < 0.01$) (Figures 2(c) and 2(d)).

3.3. Sildenafil and Riociguat Reduce Collagen Secretion and Inhibit TGF-Beta1 Induced Phosphorylation of SMAD2/SMAD3 in RV Cardiac Fibroblasts. TGF-beta is known to induce fibrosis and targeting the TGF-beta/Smad signaling pathway provides a therapeutic approach in numerous pathophysiological conditions. To confirm the beneficial *in vivo* effects of riociguat on heart fibrosis and collagen deposition, adult RV cardiac fibroblasts (CFs) were treated with either sildenafil or riociguat upon TGF-beta1 stimulation. Sildenafil, as well as riociguat, caused a significant reduction of total collagen production and secretion of TGF-beta1 stimulated

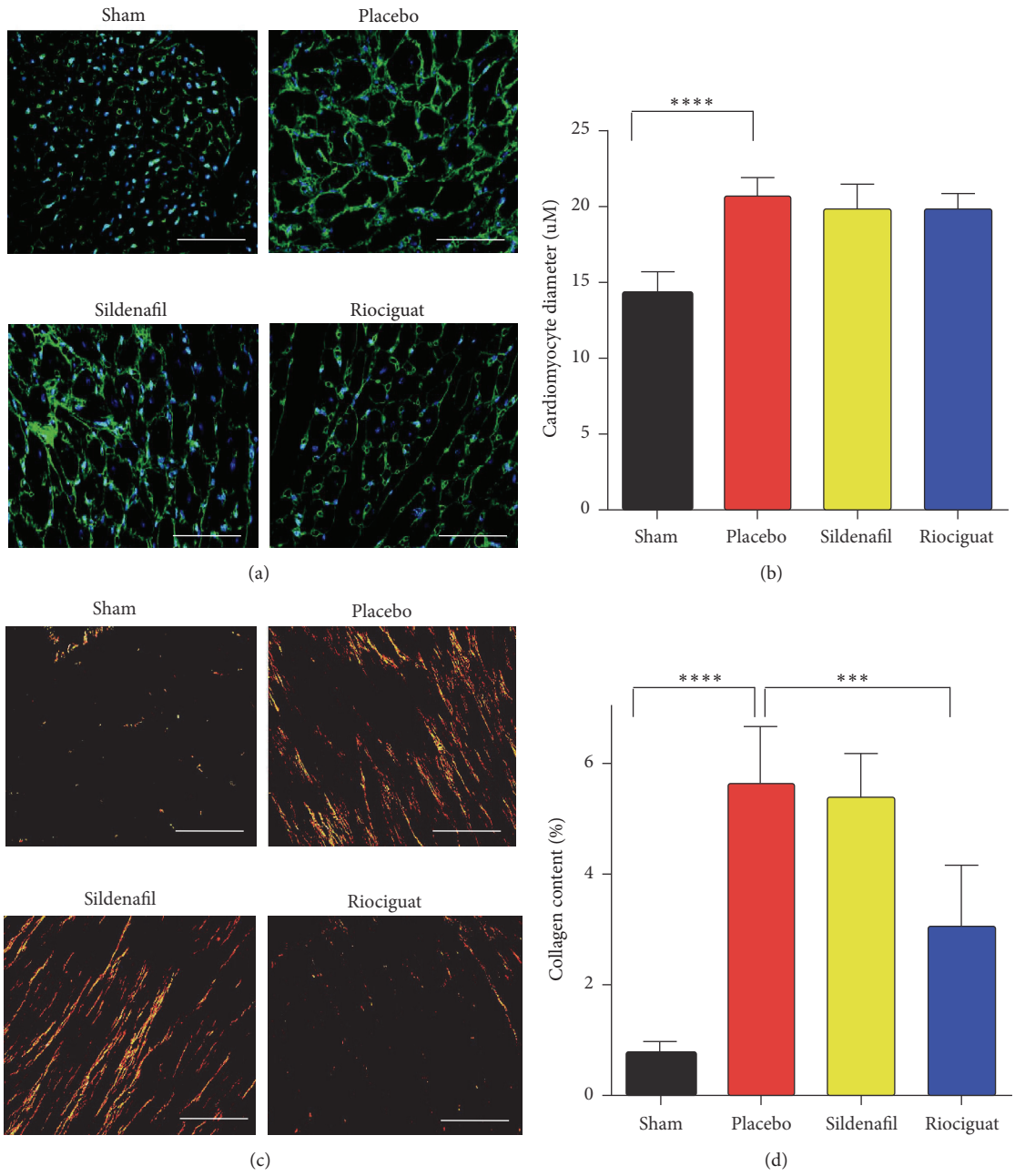

FIGURE 2: *Effects of sildenafil and riociguat and on RV cardiomyocyte size and collagen content after PAB*. (a, b) Representative pictures and quantification of cardiomyocyte cross-sectional area based on a cell plasma membrane staining with wheat germ agglutinin- (WGA-) FITC (mean ± SD, 5 mice per group, $P < 0.05$). Scale bar 100 μm. (c, d) Representative images and assessment of RV collagen area (%), representing reduced collagen content in riociguat-treated samples (mean ± SD, 5 mice per group, $^{***}P < 0.001$, $^{****}P < 0.0001$). Scale bar 100 μm.

RV CFs (100 ± 0.0% for TGF-beta1 versus 73.9 ± 16.0% for sildenafil and 76.5 ± 11.53% for riociguat; $P < 0.0001$) (Figure 3(a)). As Smad transcription factors are well established and major intracellular mediators of the TGF-beta signaling pathway, we thought to investigate the effect of cGMP pathway modulators on phosphorylation of Smad2 and Smad3, a major determinant of Smad activation. Western Blot analyses demonstrate that both sildenafil and riociguat reduce phosphorylation of both Smad2 and Smad3 proteins in CFs, indicating the involvement of both transcription factors for transmitting the TGF-beta response in RV CFs (Figure 3(b)).

4. Discussion

In this study, we investigated the therapeutic efficacy and antiremodeling potential of the phosphodiesterase 5 (PDE 5) inhibitor sildenafil and the soluble guanylate cyclase stimulator riociguat in a model of constant pressure overload due to the banding of the pulmonary artery banding (PAB) in

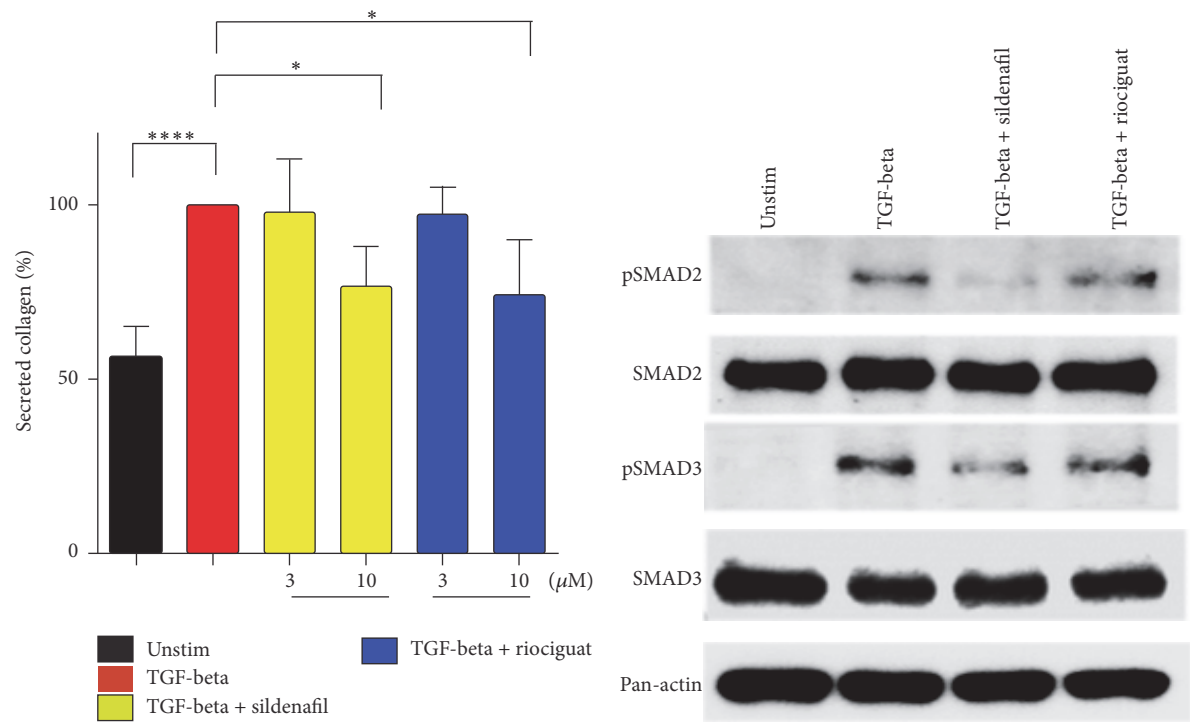

Figure 3: *Effects of sildenafil and riociguat on collagen production and phospho-Smad2/3 expression in TGF-beta stimulated RV cardiac fibroblasts.* (a) Effects of the sildenafil and riociguat on collagen secretion in RV cardiac fibroblasts (mean ± SD, $n = 6$ independent experiments, $^{*}P < 0.05$, $^{****}P < 0.0001$). (b) Western Blot images p-SMAD2/SMAD2, p-SMAD3/SMAD3, and Pan-actin from the proteins isolated from RV cardiac fibroblasts. The blot is representative of the three independent runs/experiments.

mice. Sildenafil and riociguat improved RV function but did not alleviate right heart hypertrophy. Interestingly, although TGF-beta1 induced collagen production and Smad2/Smad3 phosphorylation was significantly diminished in right ventricular CFs by both compounds *in vitro*, only riociguat attenuated PAB-induced fibrosis of the RV *in vivo*.

NO-sGC-cGMP signaling pathway plays an important physiological role in both vascular and nonvascular tissues. An activation of a key enzyme in the NO signaling pathway, soluble guanylyl cyclase, causes an increase in cGMP production. Favorable clinical effects of cGMP include vasodilation, inhibition of smooth muscle proliferation, and attenuation of pulmonary vascular remodeling, as well as anti-inflammatory, antifibrotic, and antiplatelet activity [27, 28]. The dysregulation of the NO-sGC-cGMP pathway is one of the key mechanisms in PH and cGMP, and pharmacological stimulation of this pathway, through either activation of sGC or the inhibition of PDE5, has been reported to be beneficial in various preclinical and clinical studies for PH [14, 16, 20, 23–25, 29]. The sGC stimulators BAY 41-8543, BAY 41-2272, and riociguat have been shown to induce pulmonary vasodilation, reverse vascular remodeling, and impair RVH in various models of PH [25, 28, 30–32].

Patients with chronic obstructive pulmonary disease induced pulmonary hypertension (COPD-PH) exhibited an improved cardiac index and pulmonary vascular resistance upon treatment with riociguat [27]. An improved cardiac function along with the stroke volume and cardiac index has been also reported in systolic heart failure patients upon riociguat treatment [33, 34]. Importantly, riociguat has demonstrated a protective effect against cardiac damage by reducing cardiac interstitial fibrosis in two independent rat models of renal hypertension [35].

Several classical PH animal models, such as chronic hypoxia, injections of a monocrotaline (MCT), and administration of SUGEN (SU5416, a tyrosine-kinase inhibitor of the vascular endothelial growth factor receptor VEGFR-2), associated with hypoxia (SUHx) have been established in rodents. In these models, pulmonary vascular resistance increases, resulting in a compensatory hypertrophic response of the right heart [36]. A shortcoming of these models is the inability to distinguish the mechanisms underlying RV dysfunction from accompanying changes in the pulmonary circulation. This disadvantage is overcome by the PAB model in which the direct, physical constriction of the pulmonary artery leading to an increase in RV afterload allows studying the insights of the mechanisms of right heart remodeling and function, independent of the effects on the pulmonary vasculature [31].

Limited (for riociguat), or controversial (for sildenafil) evidence of the effects of both compounds on pressure overload induced right heart hypertrophy led us to investigate the impact of both compounds upon the RV changes introduced by banding [17, 22]. Treatment with both compounds

preserved the systolic function of the RV induced by PAB. Improved function, as indicated by the decrease in ESV and increase in EF, was noted upon sildenafil and riociguat treatment, although the effect was more pronounced with riociguat. End diastolic and systolic function of the RV were similarly altered, as indicated by the decrease in EDV. The RV systolic pressure remained constant in all animals which had undergone PAB, confirming fixed pressure overload conditions. Importantly, systemic pressure revealed no changes after surgery in all studied mice, suggesting that improvements in cardiac function are mainly due to the effect on RV tissue and its remodeling. Our findings for sildenafil are in line with a study investigating the effects of PAB on rats, in which sildenafil led to improvements of RV functional parameters [24]. Despite the effect on RV dilation, both sildenafil and riociguat treatment did not cause any alterations in RV hypertrophy, as determined by assessment of RV mass and cardiomyocyte size.

Histomorphometrical analyses of RVs demonstrate the deterioration of PAB-induced fibrosis only after riociguat treatment. Importantly, the cGMP increase by sGC stimulators exerts direct antifibrotic effects in various organs [10]. Application of BAY 41-8543 showed protective effects against renal fibrosis. The authors proposed that BAY 41-8543 by activating cGKI restricts TGF-beta signaling via inhibition of a Smad translocation in Smad-dependent pathway, or via inhibition of phosphorylation of Erk1/2 in Smad-independent pathway [37]. Another cGMP stimulator, BAY, 41-2272 caused a reduction in cardiac fibrosis through inactivation of fibroblasts to myofibroblasts via angiotensin-converting enzyme (ACE) [38]. Members of TGF-beta superfamily play a crucial role in the pathogenesis of cardiac remodeling and fibrosis of the pressure-overloaded hearts [39, 40]. Besides high levels of TGF-beta in infarcted or pressure-overloaded hearts, Smad2/3 and 4 have been shown to be transcriptionally active, which has been attributed to the elevation of cardiac fibrosis [41–43]. Sildenafil and riociguat treatment of RV CFs resulted in an inhibition of TGF-beta induced phosphorylation and probably translocation of Smad2 and Smad3 transcription factors. Although sildenafil driven inhibition of Smads has been already reported [44], the inhibition of TGF-beta1 induced phosphorylation of Smad2/3 by riociguat is unknown. We postulate that riociguat effects on fibrosis in CFs are mediated by TGF-beta1/Smad signaling pathway. Interestingly, strong beneficial cardioprotective effects of riociguat on left ventricular (LV) infarct size and function detected in a model of myocardial infarction (MI) and post-MI chronic heart failure have been also associated with slight, but not significant reduction of fibrosis-activated markers [45]. In a model of chronic cardiac volume and pressure overload, riociguat application has led to the attenuation of systemic hypertension and diminution of cardiac fibrosis, as well as an improvement of systolic heart function in salt sensitive rats [35, 46].

Although both sildenafil and riociguat caused a significant decrease in a secreted collagen content of CFs *in vitro*, beneficial effects on collagen deposition *in vivo* have been noted only for riociguat. In contrast to the study by Borgdorff et al. [24], in our experimental settings sildenafil treatment did not have an outcome in a reduction of interstitial fibrosis. These discrepancies might be due to the differences in the time-course study and severity of the PAB [24]. Recently it has been demonstrated that sarcomere-derived cardiomyocyte diastolic stiffness and myocardial fibrosis of the RV may contribute to the disease progression in PAH. Importantly, in rats with severe RV dysfunction, an increase of both fibrosis-mediated and myofibril-mediated stiffness have been detected, whereas in animals with mild RV dysfunction, only myofibril-mediated stiffness was noted [47]. These data might explain results presented here, suggesting that the time-course study, as well as the severity of the disease, might explain the differences between sildenafil promoted collagen reduction *in vitro* and lack of the effect on collagen deposition *in vivo*. Taken together, our results indicate that riociguat and sildenafil play a beneficial role in RV function in pressure overload induced RVH.

5. Conclusion

In this study we investigated the therapeutic efficacy and antiremodeling potential of sildenafil and riociguat in experimental pressure overload-induced RVH model with fixed afterload. Importantly, effects of riociguat have not been addressed until now in this setting. We demonstrate that administration of either of the two compounds protects from right heart failure. Furthermore, riociguat resulted in a decrease of fibrosis *in vivo* and reduction of collagen production and secretion in RV CFs *in vitro*. Our data proposes that clinically approved cGMP modulator, riociguat, might serve as a new cardioprotective agent for the treatment of RVF.

Conflicts of Interest

Johannes-Peter Stasch and Wiebke Janssen are employees at Bayer AG. All other authors declare no conflicts of interest.

Authors' Contributions

Nabham Rai, Swathi Veeroju, and Yves Schymura contributed equally to the manuscript.

Acknowledgments

The authors received funding from Universities of Giessen and Marburg Lung Centre (UGMLC), ECCPS (Excellence Cluster Cardiopulmonary System), and CRC1213 (Collaborative Research Center 1213, Projects A9 and B4).

References

[1] J. C. Grignola, "Hemodynamic assessment of pulmonary hypertension," *World Journal of Cardiology*, vol. 3, no. 1, p. 10, 2011.

[2] J. A. Leopold and B. A. Maron, "Molecular mechanisms of pulmonary vascular remodeling in pulmonary arterial hypertension," *International Journal of Molecular Sciences*, vol. 17, no. 5, article no. 761, 2016.

[3] J. J. Ryan and S. L. Archer, "The right ventricle in pulmonary arterial hypertension: Disorders of metabolism, angiogenesis

and adrenergic signaling in right ventricular failure," *Circulation Research*, vol. 115, no. 1, pp. 176–188, 2014.

[4] K. M. Chin, N. H. S. Kim, and L. J. Rubin, "The right ventricle in pulmonary hypertension," *Coronary Artery Disease*, vol. 16, no. 1, pp. 13–18, 2005.

[5] V. V. McLaughlin, "Looking to the future: A new decade of pulmonary arterial hypertension therapy," *European Respiratory Review*, vol. 20, no. 122, pp. 262–269, 2011.

[6] L. C. Price, S. J. Wort, S. J. Finney, P. S. Marino, and S. J. Brett, "Pulmonary vascular and right ventricular dysfunction in adult critical care: current and emerging options for management: a systematic literature review," *Critical Care*, vol. 14, no. 5, article R169, 2010.

[7] C. Koress, K. Swan, and P. Kadowitz, "Soluble guanylate cyclase stimulators and activators: novel therapies for pulmonary vascular disease or a different method of increasing cGMP?" *Current Hypertension Reports*, vol. 18, no. 5, article no. 42, 2016.

[8] J. O. Lundberg, M. T. Gladwin, and E. Weitzberg, "Strategies to increase nitric oxide signalling in cardiovascular disease," *Nature Reviews Drug Discovery*, vol. 14, no. 9, pp. 623–641, 2015.

[9] H. Ghofrani, M. Humbert, D. Langleben et al., "Riociguat: mode of action and clinical development in pulmonary hypertension," *Chest*, vol. 151, no. 2, pp. 468–480, 2017.

[10] P. Sandner and J. P. Stasch, "Anti-fibrotic effects of soluble guanylate cyclase stimulators and activators: A review of the preclinical evidence," *Respiratory Medicine*, vol. 122, pp. S1–S9, 2017.

[11] M. Gheorghiade, C. N. Marti, H. N. Sabbah et al., "Soluble guanylate cyclase: A potential therapeutic target for heart failure," *Heart Failure Reviews*, vol. 18, no. 2, pp. 123–134, 2013.

[12] T. A. McKinsey and D. A. Kass, "Small-molecule therapies for cardiac hypertrophy: moving beneath the cell surface," *Nature Reviews Drug Discovery*, vol. 6, no. 8, pp. 617–635, 2007.

[13] J. R. Kraehling and W. C. Sessa, "Contemporary approaches to modulating the nitric oxide-cGMP pathway in cardiovascular disease," *Circulation Research*, vol. 120, no. 7, pp. 1174–1182, 2017.

[14] H. A. Ghofrani, N. Galiè, F. Grimminger et al., "Riociguat for the treatment of pulmonary arterial hypertension," *The New England Journal of Medicine*, vol. 369, no. 4, pp. 330–340, 2013.

[15] A. J. Wardle, R. Wardle, K. Luyt, and R. Tulloh, "The utility of sildenafil in pulmonary hypertension: A focus on bronchopulmonary dysplasia," *Archives of Disease in Childhood*, vol. 98, no. 8, pp. 613–617, 2013.

[16] N. Galiè, H. A. Ghofrani, A. Torbicki et al., "Sildenafil citrate therapy for pulmonary arterial hypertension," *The New England Journal of Medicine*, vol. 353, no. 20, pp. 2148–2157, 2005.

[17] M. A. J. Borgdorff, B. Bartelds, M. G. Dickinson et al., "Sildenafil enhances systolic adaptation, but does not prevent diastolic dysfunction, in the pressure-loaded right ventricle," *European Journal of Heart Failure*, vol. 14, no. 9, pp. 1067–1074, 2012.

[18] A. M. S. Fernandes, A. C. Andrade, N. D. Barroso et al., "The immediate effect of Sildenafil on right ventricular function in patients with heart failure measured by cardiac magnetic resonance: A randomized control trial," *PLoS ONE*, vol. 10, no. 3, Article ID e0119623, 2015.

[19] M. Guazzi, G. Tumminello, F. Di Marco, C. Fiorentini, and M. D. Guazzi, "The effects of phosphodiesterase-5 inhibition with sildenafil on pulmonary hemodynamics and diffusion capacity, exercise ventilatory efficiency, and oxygen uptake kinetics in chronic heart failure," *Journal of the American College of Cardiology*, vol. 44, no. 12, pp. 2339–2348, 2004.

[20] H. K. Bae, H. Lee, K. C. Kim, and Y. M. Hong, "The effect of sildenafil on right ventricular remodeling in a rat model of monocrotaline-induced right ventricular failure," *Korean Journal of Pediatrics*, vol. 59, no. 6, pp. 262–270, 2016.

[21] R. Yoshiyuki, R. Tanaka, R. Fukushima, and N. Machida, "Preventive effect of sildenafil on right ventricular function in rats with monocrotaline-induced pulmonary arterial hypertension," *Journal of Experimental Animal Science*, vol. 65, no. 3, pp. 215–222, 2016.

[22] S. Schafer, P. Ellinghaus, W. Janssen et al., "Chronic inhibition of phosphodiesterase 5 does not prevent pressure-overload-induced right-ventricular remodelling," *Cardiovascular Research*, vol. 82, no. 1, pp. 30–39, 2009.

[23] M. Lang, B. Kojonazarov, X. Tian et al., "The soluble guanylate cyclase stimulator riociguat ameliorates pulmonary hypertension induced by hypoxia and SU5416 in rats," *PLoS ONE*, vol. 7, no. 8, Article ID e43433, 2012.

[24] M. A. Borgdorff, B. Bartelds, M. G. Dickinson et al., "Sildenafil treatment in established right ventricular dysfunction improves diastolic function and attenuates interstitial fibrosis independent from afterload," *American Journal of Physiology-Heart and Circulatory Physiology*, vol. 307, no. 3, pp. H361–H369, 2014.

[25] R. T. Schermuly, J.-P. Stasch, S. S. Pullamsetti et al., "Expression and function of soluble guanylate cyclase in pulmonary arterial hypertension," *European Respiratory Journal*, vol. 32, no. 4, pp. 881–891, 2008.

[26] T. Novoyatleva, Y. Schymura, W. Janssen et al., "Deletion of Fn14 receptor protects from right heart fibrosis and dysfunction," *Basic Research in Cardiology*, vol. 108, no. 2, article 325, 2013.

[27] J.-P. Stasch and O. V. Evgenov, "Soluble guanylate cyclase stimulators in pulmonary hypertension," *Handbook of Experimental Pharmacology*, vol. 218, pp. 279–313, 2013.

[28] J.-P. Stasch, P. Pacher, and O. V. Evgenov, "Soluble guanylate cyclase as an emerging therapeutic target in cardiopulmonary disease," *Circulation*, vol. 123, no. 20, pp. 2263–2273, 2011.

[29] K. Pradhan, A. Sydykov, X. Tian et al., "Soluble guanylate cyclase stimulator riociguat and phosphodiesterase 5 inhibitor sildenafil ameliorate pulmonary hypertension due to left heart disease in mice," *International Journal of Cardiology*, vol. 216, pp. 85–91, 2016.

[30] R. Dumitrascu, N. Weissmann, H. A. Ghofrani et al., "Activation of soluble guanylate cyclase reverses experimental pulmonary hypertension and vascular remodeling," *Circulation*, vol. 113, no. 2, pp. 286–295, 2006.

[31] B. Egemnazarov, A. Schmidt, S. Crnkovic et al., "Pressure overload creates right ventricular diastolic dysfunction in a mouse model: assessment by echocardiography," *Journal of the American Society of Echocardiography*, vol. 28, no. 7, pp. 828–843, 2015.

[32] L. B. Thorsen, Y. Eskildsen-Helmond, H. Zibrandtsen, J.-P. Stasch, U. Simonsen, and B. E. Laursen, "BAY 41-2272 inhibits the development of chronic hypoxic pulmonary hypertension in rats," *European Journal of Pharmacology*, vol. 647, no. 1-3, pp. 147–154, 2010.

[33] S. Breitenstein, L. Roessig, P. Sandner, and K. S. Lewis, "Novel sGC Stimulators and sGC Activators for the Treatment of Heart Failure," in *Journal of Cardiac Failure*, vol. 243 of *Handbook of Experimental Pharmacology*, pp. 225–247, Springer International Publishing, Cham, 2017.

[34] D. Conole and L. J. Scott, "Riociguat: First global approval," *Drugs*, vol. 73, no. 17, pp. 1967–1975, 2013.

[35] Y. Sharkovska, P. Kalk, B. Lawrenz et al., "Nitric oxide-independent stimulation of soluble guanylate cyclase reduces organ

damage in experimental low-renin and high-renin models," *Journal of Hypertension*, vol. 28, no. 8, pp. 1666–1675, 2010.

[36] G. Maarman, S. Lecour, G. Butrous, F. Thienemann, and K. Sliwa, "A comprehensive review: the evolution of animal models in pulmonary hypertension research; are we there yet?" *Pulmonary Circulation*, vol. 3, no. 4, pp. 739–756, 2013.

[37] E. Schinner, V. Wetzl, A. Schramm et al., "Inhibition of the TGFβ signalling pathway by cGMP and cGMP-dependent kinase I in renal fibrosis," *FEBS Open Bio*, vol. 7, no. 4, pp. 550–561, 2017.

[38] H. Masuyama, T. Tsuruda, Y. Sekita et al., "Pressure-independent effects of pharmacological stimulation of soluble guanylate cyclase on fibrosis in pressure-overloaded rat heart," *Hypertension Research*, vol. 32, no. 7, pp. 597–603, 2009.

[39] M. Dobaczewski, W. Chen, and N. G. Frangogiannis, "Transforming growth factor (TGF)-β signaling in cardiac remodeling," *Journal of Molecular and Cellular Cardiology*, vol. 51, no. 4, pp. 600–606, 2011.

[40] W. Song and X. Wang, "The role of TGFβ1 and LRG1 in cardiac remodelling and heart failure," *Biophysical Reviews*, vol. 7, no. 1, pp. 91–104, 2015.

[41] P. Bonniaud, P. J. Margetts, K. Ask, K. Flanders, J. Gauldie, and M. Kolb, "TGF-β and Smad3 signaling link inflammation to chronic fibrogenesis," *The Journal of Immunology*, vol. 175, no. 8, pp. 5390–5395, 2005.

[42] G. Euler-Taimor and J. Heger, "The complex pattern of SMAD signaling in the cardiovascular system," *Cardiovascular Research*, vol. 69, no. 1, pp. 15–25, 2006.

[43] M. Ruiz-Ortega, J. Rodríguez-Vita, E. Sanchez-Lopez, G. Carvajal, and J. Egido, "TGF-β signaling in vascular fibrosis," *Cardiovascular Research*, vol. 74, no. 2, pp. 196–206, 2007.

[44] W. Gong, M. Yan, J. Chen, S. Chaugai, C. Chen, and D. Wang, "Chronic inhibition of cyclic guanosine monophosphate-specific phosphodiesterase 5 prevented cardiac fibrosis through inhibition of transforming growth factor β-induced Smad signaling," *Frontiers of Medicine*, vol. 8, no. 4, pp. 445–455, 2014.

[45] C. Methner, G. Buonincontri, C.-I. Hu et al., "Riociguat reduces infarct size and post-infarct heart failure in mouse hearts: Insights from MRI/PET imaging," *PLoS ONE*, vol. 8, no. 12, Article ID e83910, 2013.

[46] S. Geschka, A. Kretschmer, Y. Sharkovska et al., "Soluble guanylate cyclase stimulation prevents fibrotic tissue remodeling and improves survival in salt-sensitive dahl rats," *PLoS ONE*, vol. 6, no. 7, Article ID e21853, 2011.

[47] S. Rain, S. Andersen, A. Najafi et al., "Right ventricular myocardial stiffness in experimental pulmonary arterial hypertension-clinical perspective," *Circulation: Heart Failure*, vol. 9, no. 7, p. e002636, 2016.

Hindawi
BioMed Research International
Volume 2017, Article ID 8217105, 15 pages
https://doi.org/10.1155/2017/8217105

Review Article

Acute Right Ventricular Dysfunction in Intensive Care Unit

Juan C. Grignola[1,2] and Enric Domingo[3,4]

[1]*Pathophysiology Department, School of Medicine, Hospital de Clínicas, Universidad de la República, Montevideo, Uruguay*
[2]*Postoperative Cardiac Critical Care Unit, Centro Cardiológico Americano, Montevideo, Uruguay*
[3]*Area del Cor, Hospital Vall d'Hebron, Barcelona, Spain*
[4]*Physiology Department, School of Medicine, Universitat Autonoma de Barcelona, Barcelona, Spain*

Correspondence should be addressed to Juan C. Grignola; jgrig@fmed.edu.uy

Received 31 May 2017; Revised 13 August 2017; Accepted 18 September 2017; Published 19 October 2017

Academic Editor: Andre La Gerche

The role of the left ventricle in ICU patients with circulatory shock has long been considered. However, acute right ventricle (RV) dysfunction causes and aggravates many common critical diseases (acute respiratory distress syndrome, pulmonary embolism, acute myocardial infarction, and postoperative cardiac surgery). Several supportive therapies, including mechanical ventilation and fluid management, can make RV dysfunction worse, potentially exacerbating shock. We briefly review the epidemiology, pathophysiology, diagnosis, and recommendations to guide management of acute RV dysfunction in ICU patients. Our aim is to clarify the complex effects of mechanical ventilation, fluid therapy, vasoactive drug infusions, and other therapies to resuscitate the critical patient optimally.

1. Introduction

The role of the left ventricle (LV) in ICU patients with circulatory shock has long been considered. However, acute right ventricle (RV) dysfunction causes and exacerbates many common critical illnesses (e.g., acute respiratory distress syndrome (ARDS), pulmonary embolism (PE), inferior acute myocardial infarction, and postoperative cardiac surgery).

There is a variety of definitions for acute RV dysfunction (RVD), RV failure (RVF), and right heart failure (RHF) in the literature that must be clarified and not used interchangeably.

RHF can be defined by a clinical syndrome due to an alteration of structure and/or function of the right heart circulatory system (comprised from the systemic veins up to the pulmonary capillaries) that reduces the ability to propel blood to the pulmonary circuit and/or high systemic venous pressures at rest or with effort [1]. Failure of the RV is a frequent component of RHF but not a mandatory feature of the RHF syndrome.

Acute RVD is defined as at least one of the following (Table 1) [2, 3]:

(i) Acute occurrence of RV systolic dysfunction by measuring the longitudinal systolic displacement and dilation [4–6]

(ii) Unexplained increase of natriuretic peptides in the absence of LV or renal disease

(iii) Electrocardiographic (ECG) RV strain patterns which are strong markers of moderate-to-severe RV strain. While specific, they are limited by a lack of sensitivity.

Evidence of cardiomyocyte death (elevation of troponin $I > 0.4$ ng/mL, troponin $T > 0.1$ ng/mL) predicts severe RVD. Although evidence of cardiomyocyte death can be seen in the absence of RVD, such patients are at risk for progression to circulatory collapse.

Acute cor pulmonale (ACP) is a form of RVD due to an acute increase in RV afterload.

Acute RVF is defined as acute RVD plus low cardiac output (CO) and hypoperfusion with the consequent multiorgan dysfunction/failure. RVF occurs when the RV fails to provide enough blood flow to the pulmonary circulation to accomplish adequate LV filling [7] (Figure 1). It can be suspected whenever the ratio of the right atrial pressure to

Table 1: Acute right ventricular dysfunction definition*.

Echo parameters		ECG signs	Biomarkers
RV systolic function	RV dilation		
TAPSE < 16 mm	ED RVD/LVD ratio > 0.9	Complete RBBB	BNP > 100 pg/mL
S < 10 cm/sec	ED RVA/LVA ratio > 0.6	Incomplete RBBB	NT-proBNP > 900 pg/mL
RV fractional area change < 35%	ED RVD > 42 mm (at the base)	Anteroseptal ST elevation	
RV ejection fraction < 45%	ED RVD > 33 mm (at the middle third of RV)	Anteroseptal ST depression	
	Septal dyskinesia in the RV focused view	Anteroseptal T-wave inversion	

BNP: B-type natriuretic peptide; ED RVD/LVD ratio: end-diastolic RV diameter/LV diameter ratio; ED RVA/LVA ratio: end-diastolic RV area/LV area ratio; ED RVD: end-diastole RV diameter; NT-proBNP: N-terminal pro-BNP; S: pulsed Doppler S wave; TAPSE: tricuspid annular plane systolic excursion. *At least one of the items must be present (echo parameters, ECG signs, and biomarkers) [30].

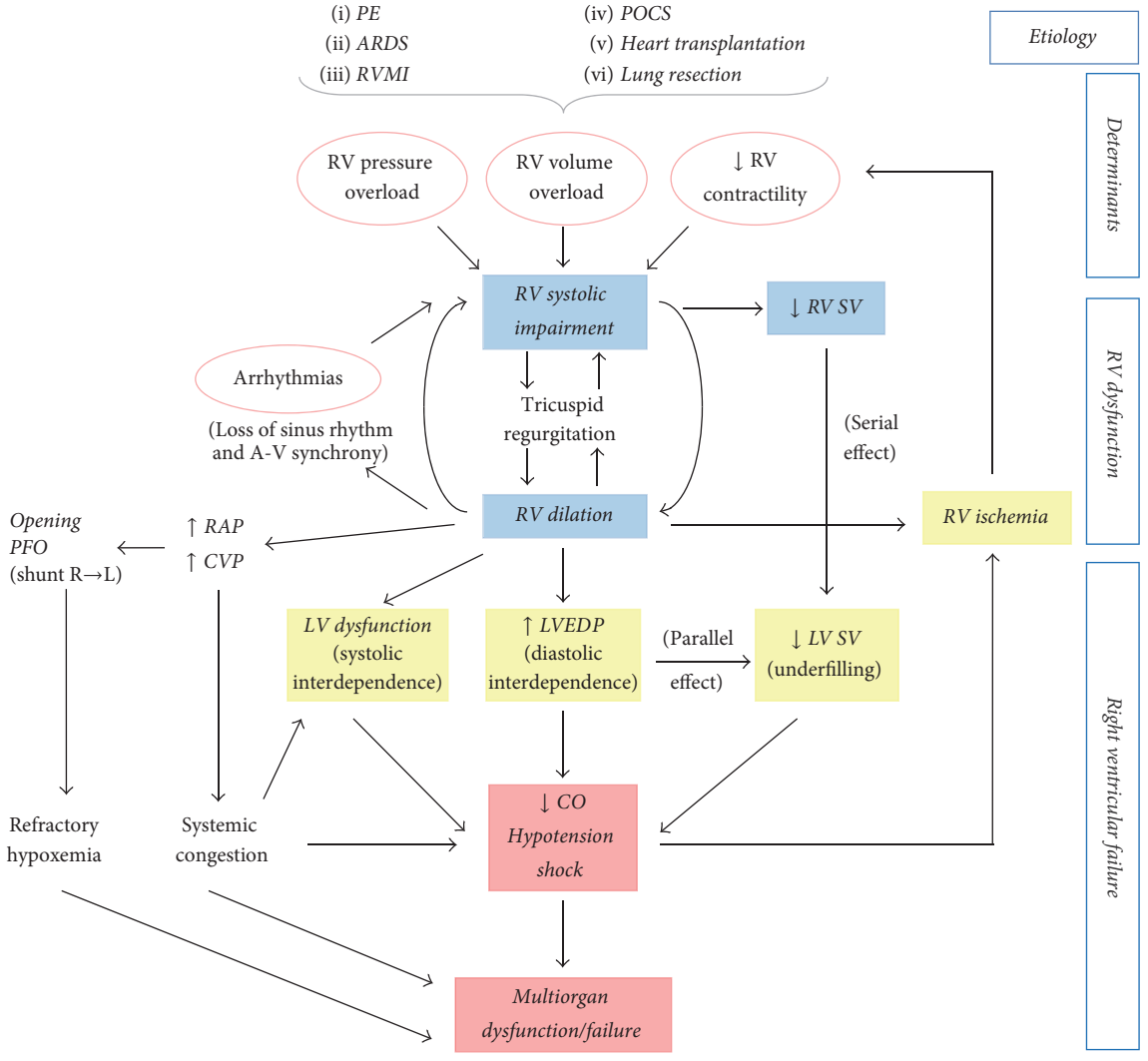

Figure 1: Mechanisms of acute right ventricular dysfunction/failure (RVD/RVF). RV dysfunction begins with excessive increases in preload or afterload or injury that results in decreased contractility. RV ischemia and LV function impairment ensue a vicious cycle worsening hemodynamics and precipitate the transition to RVF. ARDS: acute respiratory distress syndrome; A-V: atrioventricular; CO: cardiac output; CVP: central venous pressure; MI: myocardial infarction; PE: pulmonary embolism; PFO: patent foramen oval; POCS: postoperative cardiac surgery; RAP: right atrial pressure; R → L: right-to-left; SV: stroke volume.

the pulmonary arterial occlusion pressure ≥ 0.8–1.0 with a reduction in the cardiac index.

In the present work, we will focus on the epidemiology, pathophysiology, diagnosis, and treatment of acute RVD/RVF.

2. Epidemiology

Acute RVD is both common and potentially lethal in critically ill patients. Different clinical entities can produce acute RVF in ICU as a consequence of alterations in one or more of the determinants of RV performance (preload, afterload, and contractility). We will discuss the clinically most important etiologies of acute RVD/RVF:

(i) Acute PE is a common cause of acute RVD/RVF due to an excessive increase in afterload secondary to obstruction by clots, vasoconstriction in nonobstructed areas, and intracardiac hemolysis (resulting from the turbulent flow across the pulmonary value). Echocardiographic RVD is present between 30 and 56% of normotensive patients with PE. All-cause mortality rate at 30 days in the patients with confirmed PE was 5.4 to 10%, and in-hospital mortality rate directly attributed to PE was 1.1 to 3.3%, depending on whether it is in-patients versus outpatients registry and the degree of illness [8–11]. Cardiogenic shock occurs in ~5% of acute PE cases with a 90-day mortality rate of more than 50% [12]. In general, in previously healthy and nonremodeled RV-pulmonary unit at least 40% of the cross-sectional area must be obstructed to significantly increase the pulmonary arterial pressure (PAP), and besides RV cannot acutely overcome a systolic PAP more than 50 mmHg [13]. Conversely, acute-on-chronic RVF can tolerate significantly higher PAP [14].

(ii) ARDS is one of the most common entities to challenge the RV. The incidence of acute RVD in ARDS varies from 30 to 56%, depending on the definition criteria of RVD, the severity of lung injury, and ventilatory strategy which is associated with increased 28-day mortality even in the lung-protective mechanical ventilation era and Berlin definition of ARDS [15–17]. Both pulmonary hypertension and RV contractile impairment are the main factors involved in RVD [18, 19]. Mechanisms of ARDS-induced acute RVD include hypoxic/hypercarbic vasoconstriction, an increased alveolar dead space, pulmonary microthrombi, and proinflammatory cytokine activation. A recent study identified four predictors of acute RVD in ARDS: (1) pneumonia-induced ARDS, (2) partial pressure of arterial oxygen/fraction of inspired oxygen ratio < 150 mmHg, (3) partial pressure of carbon dioxide ≥ 48 mmHg, and (4) driving pressure (plateau pressure – total positive end-expiratory pressure) ≥ 18 cmH_2O [17]. Routine echocardiography is recommended in all ARDS patients with a score ≥ 2 (incidence of RVD ≥ 20%) allowing an early implementation of RV-protective strategy that might prevent RVD.

(iii) RV myocardial infarction (RVMI) can be complicated by acute RVD in 30–50% of patients with inferior wall ST-elevation MI. Meanwhile, severe hypotension and low CO are present in 10% on admission in the reperfusion era [19]. The right coronary artery (RCA) usually is the culprit vessel in RVMI, and more extensive RV myocardial necrosis is associated with proximal RCA occlusions [20]. The RV tolerates ischemic injury better than the LV because it has a lower oxygen demand, greater coronary flow reserve, dual, right and left, coronary arteries supply, and homogeneous transmural perfusion across the cardiac cycle [21]. Although RVMI increases the risk of complications in patients with inferior MI, several studies have reported that the acute outcome of patients with RVMI is primarily determined by the amount of accompanying LV necrosis [22].

(iv) Acute RVF is a serious problem after cardiothoracic surgery. It occurs in 0.1% of patients after cardiotomy, in 2-3% of patients undergoing heart transplantation, and in 10–20% of patients needing LV assist device insertion [23]. PH and myocardial depression after cardiopulmonary bypass are usually mild, except in vulnerable patients, to whom it may contribute to postoperative RVF. In the postoperative cardiac surgery (POCS) patient, acute RVD (RV fractional area change ≤ 25% or severe RV dilation) was present in almost half of the patients hemodynamically unstable. Several factors may be implicated to RVD/RVF in the POCS patient: (a) long cardiopulmonary bypass time, (b) right coronary embolism or bypass graft occlusion, (c) inadequate myocardial protection during surgery, (d) reperfusion lung injury with secondary PH, (e) protamine-induced pulmonary hypertension (PH), (f) atrial arrhythmias or loss of atrioventricular synchrony, and (g) preexisting pulmonary vascular disease [24, 25].

(v) The extent of pulmonary parenchymal resection (loss of pulmonary tissue) and the preexisting PVD/RVD predict the risk and severity of postoperative RVD in patients undergoing lung resection. Hypoxia, atelectasis, and hypercarbia may precipitate acute RVD [26].

3. Pathophysiology of Acute RV Dysfunction and Failure

3.1. Anatomy and Mechanics of RV. The anatomy and physiology of the RV are both unique and complex and quite different from LV. In contrast to the ellipsoidal shape of the LV, the RV appears triangular and crescent-shaped. Anatomically, RV can be described regarding three components: (1) the inlet, which consists of the tricuspid valve, chordal tendineae, and papillary muscles; (2) the trabeculated apical myocardium; and (3) the infundibulum, or conus, which corresponds to the outlet region [27]. Data from phylogeny

suggest that the infundibulum can be found as early as in primitive chordates and the RV sinus is found quite later in vertebrates, presumably as an adaptation of the cardiovascular system to air breathing. In crocodiles, venous and arterial circulation diverged for the first time, with an infundibulum incorporated to the RV. In birds and mammals, this incorporation is complete [27, 28]. According to which ontogeny reflects the phylogeny, the infundibulum is present in very early stages of mammalian embryonic development (20 days after fecundation), while the RV sinus develops later (approximately 22 to 24 days after fecundation) [29].

Regarding the myofiber architecture of the heart and according to Torrent-Guasp and other authors, the ventricular myocardium is constituted by a continuous band of muscle that extends from the pulmonary artery root to the aortic root, forming a helical structure with two spirals and delimiting the two ventricular cavities. This myocardial band would be composed of the "basal loop" and the "apical loop." The basal loop is predominantly horizontal and comprises the right and left segments; the apical loop is predominantly vertical and consists of the descending segment ("left septum") and the ascending segment ("right septum") [32–35].

Under normal afterload, RV contraction begins at the sinus (inlet chamber) and progresses toward the conus or infundibulum (outlet chamber) (approximately 25 to 50 ms apart), indicating a peristaltic/asynchronous bellows-like pattern of contraction from apex to base. In contrast, LV contracts in a squeezing/synchronous pattern by twisting and rotational movements from apex to base (likened to wringing a towel) [36]. The RV contracts by three mechanisms: (1) inward movement of the free wall secondary to the contraction of the right segment of the basal loop (transverse orientation), which produces a bellows effect; (2) contraction of the ascending segment of the apical loop (oblique orientation), which shortens the long axis, drawing the tricuspid annulus toward the apex; and (3) traction on the free wall at the points of attachment secondary to LV contraction [37–39]. The shortening of the RV is mainly longitudinal compared to radial, and the sinus chamber made up $81 \pm 6\%$ of the RV end-diastolic volume and $87 \pm 4\%$ of the stroke volume [36].

The low impedance and the high capacitance of the normal pulmonary circulation are reflected in the triangular shape of the RV pressure-volume loop, without distinct periods of isovolumic contraction and relaxation [40–43]. RV ejection begins early during the increase of intraventricular pressure and continues during its fall. This prolonged low-pressure ejection implies that RV emptying is very sensitive to changes in afterload and that RV keeps on ejecting (late phase of ejection) while the LV is in diastole (isovolumic relaxation and rapid filling phases or presuction and suction phases, resp.). It corresponds to the contraction of the ascending segment of the apical loop without opposition of the descending segment that is relaxed (named by Torrent-Guasp "late isovolumetric contraction") [38].

3.2. Pathogenesis of Acute RV Dysfunction and Failure. RV mechanics and function can be altered in the setting of either pressure/volume overload and primary reduction of contractility owing to myocardial ischemia (Figure 1). The compliant and thin walled RV is better suited to accommodate significant increases in preload but tolerates acute increases in afterload poorly.

The heart has intrinsic mechanisms to maintain CO to beat-to-beat changes in preload and afterload by a heterometric dimension adaptation described by Starling's law of the heart. Myocardial stretch elicits a rapid increase in developed force, which is mainly caused by an increase in myofilament calcium sensitivity (Frank-Starling mechanism). In the next 10–15 min, a second gradual increase in force takes place (slow force response), increasing the calcium transient amplitude secondary to a cardiac autocrine-paracrine nongenomic mechanism and named homeometric autoregulation described by Von Anrep more than 100 years ago [44]. Although this homeometric adaptation to afterload has been demonstrated in the RV exposed to pulmonary arterial constriction, RV stroke volume falls sharply beyond mean PAP of 30 mmHg [45]. Our group, working with anesthetized, opened pericardium sheep, observed that the asynchronous and sequential RV contraction with normal afterload changed to a synchronic contraction pattern during acute and moderate PH. RV contraction synchronization allowed RV to increase contractility, keeping both CO and end-diastolic volume constant [46]. In another experimental model of a stepwise increased pulmonary arterial pressure, we showed that the RV could initially (systolic PAP of 30 mmHg) improve its systolic function through an homeometric autoregulation mechanism. When systolic PAP reached 35 mmHg the systolic performance increase was lost, returning to the baseline value and the active diastolic function was impaired without either dilation or significant changes in ventricular compliance. Acute RVF and circulatory collapse came at a systolic PAP > 40 mmHg [47].

Acute adaptation of the RV to PH depends on both the stationary (pulmonary vascular resistance) and the pulsatile (PA stiffness, total pulmonary capacitance, and reflected wave) components of afterload [48]. It should be considered that the dynamic afterload may be different according to the clinical scenarios. We have shown that, during active PH (phenylephrine induced vasoconstriction), the RV pulsatile load was attenuated through preserving proximal PA stiffness and total pulmonary capacitance and decreasing the magnitude of the reflected wave in comparison with isobaric PA banding [49]. Both the PE and the increase of the mPAP secondary to the increase in the left atrial pressure would determine a predominant increase of the pulsatile load unlike the ARDS with an effect preferably on the stationary load [50–53]; therefore the former could present circulatory collapse at a lower mPAP.

RV systolic impairment and dilation emerge once both myocardial intrinsic adapting mechanisms are exhausted. Several molecular and cellular mechanisms have been proposed in the development of acute RVD secondary to PH. RV wall tension increase leads to the cardiomyocyte stress and injury secondary to ischemia, substrate depletion, and mitochondrial energy metabolism impairment [54]. Different amplifying loops have been involved in the contractile dysfunction, enforcing further stress on the remaining

Table 2: Cut-off values of RV structural and functional parameters and RV afterload assessment.

RV structural parameters	RV functional parameters	RV afterload assessment
Basal RV diameter[$] > 42 mm	RV fractional area change ≥ 35%	AccT < 100 msec
RV mid-diameter[$] > 33 mm	MPI[$] > 0.43 (pulsed Doppler); >0.54 (tissue Doppler)	Shape of doppler RV outflow tract envelope[#]:
RV EDD/LV EDD[$] > 0.9	TAPSE[‡] < 16 mm	(i) No notch
RV/LV EDA[$] > 0.6	S wave[°] < 10 cm/s	(ii) Late notch
LV eccentricity index[†] > 1	Peak RV free wall 2D strain[*] > −20%	(iii) Midsystolic notch
McConnell's sign[$]		
RV wall thickness > 5 mm		

AccT: acceleration time of RV outflow tract flow; EDD: end-diastolic diameter; EDA: end-diastolic area; LV: left ventricle; RV: right ventricle; MPI: myocardial performance index (the ratio of the sum of isovolumic contraction plus relaxation time and ejection time intervals); S wave: peak velocity of systolic excursion at the lateral tricuspid annulus; TAPSE: tricuspid annular plane systolic excursion. [#]The presence and position of the systolic notching are related to the pulmonary dynamic afterload severity and RV dysfunction in patients referred for PH [31]. The presence of midsystolic notch is associated with the worst hemodynamic profile. [$]TTE: apical four-chamber; TEE: mid esophageal four-chamber; [†]TTE: parasternal midpapillary short axis; TEE: transgastric midpapillary short axis; [°]TTE: apical four-chamber; TEE: deep transgastric RV; [*]RV-focused four-chamber view. [‡]M-mode imaging at the lateral tricuspid valve plane.

cardiomyocytes. Among them, neutrophil-mediated inflammation secondary to the influx of proinflammatory cells and chemokine/cytokine activation play the main role by producing oxidative damage, cardiomyocyte apoptosis, and direct negative inotropic effects (myosin heavy chain switch and the decrease of myofibrillar sensitivity to calcium). All of them state a proinflammatory phenotype of RV [54–57].

The biochemical and mechanical changes accounting for the transition from acute RVD to failure remain a subject of intense study. Some authors have proposed that acute RV failure begins when the coronary vasodilator reserve is exhausted as a consequence of RV ischemia although it is not possible to discard the concomitant existence of a primary RV failure, related to an overdistension of the ventricle [58, 59]. Another mechanism proposed is LV mechanical dysfunction by ischemia and edema, which can lead to RVD through systolic and diastolic ventricular interdependence [60, 61]. The upstream transmission of LV end-diastolic pressure to left atrial pressure, pulmonary arterial wedge pressure, and mean PAP may approach a 1 : 1 ratio, producing a vicious cycle.

Finally, RV cardiomyocyte ischemia produces another vicious cycle of increased oxygen demand in the setting of decreased oxygen delivery, leading to circulatory collapse and multiorgan failure (Figure 1).

4. Clinical Presentation and Diagnosis of RVD/RVF in ICU

The clinical presentation of acute RVF varies depending on the underlying cause, the presence of comorbidities, and the cardiovascular reserve of the right ventricle-arterial unit. It can occur suddenly or catastrophic in a previously "healthy heart" or in a hidden way, worsening of compensated RVD in the setting of a chronic heart and lung disease. The diagnosis of acute RVF in ICU patients can become very difficult due to the presence of comorbid conditions that may cause organ hypoperfusion even in the absence of RVD (e.g., sepsis, LV dysfunction, and hypovolemia).

Clinical clues and ECG signs of acute RVD are varied and limited by a low sensitivity and specificity. Therefore, diagnosis typically relies on echocardiography. The ascendance of intensivist-conducted echocardiography has become important not only for early detecting acute RVD in ICU patients but also for monitoring and guiding a rational therapy preventing RVF from occurring.

4.1. The Role of Echocardiography. Measurements by two-dimensional echocardiography (2DE) are challenging becaus e of the complex three-dimensional geometry of the RV and sonographic interference from the lungs. While transthoracic echocardiography (TTE) provides adequate imaging in 99% of critically ill patients for diagnosing acute RVD and cardiac cause of shock [62], transesophageal echocardiography (TEE) is adequately suited for identification of ACP and patent foramen ovale [63, 64].

Multiple views are required to an accurate assessment of RV structure and function. We can resume the following views to be used in ICU patients: the parasternal long and short axis, apical four-chamber, and subcostal four-chamber views on TTE and mid-esophageal four-chamber, RV inflow-outflow, and transgastric short axis views on TEE [6, 30, 65, 66].

It is advisable to gather three groups of parameters (Table 2):

(i) RV structural parameters: linear and areas measurements to assess RV dilation (absolute and relative to LV) predominantly at inlet chamber

(ii) RV functional parameters: predominantly global longitudinal systolic function (since shortening of the RV is greater longitudinally than radially, drawing the tricuspid annulus toward the apex)

(iii) RV afterload assessment.

4.2. Pulmonary Artery Catheter (PAC). Given the potential risks of placing a PAC and the availability of bedside echocardiography, the use of PAC is much less common nowadays. In general, invasive monitoring should be reserved for those patients with echocardiographic evidence of severe RVD at risk of acute RVF or patients with established RVF, since we can perform repeated measurements rapidly [67].

The usual PAC findings suggestive of acute RVD include an elevated CVP (greater than 20 mmHg), an inverse pressure gradient (CVP > PAWP), and a low cardiac index (<2 L/min/m^2), stroke volume index (<30 mL/m^2), and mixed-venous oxygen saturation (SvO_2 < 55%) [68, 69].

One of the challenges of using PAC is the accuracy and precision of PAWP assessment due to the influence of respirophasic effects of mechanical ventilation, end-expiratory versus mean digital measurements, the volume of balloon inflation, and increase extension of zones 1 and 2 (West) [70, 71]. We should be aware that when PEEP is higher than 10 cm H_2O, PAWP is higher than LV end-diastolic pressure.

In summary, combining the use of real-time echocardiographic evaluation bedside with the knowledge of RV physiology is the desirable way to diagnose acute RVD/RVF in ICU patients. PAC might contribute to the monitoring and adjustment of the treatment.

5. Treatment

Effective treatment of acute RVF requires a skilled multidisciplinary team to rapidly assess and triage the patient. The treatment of acute RVD can be divided into the following bundles: (a) general measures including avoiding increasing RV afterload, decreasing RV contractility and optimization of RV preload, applying an "RV-protective" ventilation strategy, and maintaining sinus rhythm and atrioventricular synchrony; (b) pharmacological treatment with a guided inotropic and vasoactive supports; (c) mechanical circulatory support devices. Real-time monitor with bedside echocardiography assessment and the invasive hemodynamic monitoring remain the most valuable methods to guide a rational therapy of acute RVD/RVF in critically ill patients.

5.1. General Measures. The prevention of acute RVF in ICU begins with the identification of high-risk patients, for example, patients with severe ARDS and inferior AMI and patients undergoing cardiac surgery with long cardiopulmonary bypass times and receiving cardiac allografts with either long ischemic time or mismatched in size. Once the severe RVD or RVF is recognized, we have to identify and treat any underlying reversible conditions that are either primarily responsible for (triggering factors) or contributing to the progressive impairment of RV function.

Proper management of *volume status* is essential for the failing RV, as both hypovolemia and hypervolemia may result in reduced CO. The RV has a flatter function curve than the LV, meaning that there is less change in RV performance over a wide range of filling pressures. When volume overload is present, the use of diuretics or renal replacement therapy is required [14]. Continuous infusion of diuretics may be preferable over bolus dosing, and the combination of a loop diuretic with a thiazide-like diuretic is indicated whenever diuretic resistance is suspected [72]. Overdiuresis may also be detrimental to RV function, leading to reduced CO, prerenal azotemia, and systemic hypotension.

We should be aware of the limitation of the dynamic fluid responsiveness predictors in fluid management whenever RV dysfunction is present. It is well known that the presence of RV failure should be suspected when a patient has significant variations of stroke volume or pulse pressure but does not respond to fluids [73]. However, the performance of the stroke volume variation and pulse pressure variation could depend on the volume status: during normovolemia their high values failed to predict volume responsiveness (false positive) [74]; by contrast, during hypovolemia their normal values predict volume unresponsiveness (true negative), avoiding dangerous fluid loading [75].

Besides, RV preload requirements differ substantially based on whether afterload is normal or increased. When acute RVD occurs in the setting of increased RV afterload, we should be restrictive with volume management. Increasing blood volume to an already overloaded RV (e.g., PE, ARDS) will not only improve perfusion but also impair CO, aggravating RV dilatation, increasing tricuspid regurgitation and right-sided venous congestion and subsequent underfilling of the LV (ventricular interdependence and serial effect), all of which will lead to hypoperfusion and multiorgan dysfunction. On the contrary, when acute RVD occurs in the setting of normal pulmonary vascular resistance (e.g., RV myocardial infarction), we can be more liberal with fluid reposition to maintain CO. Some authors have proposed a mini-fluid challenge (100 mL of colloid or crystalloid fluid over 1 minute) as a safer and rational approach in some clinical scenarios (e.g., ARDS) [76].

The dominant RV effects of *mechanical ventilation* are to reduce the preload and raise the afterload, which in the setting of acute RVD may be a critical issue. The ventilatory strategy is the main nonpharmacological treatment of the RV afterload through the control of hypoxemia, hypercapnia, acidemia, and inspiratory airway pressure. The main principles of mechanical ventilation for patients with acute RVD include (a) limiting tidal volume and PEEP, therefore limiting plateau (<27 cmH_2O) and driving pressures (<18 cmH_2O), (b) avoiding hypercapnia (<60 mmHg) and acidosis, and (c) preventing or reversing hypoxic pulmonary vasoconstriction [30]. Additionally, in ARDS, the presence of RVD (hemodynamic status) and not PaO_2/FiO_2 ratio could be an indication for proning to unload the RV by recruiting collapsed alveoli without causing overdistention and reducing airway pressure and hypercapnia ("RV-protective" ventilation strategy) [77–79].

Right atrial contraction contributes up to 40% of RV filling and is more important when the RV compliance is impaired (e.g., RV dilatation). Appropriate sinus heart rate and rhythm, and the maintenance of atrioventricular synchrony and atrial kick, can be among the simplest methods of maintaining and avoiding RV contractility impairment. Electrical or pharmacological cardioversion for the restoration of sinus rhythm and the placement of a temporary pacemaker if heart block is present should be considered [80].

5.2. Pharmacological Treatment. The pharmacological treatment will be focused on reducing the RV afterload and preserving an appropriate systemic pressure (vasoactive support) and increasing the RV contractility (inotropes drug therapy). The ideal cardiovascular drug for use in acute RVF would

Table 3: Cardiovascular drugs for the management of acute RVF.

Agent	Receptors agonism					Cardiovascular properties				
	α1	β1	β2	D	V1	CI	PVR	SVR	PVR/SVR	↑ HR
Vasopressors										
Norepinephrine	++	+				+	+	++	−/+	+
Phenylephrine	++					−	++	+	+	−
AVP (0.01–0.03 UI/min)				+	+	+/−	+/−	++	−	−
Inotropes										
Epinephrine	++	++	+			++	−	++	−	++
Dopamine										
<5 μg/kg/min		+		++		+	−	−	−	+
5–10 μg/kg/min	+	++		++		+	+	+	+/−	+
>10 μg/kg/min	++	++		++		+	+	++	+	+
Dobutamine		++	+			++	−	−	−	+
Inodilators										
Milrinone						++	−	−	−	+/−
Levosimendan						++	−	−	−	+

α1, β1, and β2: adrenergic receptors; D: dopaminergic receptor; V1: vasopressin receptor; +: low-moderate affinity; ++: moderate-high affinity; AVP: arginine vasopressin; CI: cardiac index; PVR and SVR: pulmonary and systemic vascular resistance; HR: heart rate. Drugs in italic are the most preferable. −: neutral effect.

be an agent that enhances systemic arterial pressure and RV contractility without raising pulmonary vascular resistance (PVR). In summary, the pharmacological treatment should provide the following properties: (1) a predominant inotropic property, (2) avoiding pulmonary vasoconstriction, preferably vasodilation, and (3) maintaining systemic perfusion pressure (which is fundamental to RV coronary perfusion) with an adequacy of perfusion (venous oximetry, stroke volume, and CO) [34].

Regarding the *vasopressor support*, the primary objectives are to avoid systemic hypotension, achieving systemic pressure higher than the pulmonary pressure and an optimal PVR/SVR (PVR/systemic vascular resistance) ratio (Table 3). Norepinephrine and a low dose of vasopressin are the preferable drugs (Table 3). Except at high doses, norepinephrine has been shown to increase SVR while reducing pulmonary arterial pressure and PVR/SVR ratio (doses less than 0.5 μg/kg/min) [81]. Norepinephrine is also positively inotropic through the β1 adrenergic agonism, increasing cardiac index and improving RV-pulmonary coupling in studies of RVD secondary to PH [14, 82]. Arginine vasopressin (<0.03 U/min) is another vasopressor that preferentially increases SVR over PVR. At higher doses, it should be used with caution since it increases PVR and causes dose-related adverse myocardial effects and coronary vasoconstriction [83]. Phenylephrine improves right coronary perfusion in RVF, although this benefit may be offset by worsening RV function due to increased PVR, and it is not recommended [59, 84].

The next major goal is to improve RV myocardial contractility by using *inotropes*. Dobutamine has favorable pulmonary vascular effects at lower doses (<5 μg/kg/min), although it leads to increased PVR, tachycardia, and systemic hypotension at doses exceeding 10 μg/kg/min [85]. If hypotension occurs, it should be used in combination with vasopressors agents, such as norepinephrine.

Both dopamine and epinephrine are not recommended for tachycardia, arrhythmic events, and an increase in the myocardial oxygen consumption. At moderate-high doses of dopamine, PVR/SVR ratio increases [86] (Table 3).

Among *inodilators* (inotropic and vasodilatory properties), both milrinone and levosimendan have been recommended for acute RVD treatment. Milrinone is a bipyridine phosphodiesterase III inhibitor that prevents the degradation of cyclic AMP increasing the intracellular calcium influx such that myocardial contractility improved. Similar to dobutamine, systemic vasodilatation may limit its use. This effect is minimized by the use of inhaled milrinone (Figure 2). Milrinone is usually used in patients with mild-to-moderate RVD undergoing cardiac surgery, but without severe hypotension [25, 87]. Levosimendan is a calcium sensitizer that enhances cardiac contractility without increasing oxygen consumption by increasing calcium sensitivity of cardiomyocyte contractile apparatus during systole, without increasing intracellular calcium concentration, resulting in the acceleration of actin-myosin cross bridge formation rate without prolonging relaxation time (positive lusitropy). It also opens sarcolemma K channels and calcium desensitization in smooth muscle cells, determining vasodilatation in different vascular beds. The opening of mitochondrial inner membrane K_{ATP} channels in cardiomyocytes may be protective for the energy production during ischemia-reperfusion, by preventing mitochondrial calcium overload and preserving high-energy phosphates [88–90]. Among different experimental models, levosimendan improves RV-arterial coupling in acute RVF more than dobutamine [91–93]. We have shown that levosimendan increased RV contractility and improved RV diastolic function and RV-arterial coupling in an experimental model of

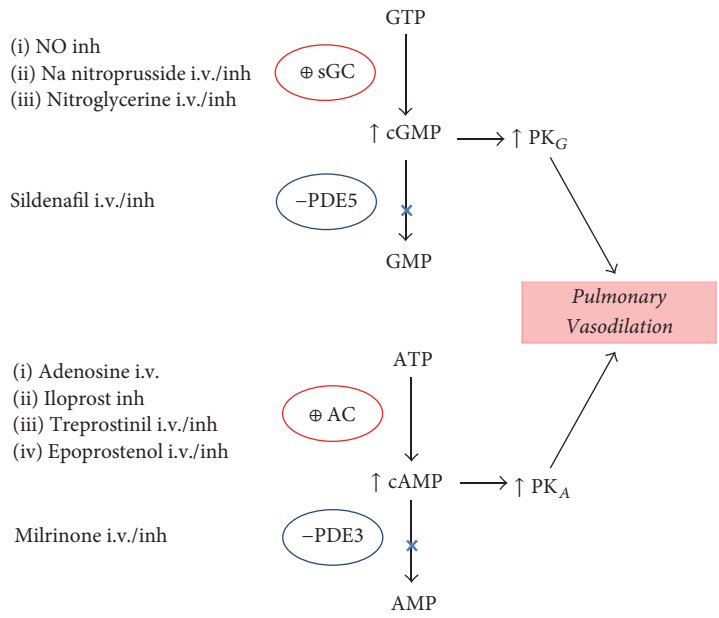

Figure 2: Pulmonary vasodilators drugs, pathways, and mechanisms of action. AC: adenylate cyclase; sGC: soluble guanylate cyclase; ATP and GTP: adenosine and guanosine triphosphate, respectively; cAMP and cGMP: cyclic adenosine and guanosine monophosphate, respectively; inh: inhaled; i.v.: intravenous; NO: nitric oxide; −PDE: phosphodiesterase inhibitor; PK: protein kinase; ⊕: stimulator.

normotensive PE. This was associated with an improvement of myocardial RV energy status, decreasing the myocardial protein carbonylation [57]. Very recently, in a rodent PE model, we have reported that levosimendan is a more specific vasodilator of resistance PA with a similar relaxant potency to mesenteric arteries, which is preserved after PE but significantly reduced during hypoxia [94]. These novel effects could improve the RV-arterial coupling and preserve an adequate ventilation/perfusion ratio, respectively, during PH treatment. Among clinical scenarios, levosimendan improves RV function and decreases PVR in ischemic RVF and ARDS and after mitral valve replacement surgery [95, 96]. Early perioperative levosimendan treatment in cardiac surgery patients with severely impaired perioperative medical condition appears to reduce mortality and morbidity, and a recent European expert opinion was suggested that the optimal time point for initiation levosimendan (0.1 μg/kg/min) is the day before cardiac surgery [97, 98]. However, very recently, two large, randomized, placebo-controlled trials of levosimendan in patients undergoing cardiac surgery have shown no clear advantage over conventional inotropic drugs for the management of perioperative low cardiac output syndrome [99, 100].

Specific *pulmonary vasodilators* may be useful to reduce RV afterload in acute RVD settings particularly whenever pulmonary remodeling is suspected or confirmed. Exclusion of an isolated pulmonary venous pressure elevation is important, as increased transpulmonary flow may precipitate pulmonary edema [101]. Systemic administration of pulmonary vasodilators may decrease systemic blood pressure, potentially reducing RV preload and worsening RV ischemia. They also can worsen oxygenation by blunting hypoxic pulmonary vasoconstriction and impairing ventilation-perfusion matching. Therefore, the use of inhaled rather than systemic pulmonary vasodilators is strongly recommended [102]. Pulmonary vasodilator therapy relies on three pathways: nitric oxide (NO) donors (guanylate cyclase (GC) stimulators), adenylate cyclase (AC) stimulators, and phosphodiesterase (PDE) inhibitors (Figure 2).

Inhaled NO (iNO) is a potent pulmonary vasodilator at concentrations from 5 to 40 parts per million with a rapid onset of action and very short half-life, making it an ideal agent for management of PH and/or hypoxemia in critically ill patients in whom lowering PAP and improving RV function is paramount (e.g., ARDS, POCS, and heart transplantation) [103–105]. While iNO is the "gold standard" for pulmonary-specific PH treatment, clinicians have been interested in developing less expensive alternatives (Figure 2) [106].

The use of other currently available pulmonary vasodilators, such as the endothelin receptor antagonists (ERA) and the recently approved soluble guanylate cyclase stimulator, riociguat, should probably be avoided in acute RVF due to concerns about unreliable oral absorption. ERA use in the ICU is limited by the potential hepatotoxicity and riociguat may have significant systemic vasodilator effects, especially under conditions such as sepsis. However, oral pulmonary vasodilators can be useful when patients have become hemodynamically stable, and the medical team is planning to withdraw parenteral or inhalation agents, avoiding the rebound of PH [107]. In general, phosphodiesterase type 5 inhibitor (sildenafil) is the preferred agent due to the vast clinical experience [108, 109].

5.3. Mechanical Circulatory Support. Despite optimal medical management, some patients fail to improve and require implantation of a mechanical circulatory support device.

Table 4: Differences between venoarterial and venovenous extracorporeal membrane oxygenation (ECMO).

Venoarterial ECMO	Venovenous ECMO
Higher PaO_2 is achieved	Lower PaO_2 is achieved
Lower perfusion rates are needed	Higher perfusion rates are needed
Bypasses pulmonary circulation	Maintains pulmonary blood flow
Decreases pulmonary artery pressures	Elevates mixed venous PO_2
Provides cardiac support to assist systemic circulation	Does not provide cardiac support to assist systemic circulation
Requires arterial cannulation	Requires only venous cannulation

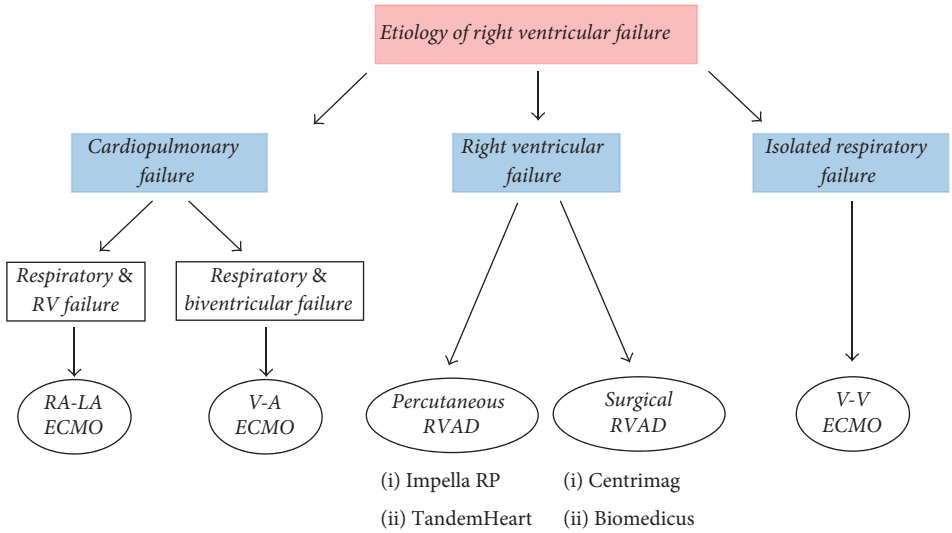

Figure 3: Schematic algorithm for selecting the appropriate extracorporeal life support in patients with refractory right ventricular failure. RA-LA: right atrial-left atrial; RVAD: right ventricular assist device; V-A: venoarterial; V-V: venovenous; ECMO: extracorporeal membrane oxygenation.

The RV may exhibit a greater capacity for rapid recovery compared with the LV. Recent literature suggests that 42% to 75% of patients with acute RVF recover hemodynamic and functional status enabling device explantation [110]. The use of extracorporeal life support provides hemodynamic and/or respiratory support in the acute setting, allowing for resolution of a potentially reversible process (bridge to recovery), or bridging who are candidates for transplantation. Options for long-term mechanical circulatory support (destination therapy) are lacking [111, 112]. One of the most important determinants of success is the correct timing of implantation to avoid significant, potentially irreversible end-organ injury [111].

Two types of mechanical circulatory assistance have been described in the setting of RVF: (a) RV assist devices (RVAD) and (b) extracorporeal membrane oxygenation (ECMO) [113]. RVAD may be required whenever there is isolated acute RVD/RVF refractory to medical therapy, to sustain the failing RV. All serve to unload and bypass the RV and can be percutaneously (Impella RP®, TandemHeart®) or surgically (Centrimag®, Biomedicus®) implanted [114]. Among the clinical situations to be RVAD considered, we highlight RV myocardial infarction, PE, myocarditis, and postoperative low cardiac output syndrome, following LV assist device implantation or primary graft failure after heart transplantation [66]. Bleeding or thrombus formation is the most common complication related to RVADs [115]. ECMO support with either peripheral or central cannulation is indicated whenever respiratory failure is present while awaiting pulmonary recovery, with or without RVF or biventricular failure. ECMO configuration may be venovenous (VV-ECMO) or venoarterial (VA-ACMO) which present different properties and indications (Table 4) (Figure 3). Infections, the formation of thrombus around the cannulae, and limb hypoperfusion are typical complications of ECMO. Each mechanical circulatory support device should only be used in carefully selected patients (Figure 3).

There was a lack of large comparison groups of patients with RVF managed with medical treatment only, RVADs, or ECMO. A prospective study that includes a clear definition of refractory RVF, guidelines for device use, and appropriate control groups is required.

5.4. Targeted Management in Specific Clinical Scenarios. We have described general management considerations for critically ill patients with acute RVF. A key principle in the management of acute RVD focuses on determination and treatment of the underlying etiology [80]. We briefly review targeted therapy for some specific causes of acute RVF (Table 5).

Table 5: Mechanisms and targeted management in specific clinical scenarios of acute RV failure.

Clinical scenario	Mechanism	Treatment
Right ventricular infarct	Decreased RV contractility	Early myocardial reperfusion (percutaneous coronary intervention, systemic thrombolysis)
Pulmonary embolism	Increase RV afterload (mechanical obstruction & vasoconstriction)	Systemic anticoagulation, systemic or catheter-directed thrombolysis, embolectomy
Decompensated PAH	Increase RV afterload	Parenteral prostanoids (with or without inhaled pulmonary vasodilators
ARDS	Increasing RV afterload/decreasing RV contractility	Limiting VT and PEEP, avoiding hypoxia, hypercapnia, and acidosis
Noncardiac surgery	Acute PH, decreasing RV contractility (RV infarct)	Pulmonary vasodilators, myocardial reperfusion, inotropic drugs
Cardiac surgery	Volume overload, myocardial ischaemia, preexisting RVD, arrhythmias	Diuretics, inotropic drugs, cardioversion, antiarrhythmic drugs

ARDS: acute respiratory distress syndrome; PAH: pulmonary arterial hypertension; RVD: right ventricular dysfunction.

Early myocardial reperfusion of patients with *RV myocardial infarct* (preferably with primary percutaneous coronary intervention) may lead to immediate improvement and later complete recovery of RV function and a better outcome [116]. Unlike the LV, the RV may remain viable for days after an MI [117]. So, late reperfusion is a valid option to consider in patients with acute inferior MI complicated by RVD.

RVF is the principal determinant of early mortality in the acute phase of *pulmonary embolism*. Unless contraindications exist, acute PE is treated with anticoagulation. Based on the contemporary risk classification, "high-risk" patients (persistent arterial hypotension or shock caused by overt RVF) and "intermediate-high-risk" patients (normotensive patients with a high clinical prognostic score plus imaging and biochemical markers of RV function) if RV dysfunction leads to hemodynamic decompensation, reperfusion treatment, preferably systemic (i.v.) thrombolysis, is recommended [3]. Surgical pulmonary embolectomy is an alternative therapy for hemodynamically unstable patients with high-risk PE (particularly if thrombolysis is contraindicated or has failed) and for intermediate high-risk patients in whom hemodynamic decompensation appears imminent, and the bleeding risks of thrombolysis are high [3]. Pharmacomechanical fibrinolysis (catheter-directed fibrinolysis through a multiside hole catheter placed into the thrombus) is another option in these clinical scenarios [118].

Patients with previously unknown *pulmonary arterial hypertension* (PAH) are occasionally seen for the first time in the ICU. Possible triggers for acute RVF in patients with PAH should be actively identified, as their presence will impact clinical management. The most frequent causes are infection/sepsis, supraventricular arrhythmias, anemia with iron deficiency, and nonadherence to or withdrawal from chronic PAH treatment. As we previously mentioned, hypoxia and hypercapnia, as well as acidosis and hypothermia, are precipitating factors of RVF by promoting pulmonary vasoconstriction and the further increase of PAP. Positive pressure ventilation should be avoided because it increases RV afterload and the sedatives should be used with caution because they may lead to systemic hypotension [119]. Fluid status should be closely monitored; if signs of venous and systemic congestion are present, intravenous diuretics should be the first option, followed by renal replacement therapy in patients with diuretic resistance. Parenteral prostanoids are the first-line therapy to achieve a safe reduction of RV afterload. Inhaled pulmonary vasodilators can be used in combination with i.v. therapy to avoid systemic hypotension [107, 120]. In very specific cases, balloon atrial septostomy can be useful to decompresses RV and improve LV filling and CO [121]. It is not recommended in patients with right atrial pressure > 20 mmHg or arterial oxygen saturation < 85% at rest in room air [121].

Acute respiratory distress syndrome is the main cause of acute RVF encountered in ICU. Mechanical ventilation can contribute to an uncoupling between pulmonary circulation and the RV, predisposing to the RVF. A protective ventilation strategy with focus on maintaining plateau pressure < 27 cmH_2O and partial pressure of arterial carbon dioxide < 60 mmHg, adapting positive end-expiratory pressure to RV function, and considering prone positioning for PaO_2/fraction of inspired oxygen < 150 mmHg has been recommended to prevent acute RV failure or ameliorate its complications [122].

In *noncardiac surgery*, perioperative RV failure is most often, although not exclusively, secondary to acute pulmonary hypertension (increased afterload). In *cardiac surgery*, RV failure is also frequently caused by volume overload, myocardial ischemia, preexisting RV dysfunction, or arrhythmias [25].

Right-sided valvular diseases have a significant and independent impact on morbimortality. Right-sided infective endocarditis accounts for 5–10% of all cases of infective endocarditis and may occur in native valves (intravenous drug abusers), prosthetic valves, congenital heart defects, and implanted devices (e.g., pacemaker) [123]. Surgery is recommended for patients with RVF, severe tricuspid regurgitation, and poor response to diuretics, large vegetation, and recurrent emboli.

6. Conclusions

Acute RVD/RVF is seen with increasing frequency in the intensive care unit and causes or aggravates many common critical diseases.

Bedside echocardiography assessment and invasive hemodynamic monitoring remain the most valuable methods to diagnose and to guide a rationale therapy of acute RVD/RVF in critically ill patients.

General precautionary measures, early diagnosis of RVD, and etiology-specific therapy may reduce the appearance of RVF. Supportive therapies focused on improving RV function via optimization of preload, enhancing contractility, and reducing afterload are the key principles in the management of acute RVF.

Future research should focus on better understanding the cellular and molecular mechanisms of acute RV cardiac dysfunction to develop novel therapies that directly target the injured myocardium.

Conflicts of Interest

The authors declare that there are no conflicts of interest regarding the publication of this paper.

References

[1] M. R. Mehra, M. H. Park, M. J. Landzberg, A. Lala, and A. B. Waxman, "Right heart failure: toward a common language," *The Journal of Heart and Lung Transplantation*, vol. 33, no. 2, pp. 123–126, 2014.

[2] M. R. Jaff, M. S. McMurtry, S. L. Archer et al., "Management of massive and submassive pulmonary embolism, iliofemoral deep vein thrombosis, and chronic thromboembolic pulmonary hypertension: a scientific statement from the American Heart Association," *Circulation*, vol. 123, no. 16, pp. 1788–1830, 2011.

[3] S. V. Konstantinides, A. Torbicki, and G. Agnelli, "2014 ESC guidelines on the diagnosis and management of acute pulmonary embolism," *European Heart Journal*, vol. 35, no. 43, pp. 3033–3073, 2014.

[4] G. Coutance, E. Cauderlier, J. Ehtisham, M. Hamon, and M. Hamon, "The prognostic value of markers of right ventricular dysfunction in pulmonary embolism: A meta-analysis," *Critical Care*, vol. 15, no. 2, article no. R103, 2011.

[5] L. G. Rudski, W. W. Lai, J. Afilalo et al., "Guidelines for the echocardiographic assessment of the right heart in adults: a report from the American Society of Echocardiography endorsed by the European Association of Echocardiography, a registered branch of the European Society of Cardiology, and the Canadian Society of Echocardiography," *Journal of the American Society of Echocardiography*, vol. 23, no. 7, pp. 685–713, 2010.

[6] R. M. Lang, L. P. Badano, V. Mor-Avi et al., "Recommendations for cardiac chamber quantification by echocardiography in adults: an update from the American Society of Echocardiography and the European Association of Cardiovascular Imaging," *J Am Soc Echocardiogr*, vol. 28, no. 1, pp. 39–e14, 2015.

[7] A. R. Cucci, J. A. Kline, and T. Lahm, "Acute Right Ventricular Failure," in *The Right Ventricle in Health and Disease*, N. F. Voelkel and D. Schranz, Eds., Respiratory Medicine, pp. 161–205, Springer New York, New York, NY, USA, 2015.

[8] M. Miniati, S. Monti, L. Pratali et al., "Value of transthoracic echocardiography in the diagnosis of pulmonary embolism: results of a prospective study in unselected patients," *American Journal of Medicine*, vol. 110, no. 7, pp. 528–535, 2001.

[9] C. V. Pollack, D. Schreiber, S. Z. Goldhaber et al., "Clinical characteristics, management, and outcomes of patients diagnosed with acute pulmonary embolism in the emergency department: Initial report of EMPEROR (multicenter emergency medicine pulmonary embolism in the real world registry)," *J Am Coll Cardiol*, vol. 57, no. 6, pp. 700–706, 2011.

[10] S. Laporte, P. Mismetti, H. Décousus et al., "Clinical predictors for fatal pulmonary embolism in 15,520 patients with venous thromboembolism: findings from the Registro Informatizado de la Enfermedad TromboEmbolica venosa (RIETE) registry," *Circulation*, vol. 117, no. 13, pp. 1711–1716, 2008.

[11] S. Z. Goldhaber, L. Visani, and M. de Rosa, "Acute pulmonary embolism: clinical outcomes in the International Cooperative Pulmonary Embolism Registry (ICOPER)," *The Lancet*, vol. 353, no. 9162, pp. 1386–1389, 1999.

[12] N. Kucher, E. Rossi, M. De Rosa, and S. Z. Goldhaber, "Massive pulmonary embolism," *Circulation*, vol. 113, no. 4, pp. 577–582, 2006.

[13] Y. M. Smulders, "Pathophysiology and treatment of haemodynamic instability in acute pulmonary embolism: the pivotal role of pulmonary vasoconstriction," *Cardiovascular Research*, vol. 48, no. 1, pp. 23–33, 2000.

[14] L. C. Price, S. J. Wort, S. J. Finney, P. S. Marino, and S. J. Brett, "Pulmonary vascular and right ventricular dysfunction in adult critical care: current and emerging options for management: a systematic literature review," *Critical Care*, vol. 14, no. 5, article R169, 2010.

[15] A. Vieillard-Baron, J.-M. Schmitt, R. Augarde et al., "Acute cor pulmonale in acute respiratory distress syndrome submitted to protective ventilation: incidence, clinical implications, and prognosis," *Critical Care Medicine*, vol. 29, no. 8, pp. 1551–1555, 2001.

[16] S. K. Wadia, T. G. Shah, G. Hedstrom, J. A. Kovach, and R. Tandon, "Early detection of right ventricular dysfunction using transthoracic echocardiography in ARDS: a more objective approach," *Journal of Echocardiography*, vol. 33, no. 12, pp. 1874–1879, 2016.

[17] A. Mekontso Dessap, F. Boissier, C. Charron et al., "Acute cor pulmonale during protective ventilation for acute respiratory distress syndrome: prevalence, predictors, and clinical impact," *Intensive Care Medicine*, vol. 42, no. 5, pp. 862–870, 2016.

[18] V. Zochios, K. Parhar, W. Tunnicliffe, A. Roscoe, and F. Gao, "The right ventricle in acute respiratory distress syndrome," *Chest*, vol. 152, no. 1, pp. 181–193, 2017.

[19] H. Bueno, R. López-Palop, E. Pérez-David, J. García-García, J. L. López-Sendón, and J. L. Delcán, "Combined effect of age and right ventricular involvement on acute inferior myocardial infarction prognosis," *Circulation*, vol. 98, no. 17, pp. 1714–1720, 1998.

[20] R. O'Rourke and L. J. Dell'Italia, "Diagnosis and management of right ventricular myocardial infarction," *Current Problems in Cardiology*, vol. 29, no. 1, pp. 6–47, 2004.

[21] S. B. Laster, T. J. Shelton, B. Barzilai, and J. A. Goldstein, "Determinants of the recovery of right ventricular performance following experimental chronic right coronary artery occlusion," *Circulation*, vol. 88, no. 2, pp. 696–708, 1993.

[22] M. Zehender, W. Kasper, E. Kauder et al., "Right ventricular infarction as an independent predictor of prognosis after acute inferior myocardial infarction," *The New England Journal of Medicine*, vol. 328, no. 14, pp. 981–988, 1993.

[23] T. Kaul and B. L. Fields, "Postoperative acute refractory right ventricular failure: incidence, pathogenesis, management and prognosis," *Cardiovascular Surgery*, vol. 8, no. 1, pp. 1–9, 2000.

[24] G. J. Vlahakes, "Right ventricular failure after cardiac surgery," *Cardiology Clinics*, vol. 30, no. 2, pp. 283–289, 2012.

[25] F. Haddad, P. Couture, C. Tousignant, and A. Y. Denault, "The right ventricle in cardiac surgery, a perioperative perspective: II. pathophysiology, clinical importance, and management," *Anesthesia & Analgesia*, vol. 108, no. 2, pp. 423–433, 2009.

[26] D. Amar, H. Zhang, A. Pedoto, D. P. Desiderio, W. Shi, and K. S. Tan, "Protective lung ventilation and morbidity after pulmonary resection," *Anesthesia & Analgesia*, vol. 125, no. 1, pp. 190–199, 2017.

[27] A. Farb, A. P. Burke, and R. Virmani, "Anatomy and pathology of the right ventricle (including acquired tricuspid and pulmonic valve disease)," *Cardiology Clinics*, vol. 10, no. 1, pp. 1–21, 1992.

[28] R. Van Praagh and S. Van Praagh, "Morphologic Anatomy," in *Nadas' Pediatric Cardiology*, D. C. Fyler, Ed., pp. 17–26, Hanley & Belfus, Inc, London, UK, 1992.

[29] M. Ridley, "Macroevolutionary Change," in *Evolution*, M. Ridley, Ed., pp. 582–609, Blackwell Science, USA, 1996.

[30] S. Krishnan and G. A. Schmidt, "Acute right ventricular dysfunction: Real-time management with echocardiography," *Chest*, vol. 147, no. 3, pp. 835–846, 2015.

[31] J. S. Arkles, A. R. Opotowsky, J. Ojeda et al., "Shape of the right ventricular Doppler envelope predicts hemodynamics and right heart function in pulmonary hypertension," *American Journal of Respiratory and Critical Care Medicine*, vol. 183, no. 2, pp. 268–276, 2011.

[32] G. D. Buckberg, "Basic science review: the helix and the heart," *The Journal of Thoracic and Cardiovascular Surgery*, vol. 124, no. 5, pp. 863–883, 2002.

[33] F. Torrent-Guasp, M. Ballester, G. D. Buckberg et al., "Spatial orientation of the ventricular muscle band: physiologic contribution and surgical implications," *The Journal of Thoracic and Cardiovascular Surgery*, vol. 122, no. 2, pp. 389–392, 2001.

[34] M. J. Kocica, A. F. Corno, F. Carreras-Costa et al., "The helical ventricular myocardial band: global, three-dimensional, functional architecture of the ventricular myocardium," *European Journal of Cardio-Thoracic Surgery*, vol. 29, no. 1, pp. S21–S40, 2006.

[35] F. Poveda, D. Gil, E. Martí, A. Andaluz, M. Ballester, and F. Carreras, "Helical structure of the cardiac ventricular anatomy assessed by diffusion tensor magnetic resonance imaging with multiresolution tractography," *Revista Española de Cardiología (English ed.)*, vol. 66, no. 10, pp. 782–790, 2013.

[36] T. Geva, A. J. Powell, E. C. Crawford, T. Chung, and S. D. Colan, "Evaluation of regional differences in right ventricular systolic function by acoustic quantification echocardiography and cine magnetic resonance imaging," *Circulation*, vol. 98, no. 4, pp. 339–345, 1998.

[37] N. Hristov, O. J. Liakopoulos, G. D. Buckberg, and G. Trummer, "Septal structure and function relationships parallel the left ventricular free wall ascending and descending segments of the helical heart," *European Journal of Cardio-Thoracic Surgery*, vol. 29, no. 1, pp. S115–S125, 2006.

[38] S. Saleh, O. J. Liakopoulos, and G. D. Buckberg, "The septal motor of biventricular function," *European Journal of Cardio-Thoracic Surgery*, vol. 29, no. 1, pp. S126–S138, 2006.

[39] G. D. Buckberg, M. Castellá, M. Gharib, and S. Saleh, "Structure/function interface with sequential shortening of basal and apical components of the myocardial band," *European Journal of Cardio-Thoracic Surgery*, vol. 29, no. 1, pp. S75–S97, 2006.

[40] M. P. Feneley, J. R. Elbeery, J. W. Gaynor, S. A. Gall Jr., J. W. Davis, and J. S. Rankin, "Ellipsoidal shell subtraction model of right ventricular volume. Comparison with regional free wall dimensions as indexes of right ventricular function," *Circulation Research*, vol. 67, no. 6, pp. 1427–1436, 1990.

[41] J. C. Grignola, J. Pontet, M. Vallarino, and F. Gines, "The characteristics proper of the cardiac cycle phases of the right ventricle," *Revista Española de Cardiología*, vol. 52, no. 1, pp. 37–42, 1999.

[42] W. L. Maughan, A. A. Shoukas, K. Sagawa, and M. L. Weisfeldt, "Instantaneous pressure-volume relationship of the canine right ventricle," *Circulation Research*, vol. 44, no. 3, pp. 309–315, 1979.

[43] A. N. Redington, B. Knight, P. J. Oldershaw, E. A. Shinebourne, and M. L. Rigby, "Left ventricular function in double inlet left ventricle before the Fontan operation: Comparison with tricuspid atresia," *Heart*, vol. 60, no. 4, pp. 324–331, 1988.

[44] H. E. Cingolani, N. G. Pérez, O. H. Cingolani, and I. L. Ennis, "The Anrep effect: 100 years later," *American Journal of Physiology-Heart and Circulatory Physiology*, vol. 304, no. 2, pp. H175–H182, 2013.

[45] A. C. Taquini, J. D. FermosO, and P. Aramendia, "Behavior of the right ventricle following acute constriction of the pulmonary artery," *Circulation Research*, vol. 8, pp. 315–318, 1960.

[46] F. Gines and J. C. Grignola, "Synchronization of the contraction of the right ventricle against an acute afterload increase. left ventricle-like mechanical function of the right ventricle," *Revista Española de Cardiología*, vol. 54, no. 8, pp. 973–980, 2001.

[47] J. C. Grignola, F. Ginés, and D. Guzzo, "Comparison of the Tei index with invasive measurements of right ventricular function," *International Journal of Cardiology*, vol. 113, no. 1, pp. 25–33, 2006.

[48] P. Wauthy, A. Pagnamenta, F. Vassalli, R. Naeije, and S. Brimioulle, "Right ventricular adaptation to pulmonary hypertension: an interspecies comparison," *American Journal of Physiology-Heart and Circulatory Physiology*, vol. 286, no. 4, pp. H1441–H1447, 2004.

[49] J. C. Grignola, E. Domingo, L. Devera, and F. Gines, "Assessment of right ventricular afterload by pressure waveform analysis in acute pulmonary hypertension," *World Journal of Cardiology*, vol. 3, no. 10, pp. 322–328, 2011.

[50] R. J. Tedford, P. M. Hassoun, S. C. Mathai et al., "Pulmonary capillary wedge pressure augments right ventricular pulsatile loading," *Circulation*, vol. 125, no. 2, pp. 289–297, 2012.

[51] J. E. Calvin Jr., R. W. Baer, and S. A. Glantz, "Pulmonary artery constriction produces a greater right ventricular dynamic afterload than lung microvascular injury in the open chest dog," *Circulation Research*, vol. 56, no. 1, pp. 40–56, 1985.

[52] M. Maggiorini, S. Brimioulle, D. De Canniere, M. Delcroix, and R. Naeije, "Effects of pulmonary embolism on pulmonary

vascular impedance in dogs and minipigs," *Journal of Applied Physiology*, vol. 84, no. 3, pp. 815–821, 1998.

[53] G. F. Mitchell, J.-C. Tardif, J. M. O. Arnold et al., "Pulsatile hemodynamics in congestive heart failure," *Hypertension*, vol. 38, no. 6, pp. 1433–1439, 2001.

[54] H. J. Bogaard, K. Abe, A. V. Noordegmaf, and N. F. Voelkel, "The right ventricle under pressure: cellular and molecular mechanisms of right-heart failure in pulmonary hypertension," *Chest*, vol. 135, no. 3, pp. 794–804, 2009.

[55] J. A. Watts, J. Zagorski, M. A. Gellar, B. G. Stevinson, and J. A. Kline, "Cardiac inflammation contributes to right ventricular dysfunction following experimental pulmonary embolism in rats," *Journal of Molecular and Cellular Cardiology*, vol. 41, no. 2, pp. 296–307, 2006.

[56] J. A. Watts, M. R. Marchick, and J. A. Kline, "Right ventricular heart failure from pulmonary embolism: key distinctions from chronic pulmonary hypertension," *Journal of Cardiac Failure*, vol. 16, no. 3, pp. 250–259, 2010.

[57] L. Malacrida, E. Taranto, M. Angulo, I. Alvez Cruz, and J. C. Grignola, "Levosimendan improves right ventricular function and energy metabolism in a sheep model of submasive pulmonary embolism," *Eur Heart J: Acute Cardiovasc Care*, vol. 1, no. S1, p. 10, 2012.

[58] G. G. Schwartz, S. Steinman, J. Garcia, C. Greyson, B. Massie, and M. W. Weiner, "Energetics of acute pressure overload of the porcine right ventricle: In Vivo31P nuclear magnetic resonance," *The Journal of Clinical Investigation*, vol. 89, no. 3, pp. 909–918, 1992.

[59] G. J. Vlahakes, K. Turley, and J. I. E. Hoffman, "The pathophysiology of failure in acute right ventricular hypertension: Hemodynamic and biochemical correlations," *Circulation*, vol. 63, no. 1, pp. 87–95, 1981.

[60] K. L. Davis, U. Mehlhorn, G. A. Laine, and S. J. Allen, "Myocardial edema, left ventricular function, and pulmonary hypertension," *Journal of Applied Physiology*, vol. 78, no. 1, pp. 132–137, 1995.

[61] B. K. Slinker and S. A. Glantz, "End-systolic and end-diastolic ventricular interaction," *American Journal of Physiology*, vol. 251, no. 5 Pt 2, pp. H1062–H1075, 1986.

[62] M. X. Joseph, P. J. S. Disney, R. Da Costa, and S. J. Hutchison, "Transthoracic echocardiography to identify or exclude cardiac cause of shock," *Chest*, vol. 126, no. 5, pp. 1592–1597, 2004.

[63] A. Mekontso Dessap, F. Boissier, R. Leon et al., "Prevalence and prognosis of shunting across patent foramen ovale during acute respiratory distress syndrome," *Critical Care Medicine*, vol. 38, no. 9, pp. 1786–1792, 2010.

[64] G. Lhéritier, A. Legras, A. Caille et al., "Prevalence and prognostic value of acute cor pulmonale and patent foramen ovale in ventilated patients with early acute respiratory distress syndrome: A multicenter study," *Intensive Care Medicine*, vol. 39, no. 10, pp. 1734–1742, 2013.

[65] S. K. Shillcutt and J. S. Bick, "A comparison of basic transthoracic and transesophageal echocardiography views in the perioperative setting," *Anesthesia & Analgesia*, vol. 116, no. 6, pp. 1231–1236, 2013.

[66] V.-P. Harjola, A. Mebazaa, J. Čelutkiene et al., "Contemporary management of acute right ventricular failure: a statement from the Heart failure association and the Working Group on pulmonary circulation and right ventricular function of the European Society of Cardiology," *European Journal of Heart Failure*, vol. 18, no. 3, pp. 226–241, 2016.

[67] S. S. Rajaram, N. K. Desai, A. Kalra et al., "Pulmonary artery catheters for adult patients in intensive care," *Cochrane Database Syst Rev*, vol. 2, 2013.

[68] D. Osman, X. Monnet, V. Castelain et al., "Incidence and prognostic value of right ventricular failure in acute respiratory distress syndrome," *Intensive Care Medicine*, vol. 35, no. 1, pp. 69–76, 2009.

[69] X. Repessé, C. Charron, and A. Vieillard-Baron, "Acute cor pulmonale in ARDS: Rationale for protecting the right ventricle," *Chest*, vol. 147, no. 1, pp. 259–265, 2015.

[70] S. Rosenkranz and I. R. Preston, "Right heart catheterisation: Best practice and pitfalls in pulmonary hypertension," *European Respiratory Review*, vol. 24, no. 138, pp. 642–652, 2015.

[71] A. R. Tonelli, K. K. Mubarak, N. Li, R. Carrie, and H. Alnuaimat, "Effect of balloon inflation volume on pulmonary artery occlusion pressure in patients with and without pulmonary hypertension," *Chest*, vol. 139, no. 1, pp. 115–121, 2011.

[72] J. Iqbal and M. M. Javaid, "Diuretic resistance and its management," *British Journal of Hospital Medicine*, vol. 75, pp. C103–C107, 2014.

[73] A. Perel, M. Habicher, and M. Sander, "Bench-to-bedside review: Functional hemodynamics during surgery - should it be used for all high-risk cases?" *Critical Care*, vol. 17, no. 1, article no. 203, 2013.

[74] Y. Mahjoub, C. Pila, A. Friggeri et al., "Assessing fluid responsiveness in critically ill patients: false-positive pulse pressure variation is detected by Doppler echocardiographic evaluation of the right ventricle," *Critical Care Medicine*, vol. 37, no. 9, pp. 2570–2575, 2009.

[75] J. P. Bouchacourt, J. Riva, and J. C. Grignola, "Pulmonary hypertension attenuates the dynamic preload indicators increase during experimental hypovolemia," *BMC Anesthesiology*, vol. 17, no. 1, article no. 35, 2017.

[76] J. Mallat, M. Meddour, E. Durville et al., "Decrease in pulse pressure and stroke volume variations after mini-fluid challenge accurately predicts fluid responsiveness," *British Journal of Anaesthesia*, vol. 115, no. 3, pp. 449–456, 2015.

[77] A. Paternot, X. Repessé, and A. Vieillard-Baron, "Rationale and description of right ventricle-protective ventilation in ARDS," *Respiratory Care*, vol. 61, no. 10, pp. 1391–1396, 2016.

[78] C. Guérin, J. Reignier, J. C. Richard et al., "Prone positioning in severe acute respiratory distress syndrome," *The New England Journal of Medicine*, vol. 368, no. 23, pp. 2159–2168, 2013.

[79] A. Vieillard-Baron, C. Charron, V. Caille, G. Belliard, B. Page, and F. Jardin, "Prone positioning unloads the right ventricle in severe ARDS," *Chest*, vol. 132, no. 5, pp. 1440–1446, 2007.

[80] J. Grinstein and M. Gomberg-Maitland, "Management of Pulmonary Hypertension and Right Heart Failure in the Intensive Care Unit," *Current Hypertension Reports*, vol. 17, no. 5, 2015.

[81] F. Kerbaul, B. Rondelet, S. Motte et al., "Effects of norepinephrine and dobutamine on pressure load-induced right ventricular failure," *Critical Care Medicine*, vol. 32, no. 4, pp. 1035–1040, 2004.

[82] C. Martin, G. Perrin, P. Saux, L. Papazian, and F. Gouin, "Effects of norepinephrine on right ventricular function in septic shock patients," *Intensive Care Medicine*, vol. 20, no. 6, pp. 444–447, 1994.

[83] B. R. Walker, J. Haynes Jr., H. L. Wang, and N. F. Voelkel, "Vasopressin-induced pulmonary vasodilation in rats," *American Journal of Physiology*, vol. 257, no. 2 Pt 2, pp. H415–H422, 1989.

[84] Y. L. Kwak, C. S. Lee, Y. H. Park, and Y. W. Hong, "The effect of phenylephrine and norepinephrine in patients with chronic pulmonary hypertension," *Anaesthesia*, vol. 57, no. 1, pp. 9–14, 2002.

[85] C. D. Vizza, G. Della Rocca, D. A. Roma et al., "Acute hemodynamic effects of inhaled nitric oxide, dobutamine and a combination of the two in patients with mild to moderate secondary pulmonary hypertension," *Critical Care*, vol. 5, no. 6, pp. 355–361, 2001.

[86] D. De Backer, P. Biston, J. Devriendt et al., "Comparison of dopamine and norepinephrine in the treatment of shock," *The New England Journal of Medicine*, vol. 362, no. 9, pp. 779–789, 2010.

[87] R. O. Feneck, K. M. Sherry, P. S. Withington, and A. Oduro-Dominah, "Comparison of the hemodynamic effects of milrinone with dobutamine in patients after cardiac surgery," *Journal of Cardiothoracic and Vascular Anesthesia*, vol. 15, no. 3, pp. 306–315, 2001.

[88] Z. Papp, I. Édes, S. Fruhwald et al., "Levosimendan: Molecular mechanisms and clinical implications: Consensus of experts on the mechanisms of action of levosimendan," *International Journal of Cardiology*, vol. 159, no. 2, pp. 82–87, 2012.

[89] A. Pathak, M. Lebrin, A. Vaccaro, J. M. Senard, and F. Despas, "Pharmacology of levosimendan: Inotropic, vasodilatory and cardioprotective effects," *Journal of Clinical Pharmacy and Therapeutics*, vol. 38, no. 5, pp. 341–349, 2013.

[90] J. Hasslacher, K. Bijuklic, C. Bertocchi et al., "Levosimendan inhibits release of reactive oxygen species in polymorphonuclear leukocytes in vitro and in patients with acute heart failure and septic shock: A prospective observational study," *Critical Care*, vol. 15, no. 4, article no. R166, 2011.

[91] F. Kerbaul, V. Gariboldi, R. Giorgi et al., "Effects of levosimendan on acute pulmonary embolism-induced right ventricular failure," *Critical Care Medicine*, vol. 35, no. 8, pp. 1948–1954, 2007.

[92] F. Kerbaul, B. Rondelet, J.-P. Demester et al., "Effects of levosimendan versus dobutamine on pressure load-induced right ventricular failure," *Critical Care Medicine*, vol. 34, no. 11, pp. 2814–2819, 2006.

[93] C. Missant, S. Rex, P. Segers, and P. F. Wouters, "Levosimendan improves right ventriculovascular coupling in a porcine model of right ventricular dysfunction," *Critical Care Medicine*, vol. 35, no. 3, pp. 707–715, 2007.

[94] C. Bedo and J. C. Grignola, "Preferential vasodilator effects of levosimendan in resistance pulmonary arteries in a rodent pulmonary embolism model," *International Cardiovascular Forum Journal*, vol. 11, no. 1, pp. 74–80, 2017.

[95] A. Morelli, J.-L. Teboul, S. M. Maggiore et al., "Effects of levosimendan on right ventricular afterload in patients with acute respiratory distress syndrome: A pilot study," *Critical Care Medicine*, vol. 34, no. 9, pp. 2287–2293, 2006.

[96] R. J. Morais, "Levosimendan in severe right ventricular failure following mitral valve replacement," *Journal of Cardiothoracic and Vascular Anesthesia*, vol. 20, no. 1, pp. 82–84, 2006.

[97] S. Treskatsch, F. Balzer, T. Geyer et al., "Early levosimendan administration is associated with decreased mortality after cardiac surgery," *Journal of Critical Care*, vol. 30, no. 4, pp. 859–859e6, 2015.

[98] W. Toller, M. Heringlake, F. Guarracino et al., "Preoperative and perioperative use of levosimendan in cardiac surgery: European expert opinion," *International Journal of Cardiology*, vol. 184, no. 1, pp. 323–336, 2015.

[99] R. H. Mehta, J. D. Leimberger, S. van Diepen et al., "Levosimendan in patients with left ventricular dysfunction undergoing cardiac surgery," *The New England Journal of Medicine*, vol. 376, no. 21, pp. 2032–2042, 2017.

[100] G. Landoni, V. V. Lomivorotov, G. Alvaro et al., "Levosimendan for hemodynamic support after cardiac surgery," *The New England Journal of Medicine*, vol. 376, no. 21, pp. 2021–2031, 2017.

[101] J.-L. Vachiery, Y. Adir, J. A. Barbera et al., "Pulmonary hypertension due to left heart diseases," *Journal of the American College of Cardiology*, vol. 62, no. 25, pp. D100–D108, 2013.

[102] C. Thunberg, S. Morozowich, and H. Ramakrishna, "Inhaled therapy for the management of perioperative pulmonary hypertension," *Annals of Cardiac Anaesthesia*, vol. 18, no. 3, pp. 394–402, 2015.

[103] A. Ardehali, K. Hughes, A. Sadeghi et al., "Inhaled nitric oxide for pulmonary hypertension after heart transplantation," *Transplantation*, vol. 72, no. 4, pp. 638–641, 2001.

[104] S. Bhorade, J. Christenson, M. O'Connor, A. Lavoie, A. Pohlman, and J. B. Hall, "Response to inhaled nitric oxide in patients with acute right heart syndrome," *American Journal of Respiratory and Critical Care Medicine*, vol. 159, no. 2, pp. 571–579, 1999.

[105] J. L. Fernandes, R. O. Sampaio, C. M. Brando et al., "Comparison of inhaled nitric oxide versus oxygen on hemodynamics in patients with mitral stenosis and severe pulmonary hypertension after mitral valve surgery," *American Journal of Cardiology*, vol. 107, no. 7, pp. 1040–1045, 2011.

[106] K. M. Muzevich, H. Chohan, and D. C. Grinnan, "Management of pulmonary vasodilator therapy in patients with pulmonary arterial hypertension during critical illness," *Critical Care (London, England)*, vol. 18, no. 5, p. 523, 2014.

[107] M. M. Hoeper and J. Granton, "Intensive care unit management of patients with severe pulmonary hypertension and right heart failure," *American Journal of Respiratory and Critical Care Medicine*, vol. 184, no. 10, pp. 1114–1124, 2011.

[108] J. J. Lepore, A. Maroo, L. M. Bigatello et al., "Hemodynamic effects of sildenafil in patients with congestive heart failure and pulmonary hypertension: Combined administration with inhaled nitric oxide," *Chest*, vol. 127, no. 5, pp. 1647–1653, 2005.

[109] J. E. Lee, S. C. Hillier, and C. A. Knoderer, "Use of sildenafil to facilitate weaning from inhaled nitric oxide in children with pulmonary hypertension following surgery for congenital heart disease," *Journal of Intensive Care Medicine*, vol. 23, no. 5, pp. 329–334, 2008.

[110] A. W. Cheung, C. W. White, M. K. Davis, and D. H. Freed, "Short-term mechanical circulatory support for recovery from acute right ventricular failure: clinical outcomes," *The Journal of Heart and Lung Transplantation*, vol. 33, no. 8, pp. 794–799, 2014.

[111] N. K. Kapur, V. Paruchuri, A. Jagannathan et al., "Mechanical circulatory support for right ventricular failure," *JACC: Heart Failure*, vol. 1, no. 2, pp. 127–134, 2013.

[112] N. K. Kapur, M. L. Esposito, Y. Bader et al., "Mechanical circulatory support devices for acute right ventricular failure," *Circulation*, vol. 136, no. 3, pp. 314–326, 2017.

[113] L. R. Punnoose, M. A. Simon, D. Burkhoff, and E. M. Horn, "Right ventricular assist devices," in *The Right Ventricle in Health and Disease*, N. F. Voelkel and D. Schranz, Eds., Respiratory Medicine, pp. 439–454, Springer New York, New York, NY, 2015.

[114] B. Kar, I. D. Gregoric, S. S. Basra, G. M. Idelchik, and P. Loyalka, "The percutaneous ventricular assist device in severe refractory

cardiogenic shock," *Journal of the American College of Cardiology*, vol. 57, no. 6, pp. 688–696, 2011.

[115] A. Maria Schürner, M. J. Wilhelm, V. Falk, F. Ruschitzka, D. Bettex, and A. Rudiger, "Recurrent clotting of a continuous-flow right ventricular assist device - repeated thrombolysis with two different protocols," *Journal of Cardiothoracic and Vascular Anesthesia*, vol. 29, no. 6, pp. 1614–1617, 2015.

[116] T. R. Bowers, W. W. O'Neill, C. Grines, M. C. Pica, R. D. Safian, and J. A. Goldstein, "Effect of reperfusion on biventricular function and survival after right ventricular infarction," *The New England Journal of Medicine*, vol. 338, no. 14, pp. 933–940, 1998.

[117] L. J. Dell'Italia, N. J. Lembo, M. R. Starling et al., "Hemodynamically important right ventricular infarction: Follow-up evaluation of right ventricular systolic function at rest and during exercise with radionuclide ventriculography and respiratory gas exchange," *Circulation*, vol. 75, no. 5, pp. 996–1003, 1987.

[118] N. Kucher, P. Boekstegers, and O. J. Muller, "Randomized, controlled trial of ultrasound-assisted catheter-directed thrombolysis for acute intermediate-risk pulmonary embolism," *Circulation*, vol. 129, pp. 479–486, 2014.

[119] C. E. Ventetuolo and J. R. Klinger, "Management of acute right ventricular failure in the intensive care unit," *Annals of the American Thoracic Society*, vol. 11, no. 5, pp. 811–822, 2014.

[120] E. Gayat and A. Mebazaa, "Pulmonary hypertension in critical care," *Current Opinion in Critical Care*, vol. 17, no. 5, pp. 439–448, 2011.

[121] J. Sandoval, J. Gaspar, H. Peña et al., "Effect of atrial septostomy on the survival of patients with severe pulmonary arterial hypertension," *European Respiratory Journal*, vol. 38, no. 6, pp. 1343–1348, 2011.

[122] A. Vieillard-Baron, L. C. Price, and M. A. Matthay, "Acute cor pulmonale in ARDS," *Intensive Care Medicine*, vol. 39, no. 10, pp. 1836–1838, 2013.

[123] G. Habib, P. Lancellotti, M. J. Antunes et al., "2015 ESC guidelines for the management of infective endocarditis: The task force for the management of infective endocarditis of the European Society of Cardiology (ESC). Endorsed by: European Association for Cardio-Thoracic Surgery (EACTS), the European Association of Nuclear Medicine (EANM)," *European Heart Journal*, vol. 36, no. 44, pp. 3075–3128, 2015.

Hindawi
BioMed Research International
Volume 2017, Article ID 3820191, 14 pages
https://doi.org/10.1155/2017/3820191

Review Article

Imaging Diagnosis of Right Ventricle Involvement in Chagas Cardiomyopathy

Minna M. D. Romano, Henrique T. Moreira, André Schmidt, Benedito Carlos Maciel, and José Antônio Marin-Neto

Medical School of Ribeirão Preto, University of São Paulo, Ribeirão Preto, SP, Brazil

Correspondence should be addressed to Minna M. D. Romano; minnaromano@gmail.com

Received 9 June 2017; Accepted 24 July 2017; Published 27 August 2017

Academic Editor: Kristina Haugaa

Right ventricle (RV) is considered a neglected chamber in cardiology and knowledge about its role in cardiac function was mostly focused on ventricular interdependence. However, progress on the understanding of myocardium diseases primarily involving the RV led to a better comprehension of its role in health and disease. In Chagas disease (CD), there is direct evidence from both basic and clinical research of profound structural RV abnormalities. However, clinical detection of these abnormalities is hindered by technical limitations of imaging diagnostic tools. Echocardiography has been a widespread and low-cost option for the study of patients with CD but, when applied to the RV assessment, faces difficulties such as the absence of a geometrical shape to represent this cavity. More recently, the technique has evolved to a focused guided RV imaging and myocardial deformation analysis. Also, cardiac magnetic resonance (CMR) has been introduced as a gold standard method to evaluate RV cavity volumes. CMR advantages include precise quantitative analyses of both LV and RV volumes and its ability to perform myocardium tissue characterization to identify areas of scar and edema. Evolution of these cardiac diagnostic techniques opened a new path to explore the pathophysiology of RV dysfunction in CD.

1. Introduction

Historically, physiology concepts about heart function considered the right ventricle as a kind of almost perfunctory chamber, although knowledge about ventricle interdependence was well recognized decades ago [1]. Weber et al., in an outstanding publication of 1981 in this field, postulated the following:

> *However, because the right and left ventricles are aligned in series and mechanically coupled, a perturbation in the mechanical events of one ventricle will influence the behavior of the other ventricle, and in nonsteady state conditions the output of the two ventricles may not be balanced. Eventually, however, a steady state of balanced outputs must occur if pulmonary or systemic venous congestion is to be avoided. [1]*

Diastolic interplay between ventricles is easy readily understandable, mainly considering the function of pericardium as the common covering layer for both ventricles. However, although the presence of pericardium accentuates this interaction, animal experimental models with the pericardium excised showed that the diastolic interplay was still present [2]. There is also a systolic interplay, so that, during systole, the pressure in one ventricle will influence the systolic pressure developed in the other. The systolic interplay has been primarily demonstrated as the predominant influence the left ventricle exerts upon the right ventricle. This is because the opposite effect of lower systolic pressure of right ventricle influencing left ventricle performance is usually minimized under normal physiologic conditions. As the interventricular septum plays an important role in the interventricular pressure relationship, its function was assessed in classic animal experiments with total destruction of RV free wall but with maintenance of septum presence [3] and,

in contrast, in experimental models of septum dysfunction because of infarction [4].

Based on these physiologic aspects and adding to the fact that many of the studies were designed on a volume-pressure relation basis, it is possible to understand why cardiology science neglected the RV as a "secondary chamber" or a "passing chamber" [5]. Nonetheless, knowledge about primary myocardial conditions affecting the RV, without concomitant pressure overload of this chamber, as in Uhl's anomaly and RV dysplasia, reinforces the need of other theories to explain the real influence of right ventricular function in cardiovascular physiology. The fact that RV dysplasia includes a phase of right-sided cardiac failure beyond the arrhythmic clinical complications gives an insight to the fact that advanced RV muscle impairment can be clinically significant and directly leads to intrinsic heart failure syndrome [6].

There is evidence that CD causes a peculiar right ventricle involvement first because evolution of the disease to heart failure usually includes prominent right heart failure symptoms in absence of or with only mild pulmonary congestion [7, 8]; second, because there is direct evidence of myocardial damage of the right ventricle in human myocardial biopsies and postmortem studies, as well as in animal experimental models of *T. cruzi* infection; and, finally, because there is a proportion of patients with early and isolated right ventricle dysfunction when evaluated by different cardiac image methods [9, 10].

However, exploring the right ventricle with imaging diagnostic tools is still a challenge. The accumulated evidence about ventricular systolic function in most diseases is derived from echocardiography. Two-dimensional echocardiography needs geometrical assumptions to estimate ventricular volumes and the right ventricle simply does not have a mathematically defined geometrical form.

This review explores the right ventricle anatomic and functional involvement in Chagas cardiomyopathy (CC) while highlighting the contribution of cardiac imaging diagnostic methods in the field.

2. Chagas Cardiomyopathy (CC)

CD was recognized by WHO as one of the world's 13 most neglected tropical diseases with a high prevalence of individuals at risk of infection in South and Central America and with the highest rates of mortality between all neglected diseases [14]. Although its prevalence had slightly declined through the last decade, it can reach 11.4% of heart failure causes in specific endemic regions of Brazil [15]. Although originally confined to poor rural areas of Latin America, migration movements contributed to spread CD to nonendemic countries in Europe, Canada, and USA [16, 17].

CD is caused by the *T. cruzi* protozoan infection that leads, in most cases, to a myocardial chronic inflammatory response [7]. Myocardial damage is probably a result of imbalance between parasite persistence and adverse immune-inflammatory response [18] which result in a broad spectrum of tissue lesions. Myocardium disease is characterized by a low-intensity, slowly progressive but incessant myocarditis which leads to impairment of contractile function and dilatation of cardiac chambers [7]. Histologically, there is a widespread destruction of myocardial cells, edema, diffuse fibrosis, mononuclear cell infiltration, and scarring of the conduction system and the contractile myocardium [11, 19] (Figure 1). Early stages of the disease are still not fully understood, but conduction system abnormalities can occur before myocardium contractile function impairment [20]. Cardiac autonomic dysfunction may also be an early consequence of the loss of cardiac neuronal parasympathetic activity [21–23]. Microvascular coronary dysfunction also occurs and its mechanism is still not well known but is likely to contribute to contractile function damage [24–26]. Progression of the myocardium damage results in a scenario of widespread substitution by fibrous tissue, which is the core of both arrhythmogenesis and heart failure.

CD includes an acute and a chronic phase. Acute infection is usually underdiagnosed. There is a recent increase of cases secondary to reactivation from the chronic phase, by blood transfusion or transplantation of solid organs, and congenital or oral contaminations [27, 28]. Most of acute cases run through an asymptomatic clinical course. When symptoms occur they include fever, malaise, enlargement of liver, spleen and lymph nodes, and subcutaneous localized edema [7]. The grade and type of immunological response have a key role in controlling parasitemia during acute phase and permit most of patients to undergo to the chronic clinically silent indeterminate form of disease. However, some 30% of infected subjects will present symptoms and or signs of cardiac damage 10–30 years later [7]. Bradycardia and conduction system abnormalities can occur early in the evolution of disease, as well as frequent ventricular ectopic beats [17, 19]. Ventricular tachycardia is ominous and can be responsible for sudden cardiac death even in less advanced stages of the disease [29]. Other typical ECG alterations include right bundle branch block and left anterior fascicular bundle block, which can be combined [19, 30].

Myocardial damage typically causes regional contraction disturbances in the left ventricle and the virtually pathognomonic apical aneurisms [22, 31]. Global LV dilatation and systolic dysfunction are also often seen as the disease progresses. When heart failure supervenes, it is usually with biventricular manifestations and systemic congestion can be more impressive when compared to pulmonary congestion. Patients with cardiac form of CD are seen frequently in cardiac units and clinics all around South and Central America. They usually present with heart failure symptoms during recurrent hospital admissions. In many cases, symptoms and signs of systemic congestion are very prominent. They usually complain of lower limbs edema, weight gain, increase in abdominal volume, and pain associated with hepatomegaly. This conspicuous form of right-sided heart failure presentation was well described since the first reports on clinical CD [32–34] and still puts a challenge to treatment. Patients need high doses of diuretics and vasodilators and sometimes the use of intravenous inotropes, although it, with no proven benefit on mortality, is warranted as a symptomatic treatment resource [33].

Because of these peculiar aspects of CD cardiomyopathy, diagnostic tools capable of detecting early myocardial

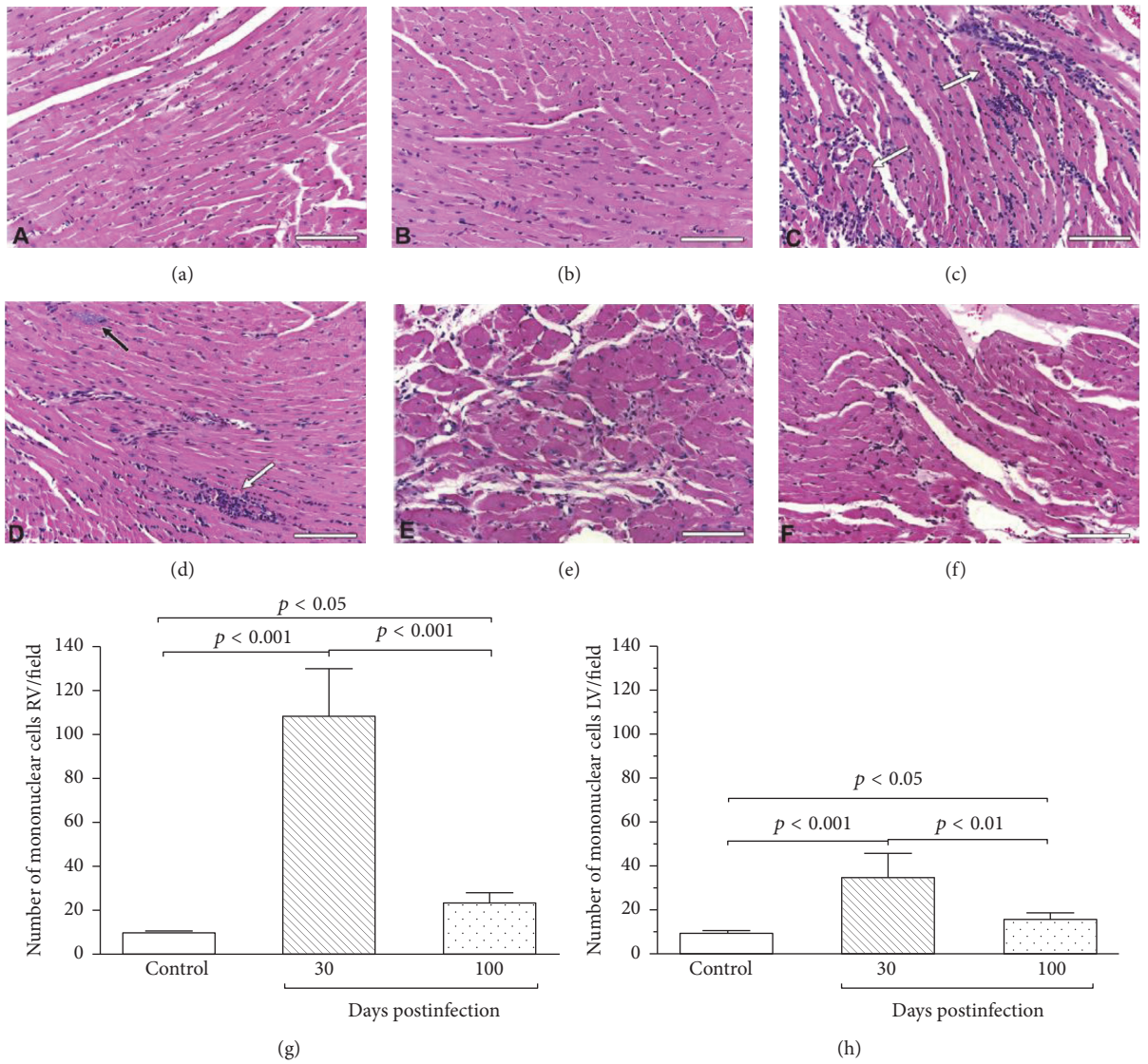

FIGURE 1: Histological analysis (HE) depicting normal cardiac fibers with regular interstitial space in the right (a) and left (b) ventricles. In a *T. cruzi*-infected mice, with 30 days post-Chagas infection (acute phase), there is an intense and diffuse myocarditis characterized by lymphomononuclear interstitial infiltrate (white arrow), multiple ruptured or unruptured pseudocysts (black arrow), and enlargement of the interstitial space ((c) and (d)). After 100 days of infection (chronic phase), the number of the lymphomononuclear inflammatory cells became significantly reduced and no parasites are detected ((e) and (f)). In this study, the numbers of interstitial mononuclear cells were quantified in both right and left ventricles. The number of cells was markedly increased at 30 days of infection as compared to 100 days of infection, mostly in the right ventricle ((g) and (h)). Bars = 100 μm, n = 6/day/group. HE = Hematoxylin-Eosin stain. Adapted from [11]. Adapted with permission from Elsevier, license number 4120251034702.

involvement in both ventricles can represent a first step towards an early and effective treatment of these patients before the development of more advanced fibrotic and irreversible changes.

3. Evidence of Right Ventricle Involvement in Chagas Disease (CD)

There is considerable evidence showing CC to be quite different from other forms of dilated cardiomyopathy from the pathologic standpoint [35]. Not only is there a prominent myocardial cell destruction associated with focally diffuse mononuclear cell infiltration, but also an intense interstitial fibrosis is seen (Figure 2), surrounding muscle cells and vessels (Figure 3) [12]. The process of inflammation and fibrosis is widespread and involves both the right [36] and left ventricles and has particular predilection for the cardiac conduction system and the apex of left ventricle [35, 37]. Higuchi et al., in a previous study using RV endomyocardium biopsies, compared ultrastructural changes in CD patients with different forms of the disease (indeterminate versus cardiac with and without ECG alterations) and did not

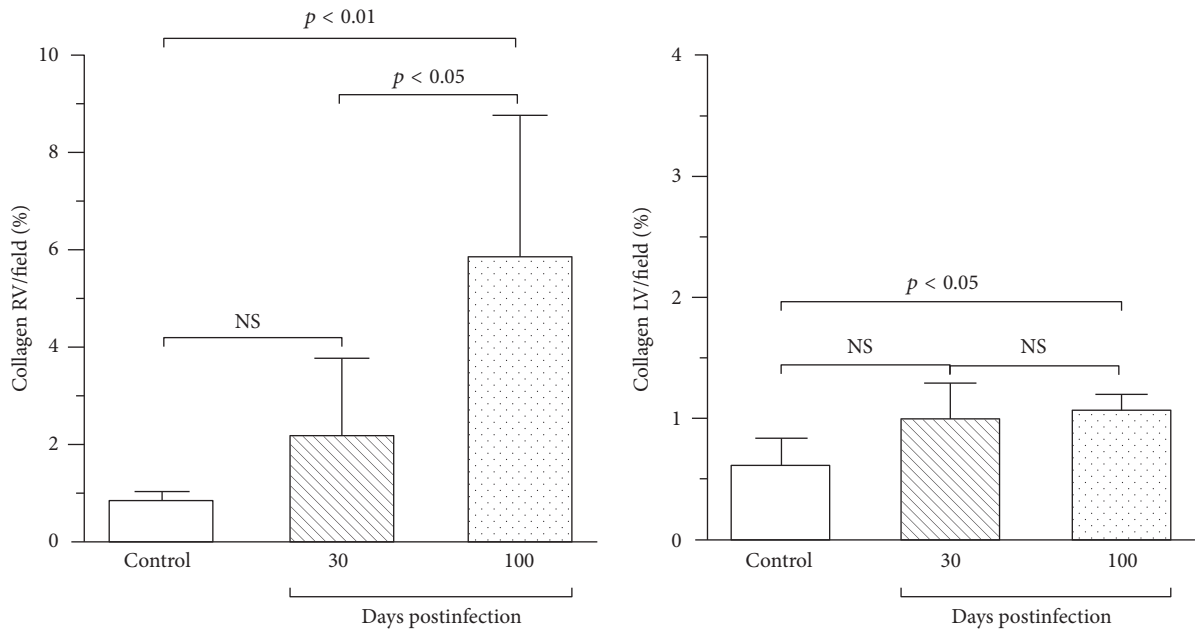

(a)

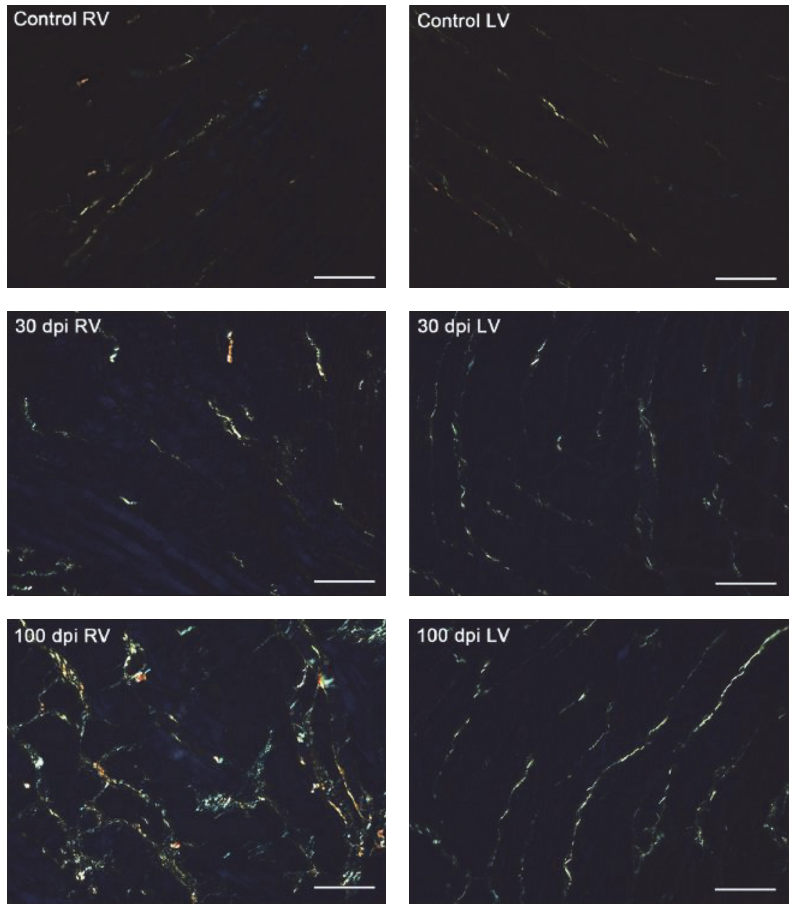

(b)

Figure 2: Interstitial collagen (Picrosirius red-stained sections) in controls and *T. cruzi*-infected mice. (a) The bar graphs show the mean fraction of fibrosis (%) in both right (left graph) and left ventricles (right graph). There is a tendency towards increased amount of collagen in acute phase (30 dpi) in both ventricles. The mean amount of collagen is significantly increased in the RV (600% higher) and LV (62% higher) in chronic phase (100 dpi). (b) Representative images illustrate these results clearly showing that the collagen increase was mainly perimysial. Bars = 50 μm, n = 6/day/group. Adapted from [11]. Adapted with permission from Elsevier, license number 4120251034702.

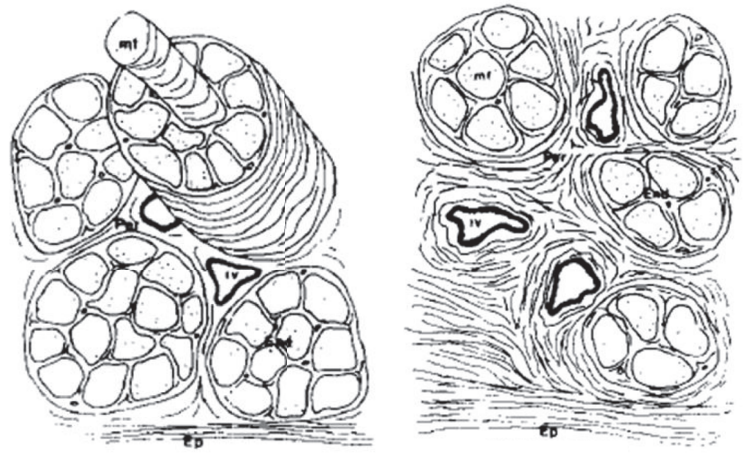

Normal Chagas' HD

Figure 3: Schematic representation of the myocardial fibrosis patterns in control myocardium (normal) and in chronic Chagas' heart disease (Chagas' HD). From [12]. Adapted with permission from Elsevier, license number 4120260350349.

encounter important differences among them. Since the pathological materials for these studies were obtained from the RV myocardial tissue and the ultrastructural alterations detected were similarly distributed in patients with the different forms of CD, these findings suggest an early involvement of the right ventricle ultrastructure in many patients [38]. Other studies with right ventricle biopsies also showed that myocardium lesions may be caused by a continuous process along all forms of the chronic disease and are found even in early stages of the disease (e.g., in patients with the indeterminate form of the disease) [39].

The peculiar clinical aspects of Chagas cardiac failure drove initial research to investigate the real role of right ventricle dysfunction in the disease physiopathology. In fact, previous studies reported on patients with CD showed that isolated right ventricle disturbances are frequent occurrences [21, 34]. It has also been reported that heart failure mortality in CD is higher when compared to mortality associated with heart failure due to ischemic causes or other cardiomyopathies [40, 41]. Among other possible factors, RV dysfunction prevalence may be responsible for high mortality of heart failure in chronic CD once; as in other causes of heart failure, it has independent prognostic impact [42]. It is also noteworthy that, in cases of reactivation of *T. cruzi* infection in immune suppressed patients, a remarkable degree of RV dilation and systolic dysfunction has been described [43–45].

Despite these findings, some controversy occurs in the literature regarding the detection of clinically apparent early right ventricle involvement in CC. Carrasco et al. [46] studied 60 subjects using cardiac catheterization and radiological contrast angiography, for both RV and LV, in patients with different forms of chronic CD and did not find right ventricular dysfunction or dilatation in a subgroup (1) of 14 patients with normal ECG and normal left ventricular function. In the three other disease severity subgroups, composed of (2) normal ECG and abnormal LV function, (3) abnormal ECG and abnormal LV function without cardiac failure symptoms, and finally (4) abnormal ECG with abnormal LV function and symptoms of cardiac failure, the proportion of RV dilatation/global RVEF reduction/segmental wall motion abnormalities was, respectively, 55%/0%/64% for group (2), 79%/32%/74% for group (3), and 71%/100%/100% for group (4). Evaluating these results under the lens of modern knowledge about the complexity of cardiac imaging methods in assessing RV function, it is plausible to conclude that there is a progression of RV disease among patients with the various forms of CD, even if apparently no abnormalities were detected in the early asymptomatic phase of the disease with the methods employed. In contrast, Marin-Neto et al. [9], studying RV function with the more accurate and quantitative method of ECG-gated radionuclide angiocardiography, were able to demonstrate, in a carefully selected group of patients with the indeterminate form of disease, a reduction in RVEF despite the presence of preserved LVEF. This investigation rescued the concept of RV early functional impairment in patients with CD, in line with the pathological findings described above and the clinical manifestations already alluded here. This was possible due to the inherent fact that radionuclide angiography allowed the concomitant evaluation of both LV and RV. After the study of Carrasco et al., without known exceptions, all studies assessing the ventricular function with contrast ventriculography were focused exclusively on the LV and coronary angiography.

The results from the study with radionuclide angiography, coupled with previous anatomopathologic data already discussed, produced the hypothesis that RV myocardial damage may be an early and direct pathophysiological consequence of CC. This hypothesis also comprehends the notion that, in a scenario of low vascular pulmonary resistance (i.e., in the absence of LV systolic and diastolic dysfunction and its retrograde effects upon the pulmonary circulation), no clinical manifestations of the RV functional impairment would be detectable. However, within this setting of RV early impairment, when the left ventricle dysfunction occurs causing the rise in pulmonary vascular resistance, compensatory mechanisms of the RV achieve their limits. From

this moment on, right-sided symptoms and signs may thus dominate the clinical expression of heart failure [34].

Mady et al., who had already shown right ventricle histologic abnormalities in 60% of patients with the indeterminate form of CD [36], also studied them, a year later, with invasive cardiac catheterization. Of note, the only hemodynamic abnormality seen in those patients with this form of CD was the RV end diastolic pressure elevation [47]. In the absence of any signs of LV dysfunction, it would be possible to conclude that the elevated diastolic pressure in the RV chamber might be due to the underlying structural abnormalities previously detected in the same patients.

Several years later, various studies using echocardiography as a noninvasive tool to assess RV geometry and function showed mixed results in diverse groups of patients with various forms of CD. Nunes et al., in 2004, using a nonquantitative echocardiography analysis, reported not being able to detect isolated RV dysfunction in a group of subjects in both early and later (28% of patients) stages of CC [48]. However, this conclusion was based only on a subjective global classification of RV systolic dysfunction. Moreover, in this study, only patients with some degree of left ventricle dilatation or systolic dysfunction were included, which, per se, makes the investigational task of finding isolated RV early involvement unfeasible. Furtado et al. also investigated the prevalence of RV systolic and diastolic dysfunction including its global performance index in a group of 60 subjects without evidence of cardiac disease by conventional diagnostic methods [49]. In contrast to the results of Nunes et al., the authors found a 26% prevalence of RV systolic dysfunction when using tissue Doppler systolic tricuspid velocity wave (S'). In that study no other echo parameters of RV function could differentiate the performance of patients with indeterminate form CD from normal controls. Ten years later, using *speckle tracking* as a new methodology echocardiography tool with potential to measure myocardium deformity, Barbosa et al. [50] reported that no RV longitudinal strain differences could be detected between patients with indeterminate form CD and normal controls.

Recently, Moreira et al. demonstrated, in a comparative investigation using cardiac magnetic resonance as a reference method, that all conventional echocardiographic parameters for right ventricular assessment studied, including TAPSE, S' of tricuspid annulus, fractional area change, and right ventricular index of myocardial performance, have a very low sensitivity to detect right ventricular systolic dysfunction in patients with CD. In contrast, analysis of right ventricular deformation by using two-dimensional speckle tracking echocardiography yielded a high ability to differentiate patients with from those without RV systolic dysfunction. The right ventricular free wall strain had a remarkably higher sensitivity in comparison with traditional echocardiographic parameters to identify RV dysfunction [13].

Cardiac magnetic resonance methods have inherent advantages for the evaluation of RVEF, since volumes can be directly measured instead of being geometrically extrapolated [51]. Studying 158 subjects with CD using cardiac magnetic resonance, Moreira et al. described reduced right ventricular ejection fraction in 37% of the patients studied [51]. Although usually associated with LV dysfunction, isolated early right ventricular dysfunction was also found in a small subset (4.4%) of patients [51]. Furthermore, right ventricular dysfunction was independently associated with atrial fibrillation.

Based on all exposed data, we can conclude that detection of incipient right ventricle dysfunction is still dependent on technical evolution of cardiac diagnosis image tools. And this concept probably can be extrapolated to any disease with a potential to primarily involve the right ventricular myocardium.

The prognostic impact of RV dysfunction in CD is not yet completely explored. Nunes et al. evaluated 158 subjects, all with left ventricle dilatation and dysfunction during a follow-up of 34 ± 23 months. The RV dysfunction parameter evaluated, Tei index of ventricular performance, was a predictor of mortality [42]. These data can be taken as the first demonstration of the role of RV dysfunction as a possible prognostic marker in CC. Nevertheless, prognostic studies have still several barriers to transpose. One of them is to compare a new parameter with others previously established and this aspect was not correctly tested considering the validated Rassi score in CC [52, 53]. In contrast, although the myocardium performance index of right ventricle (Tei index) was already proven to be able to detect RV dysfunction in other scenarios [54], in CD this index could not identify RV involvement in the indeterminate form group of patients [55].

4. Heart Conduction Disturbances in Chagas Cardiomyopathy and Its Relation to RV Function

CD frequently affects the heart conduction system and the most frequently found conduction abnormality is right bundle branch block (RBBB), often associated with left anterior fascicle bundle branch block (LAFB) [56]. Prevalence of RBBB varies between *T. cruzi* chronically infected populations from 15% to 40% [17, 57]. Among 2756 patients enrolled in the BENEFIT trial, RBBB was found in roughly 52% and in 35% of cases it was associated with LAFBB. This association was also reproducible in experimental animal models of infection with the *T. cruzi* [19]. Histologically, these regions of the cardiac conduction system show chronic fibrosis and progressive obliteration [37].

It is not clear if RBBB is really a primarily manifestation or if it is secondary to myocardial damage extending to conduction system. Also, the role of RBBB in physiopathology of CD is not well understood. One previous study showed that, in a cohort of asymptomatic patients with RBBB, patients with CD have a worse prognostic regarding cardiac sudden death when compared to other patients with RBBB and no CD [58]. Although the influence of having CD was not compared with other classic prognostic factors, these data suggest the need for further studies looking specifically to the prognosis of patients with RBBB secondary to CD. Indeed, it is well documented that having a normal ECG is a marker of good prognosis in CD but the prognostic meaning of an isolated RBBB due to CD is unclear [59].

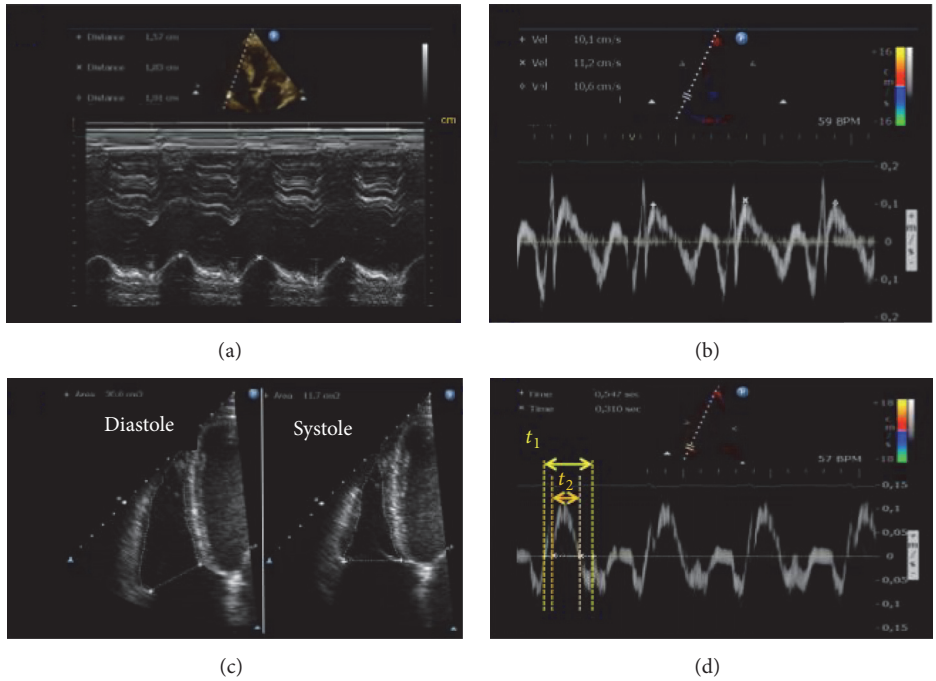

Figure 4: Echocardiographic conventional parameters of right ventricle (RV) evaluation. (a) Tricuspid Annular Peak Systolic Excursion (TAPSE) from M-mode. (b) Systolic wave velocity (S') of the lateral portion of tricuspid annulus; (c) area measurements in diastole and systole from bidimensional images to calculate fractional area change (FAC); (d) time measurements from tissue Doppler curves in tricuspid annulus to calculate myocardial performance index (MPI). [13]. Adapted with permission from Elsevier, license number 4143761084119.

The real contribution of this electrical disturbance to RV dysfunction has not been investigated. This contrasts with the conspicuous evidence that left bundle branch block (LBBB) is associated with left ventricle dysfunction [60]. Although in other disease scenarios RBBB is usually an expression of RV pressure and volume overload, in CD this electrical disturbance could be a primary reflection of myocardial damage. The understanding about the role of RBBB in inducing delayed RV contraction in RV calculations of function by cardiac diagnosing methods is frequently ignored. This effect was tested using CMR by Marterer et al., concluding that ignoring the RV physiology in RBBB patients leads to a statistically significant underscoring of RV performance parameters [61]. Thus, the impact of RBBB in CD as a primary mechanism to RV mechanical dyssynchrony and dysfunction warrants further investigation with dedicated study design.

5. Current Imaging Evaluation of the Right Ventricle in CD: Focus on Noninvasive Cardiac Diagnostic Tools

5.1. Echocardiography. Evaluation of right ventricle anatomy and function with echocardiography is always challenging. Right ventricle unique macroscopic morphology, which includes an inflow and outflow regions and the main cavity, cannot be represented by a simple mathematical geometric model. Because of this, geometric extrapolations to estimate chamber volumes, so useful for bidimensional echocardiographic assessment of the LV, cannot be applied in the case of the RV [62]. Although understanding right ventricle involvement in several disease processes has gained a recent interest, it is still not yet adequately addressed in cardiology [63]. Tridimensional echocardiography, while promising, still has some difficulties when imaging the right ventricle, as the need to improve the technical spatial resolution to assess the right ventricle free wall [64]. Other unique characteristics of right ventricle are additional barriers, as the thin myocardium walls, its prominent trabeculation, and its contraction mechanics, characterized by a predominant long-axis (apex-to-basal) shortening of myocardium fibers.

Recognizing these problems, a guide on how to measure right ventricle geometry and function with echocardiography was released in 2010 and was further updated and included in an echocardiography chamber quantification recommendation in 2015 [65, 66]. The document comprises bidimensional linear measures of RV cavity at different levels and projections and functional nonvolumetric parameters such as longitudinal excursion of tricuspid annulus (TAPSE), tissue Doppler velocity of systolic wave at the lateral portion of tricuspid annulus (S' wave), fractional area change (FAC) during systole, myocardium performance index (MPI) also recognized as Tei index [67], and the estimate of dP/dT from systolic time of the tricuspid regurgitation Doppler spectrum [65] (Figure 4).

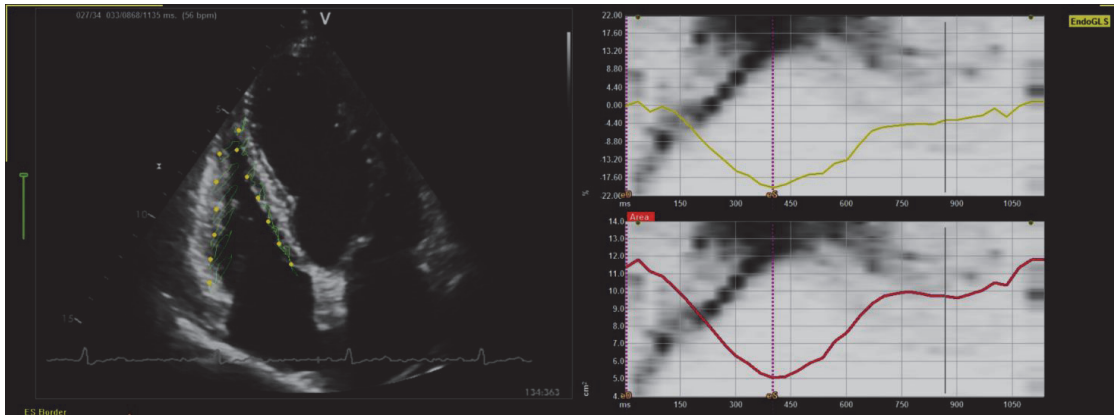

(a)

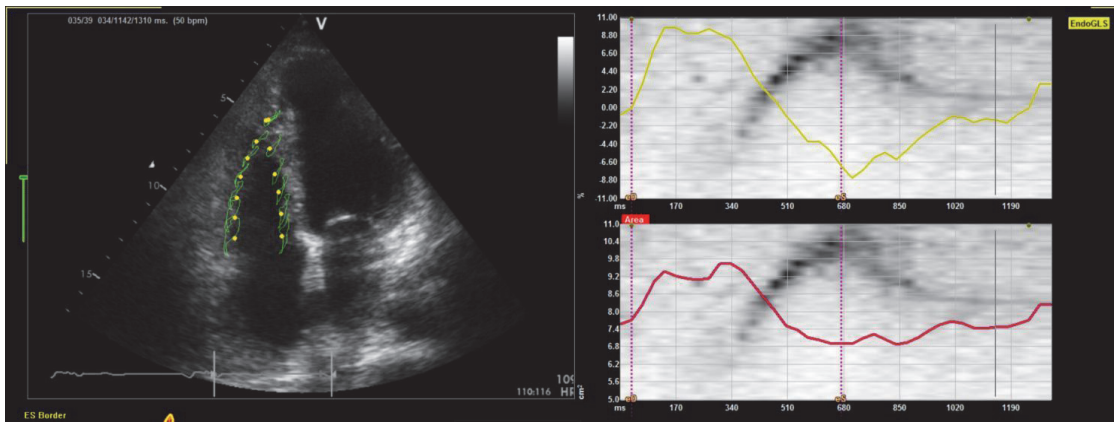

(b)

Figure 5: Myocardial deformation analysis of right ventricle (RV) from speckle tracking echocardiography. Strain analysis of RV from representative CC patients demonstrating preserved systolic function in Panel (a) (GLS: −17.8%, FAC: 55.7%) and reduced systolic function in Panel (b) (GLS: −8.4%, FAC: 10.5). Both patients have preserved left ventricle ejection fraction. Graphics in each panel represent myocardial strain in % (superior right, yellow trace) and RV area change in cm^2 (inferior right, red trace). RV: right ventricle; EndoGLS: Endocardial Global Longitudinal Strain; FAC: Fractional Area Change; es: end-systolic time.

Considering the overall neglectful cardiology approach to the right ventricle, it is understandable why the same gaps of knowledge also exist for CD studies. Acquatella, in an outstanding publication survey in 2007, extensively reviewed echo contributions to the field of CD without fully addressing the mixed results of studies of echocardiographic evaluation of RV in CD [68]. Despite this neglect, from most echocardiographic studies primarily focusing on the LV assessment, it is possible to conclude that 2D echocardiography can detect right ventricular systolic dysfunction in a high proportion of patients who already have decreased global LV systolic impairment, even at earlier stages of the cardiomyopathy [13, 48]. Other publications also addressed the potential of echocardiographic conventional parameters such as S', TAPSE, and MPI to detect right ventricular dysfunction in more advanced stages of disease and symptomatic patients [69]. Some publications also endorsed the ability of echocardiographic parameters to detect right ventricle dysfunction even in patients with the indeterminate form of the disease using tissue Doppler techniques [49, 70]. However, using myocardium performance index (MPI), investigators were not able to differentiate patients with the indeterminate form of CD from controls [49]. Also, using 2D speckle tracking, Barbosa et al., in a study of biventricular function, published negative results of strain evaluation to differentiate patients with indeterminate form of CD from controls [50].

Speckle tracking is a relatively new echocardiography tool and discussion about its methodology advantage over other approaches is still a topic of interest [71]. With this technique, the myocardium systolic function can be measured along the entire myocardium as deformation (Figure 5). The myocardium deformation analysis is relatively independent from overload conditions [72, 73] and because of this, in theory, it can be applied to detect myocardial damage even when compensatory physiological adjustments are still preserving the ejection fraction within normal limits [72]. Normality values of RV strain by 2D speckle tracking analysis were recently published [74].

Most of published data using *speckle tracking* in CD were focused on left ventricle analysis assessment [50, 75–77]. These investigations used specific vendor software for the analysis and their methodological approach, mainly about timing of measured peak (if global or systolic), end-systole definitions, and also if endocardial or mesocardial layer, were neither technically uniform [50, 75] nor even were they completely reported in some of them. A definite standardization [71] in speckle tracking measurements is necessary to evolve the applicability of this method not only in the evaluation of LV deformation but also for the RV assessment. Results of a recent published study following a standardization methodology of measurements of speckle tracking concluded that right ventricular free wall strain measurement seems to be a method of choice [13], since the sensitivity of the conventional echocardiographic parameters to detect right ventricular dysfunction in CD is intrinsically very low.

In summary, echocardiography can be used to detect RV dysfunction in CD but with some inherent methodological limitations. *Speckle tracking* is a promising tool to assess RV dysfunction in this disease overcoming the lack of sensitivity of conventional 2D and Doppler measurements of function.

5.2. Cardiac Magnetic Resonance. With its inherent capability for the direct measurement of chamber volumes and the calculation of biventricular ejection fraction without geometric extrapolations, CMR is clearly a more advantageous method than echocardiography for that purpose. In this regard, the method is already considered a gold standard of ventricle volumes quantification [78]. This has been assumed in general, despite the fact that it has not been studied in comparison with the estimation of ejection fraction based on ECG-gated radionuclide angiography. In the absence of direct comparative studies of both methods, it may well be that the nuclear method, which also has no need for any geometric extrapolation (scintigraphy counts are directly proportional to volumes throughout the cardiac cycle), and has the advantage of allowing a precise averaging of hundreds of cardiac cycles, may stand the test of a comparison with CMR. In addition, the method of measuring EF with CMR has not been fully standardized, and there are still challenges on its way to more widespread clinical application. In particular, right ventricle ejection fraction normal reference values are still not consolidated. Despite these caveats, it is relevant to emphasize that in CD patients CMR can be used not only to calculate ventricular volumes and ejection fraction (Figure 6) but also to characterize myocardial tissue alterations (Figure 7).

The utility of CMR in CD was first demonstrated for the study of left ventricle systolic function and the detection of left ventricle myocardial fibrous tissue and its significance [79–82]. As mentioned above, a recent study by Moreira et al., using CMR, evaluated the prevalence of RV systolic dysfunction in a sizable population of patients with chronic CD. In that study a reduction of right ventricular ejection fraction was detected in 37% of the patients studied, usually associated with left ventricle dysfunction. Corroborating the findings from previous studies with other methods, Moreira et al. showed the presence of right ventricular systolic dysfunction in a small subset of these *T. cruzi* chronically infected subjects with preserved left ventricular ejection fraction [51].

Therefore, even considering the intrinsic difficulties in using CMR in clinical settings, most of them related to cost and availability, especially curtailed by scarce resources in endemic regions of CD, there is now a definite drive for the clinical approach with CMR to evaluate early biventricular damage in CD.

5.3. Future Perspectives

5.3.1. Echocardiography. Recent research using a mammalian experimental model of *T. cruzi* infection that closely mimics human chronic Chagas, with the advantage of a relatively short 8–10 months of evolution to chronic phase, has allowed the integration of echocardiography analyses with anatomopathologic findings [83, 84]. Somewhat unexpectedly, it was first shown that left ventricle segmental motion abnormalities are more related to the underlying inflammation process than to myocardium fibrosis [85]. This is an emerging area of research with a great potential for "bench to bed" approach. Future correlation between anatomopathologic studies and clinical studies can advance knowledge of the disease pathophysiology and of therapeutic unfolding. Translational science thinking can guide clinical research to design studies testing a more detailed segmental systolic quantification not only in the left but also in the right ventricle to detect early myocardium involvement. Regional *speckle tracking* quantification can be a useful tool, despite its reproducibility still being a controversy theme.

5.3.2. Cardiac Magnetic Resonance. Based on the concepts described along this review of CC being an immune-inflammatory disease affecting both the left and the right ventricles, CMR has the potential to detect not only fibrosis but also myocardium edema and inflammation, in order to further extend seeking for detection of early myocardial damage. CMR techniques as T2 sequences are recently emerging in diverse scenarios of myocardial diseases, including infarction and acute myocarditis [86], and the utility of the method in CD is an open field for new exploits [80]. The potential role of the method in allowing a more accurate assessment of the right ventricular function has already been documented in various clinical settings [87].

6. Conclusion

Right ventricle role in cardiovascular physiology and pathology has been historically neglected. Cardiology science is still "on the way" to understand the right ventricle role into cardiovascular physiology and to detect structural and function abnormalities in this geometrically complex chamber.

Different from other dilated cardiomyopathies, CD has a unique characteristic of frequently early and progressive

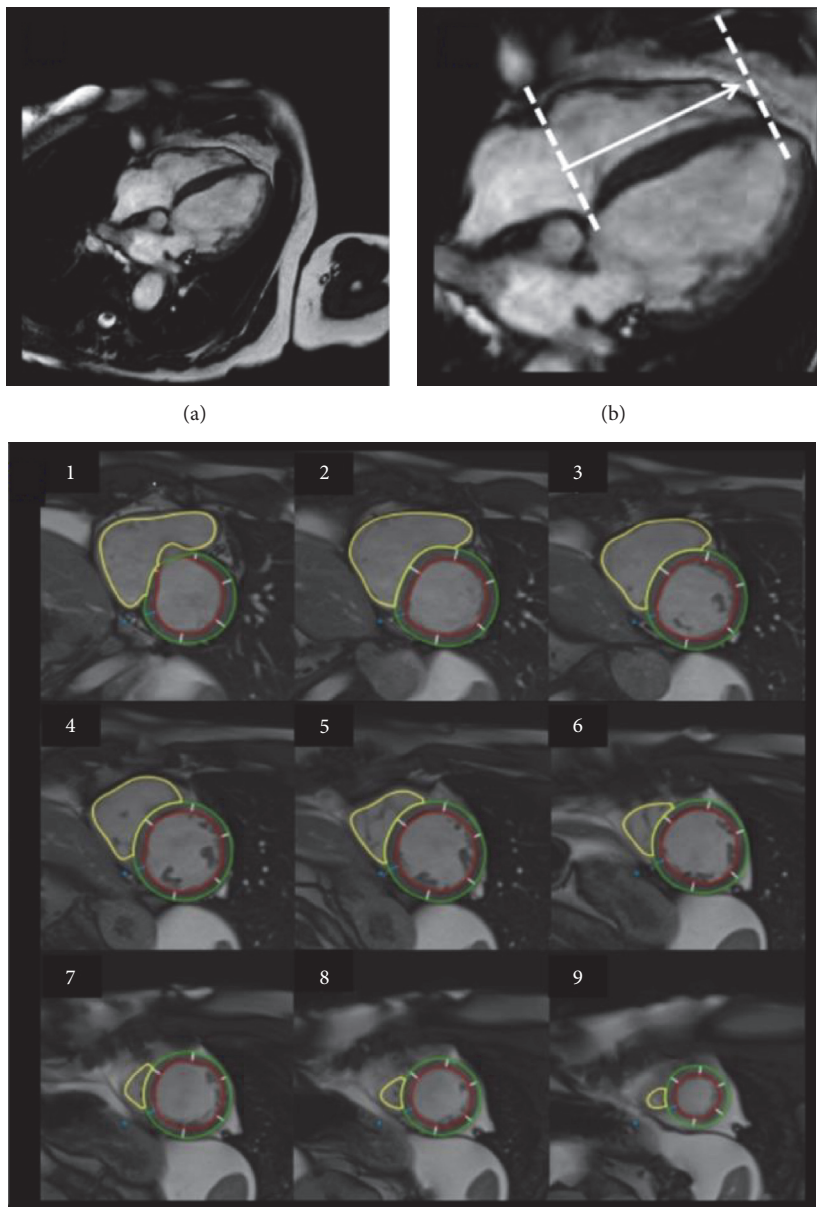

Figure 6: Volumetric assessment of the RV using CMR. Image acquired from cine-resonance using pulse sequences SSFP *(Steady-State Free Precession)*, showing the tomographic slicing of RV long-axis and limiting adjustments to transversal views from base to apex ((a) and (b)). Yellow lines shows delineation of endocardial borders of RV (c) to further calculation of volumes. Adapted from Moreira, HT (2015). "Análise ecocardiográfica do ventrículo direito na doença de Chagas: estudo comparativo com a ressonância magnética cardíaca" (Doctoral Dissertation), University of São Paulo, Ribeirão Preto, Brazil, Circ Cardiovasc Imaging, 2017, 10:e005571. Adapted with permission from Wolters Kluwer, license number 4143770060198.

damage involving cell death, inflammation, and fibrosis not only in the left but also in the right ventricle myocardium. Evolution of cardiac imaging modalities added current analyses of myocardial deformation by speckle tracking echocardiography and both chamber volumetric evaluation and tissue characterization using cardiac magnetic resonance. These novel technologies offer new perspective to study right ventricular involvement and to understand the associated aspects of CD progression in terms of malignant arrhythmias and heart failure. Sudden death, the most frequent mode of death in patients with CC, occurring even when there is preserved global LV systolic function, should be especially amenable to investigations using CMR.

Additional Points

Methods for Search Strategy and Selections. Data for this review were identified by searching Medline, PubMed, and

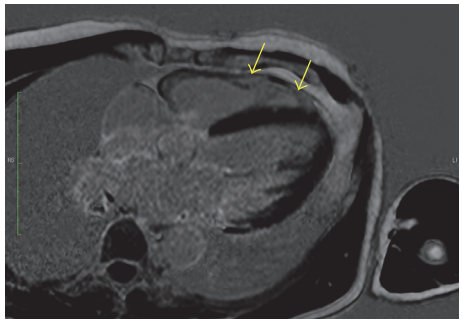

Figure 7: Four-chamber slice using CMR with LGE (late gadolinium enhancement) sequence in a patient with Chagas cardiomyopathy. Distinct extensive areas of fibrosis (white signal) (yellow arrows) are seen in the right ventricle free wall. Right ventricle dimensions are still within normal limits. Discrete isolated areas of fibrosis are also noted in the left ventricle.

Lilacs Databases and publications in English, Spanish, or Portuguese language were accepted. No other kind of selection of manuscripts to be cited was applied, considering most of available published data.

Conflicts of Interest

The authors declare that there are no conflicts of interest regarding the publication of this paper.

References

[1] K. T. Weber, J. S. Janicki, S. Shroff, and A. P. Fishman, "Contractile mechanics and interaction of the right and left ventricles," *The American Journal of Cardiology*, vol. 47, no. 3, pp. 686–695, 1981.

[2] J. S. Janicki and K. T. Weber, "Factors influencing the diastolic pressure-volume relation of the cardiac ventricles," *Federation Proceedings*, vol. 39, no. 2, pp. 133–140, 1980.

[3] I. Starr, W. A. Jeffers, and R. H. Meade Jr., "The absence of conspicuous increments of venous pressure after severe damage to the right ventricle of the dog, with a discussion of the relation between clinical congestive failure and heart disease," *American Heart Journal*, vol. 26, no. 3, pp. 291–301, 1943.

[4] H. Brooks, R. Holland, and J. Al-Sadir, "Right ventricular performance during ischemia: an anatomic and hemodynamic analysis," *The American journal of physiology*, vol. 233, no. 4, pp. H505–H513, 1977.

[5] L. J. Dell'Italia, "Anatomy and Physiology of the Right Ventricle," *Cardiology Clinics*, vol. 30, no. 2, pp. 167–187, 2012.

[6] C. Basso, D. Corrado, F. I. Marcus, A. Nava, and G. Thiene, "Arrhythmogenic right ventricular cardiomyopathy," *The Lancet*, vol. 373, no. 9671, pp. 1289–1300, 2009.

[7] A. Rassi Jr., A. Rassi, and J. A. Marin-Neto, "Chagas disease," *The Lancet*, vol. 375, no. 9723, pp. 1388–1402, 2010.

[8] A. Z. Prata A. and A. Guimarães, "Chagas Heart Disease," in *Proceedings of the Cardiovascular diseases in the tropics*, H. M. e. a. Shaper A., Ed., pp. 264–281, London, UK, 1974.

[9] J. A. Marin-Neto, P. Marzullo, A. C. Sousa et al., "Radionuclide angiographic evidence for early predominant right ventricular involvement in patients with Chagas' disease," *Canadian Journal of Cardiology*, vol. 4, no. 5, pp. 231–236, 1988.

[10] Moreira H. T., G. J. Volpe, H. S. Trad et al., "Right ventricular dysfunction in Chagas'cardiomyopathy. Primary involvement or a resonant manifestation of left ventricular dysfunction?" *Journal of Cardiovascular Magnetic Resonance*, vol. 16, Supplement 1, p. 1, 2014.

[11] C. M. Prado, M. R. N. Celes, L. M. Malvestio et al., "Early dystrophin disruption in the pathogenesis of experimental chronic Chagas cardiomyopathy," *Microbes and Infection*, vol. 14, no. 1, pp. 59–68, 2012.

[12] M. A. Rossi, "The pattern of myocardial fibrosis in chronic Chagas' heart disease," *International Journal of Cardiology*, vol. 30, no. 3, pp. 335–340, 1991.

[13] H. T. Moreira, G. J. Volpe, J. A. Marin-Neto et al., "Right ventricular systolic dysfunction in chagas disease defined by speckle-tracking echocardiography: a comparative study with cardiac magnetic resonance imaging," *Journal of the American Society of Echocardiography*, vol. 30, no. 5, pp. 493–502, 2017.

[14] WHO Expert Committee on the Control of Chagas Disease, "Control of Chagas' disease: second report of the WHO expert committee [meeting held in Buenos Aires from 16 to 20 October 1989]," WHO Tecnical Report Series 905, WHO Library Cataloguing-In-Publication Data, Brasilia, Brasi, 1991.

[15] C. Global Burden of Disease Study, "Global, regional, and national incidence, prevalence, and years lived with disability for 301 acute and chronic diseases and injuries in 188 countries, 1990-2013: a systematic analysis for the Global Burden of Disease Study 2013," *The Lancet*, vol. 386, no. 9995, pp. 743–800, 2015.

[16] C. Bern, S. Kjos, M. J. Yabsley, and S. P. Montgomery, "*Trypanosoma cruzi* and Chagas' disease in the united states," *Clinical Microbiology Reviews*, vol. 24, no. 4, pp. 655–681, 2011.

[17] M. I. Traina, S. Hernandez, D. R. Sanchez et al., "Prevalence of Chagas Disease in a U.S. Population of Latin American Immigrants with Conduction Abnormalities on Electrocardiogram," *PLOS Neglected Tropical Diseases*, vol. 11, no. 1, article e0005244, 2017.

[18] K. M. Bonney and D. M. Engman, "Chagas heart disease pathogenesis: One mechanism or many?" *Current Molecular Medicine*, vol. 8, no. 6, pp. 510–518, 2008.

[19] Z. A. Andrade, S. G. Andrade, G. B. Oliveria, and D. R. Alonso, "Histopathology of the conducting tissue of the heart in Chagas' myocarditis," *American Heart Journal*, vol. 95, no. 3, pp. 316–324, 1978.

[20] D. S. Amorin, J. A. Mello de Oliveira, J. S. Meira de Oliveira et al., "Heart block in Chagas' disease," *Arquivos Brasileiros de Cardiologia*, vol. 28, no. 1, pp. 79–82, 1976.

[21] J. A. Marin-Neto, G. Bromberg-Marin, A. Pazin-Filho, M. V. Simões, and B. C. Maciel, "Cardiac autonomic impairment and early myocardial damage involving the right ventricle are independent phenomena in Chagas' disease," *International Journal of Cardiology*, vol. 65, no. 3, pp. 261–269, 1998.

[22] F. Köberle, "Chagas' Disease and Chagas' Syndromes: The Pathology of American Trypanosomiasis," *Advances in Parasitology*, vol. 6, no. C, pp. 63–116, 1968.

[23] J. A. Marin-Neto, E. Cunha-Neto, B. C. Maciel, and M. V. Simões, "Pathogenesis of chronic Chagas heart disease," *Circulation*, vol. 115, no. 9, pp. 1109–1123, 2007.

[24] M. A. Rossi, H. B. Tanowitz, L. M. Malvestio et al., "Coronary microvascular disease in chronic chagas cardiomyopathy including an overview on history, pathology, and other

proposed pathogenic mechanisms," *PLoS Neglected Tropical Diseases*, vol. 4, no. 8, article e674, 2010.

[25] M. V. Simões, A. O. Pintya, G. Bromberg-Marin et al., "Relation of regional sympathetic denervation and myocardial perfusion disturbance to wall motion impairment in Chagas' cardiomyopathy," *American Journal of Cardiology*, vol. 86, no. 9, pp. 975–981, 2000.

[26] S. A. Morris, H. B. Tanowitz, M. Wittner, and J. P. Bilezikian, "Pathophysiological insights into the cardiomyopathy of Chagas' disease," *Circulation*, vol. 82, no. 6, pp. 1900–1909, 1990.

[27] D. V. Andrade, K. J. Gollob, and W. O. Dutra, "Acute Chagas Disease: New Global Challenges for an Old Neglected Disease," *PLoS Neglected Tropical Diseases*, vol. 8, no. 7, article e3010, 2014.

[28] A. A. Nóbrega, M. H. Garcia, E. Tatto et al., "Oral transmission of chagas disease by consumption of Açaí palm fruit, Brazil," *Emerging Infectious Diseases*, vol. 15, no. 4, pp. 653–655, 2009.

[29] M. Z. Tavora, N. Mehta, R. M. Silva, F. A. Gondim, V. M. Hara, and A. A. de Paola, "Characteristics and identification of sites of chagasic ventricular tachycardia by endocardial mapping," *Arquivos Brasileiros de Cardiologia*, vol. 72, no. 4, pp. 451–474, 1999.

[30] S. G. Andrade and M. Sadigursky, "The conduction system of the heart in mice chronically infected with Trypanosoma cruzi: histopathological lesions and electrocardiographic correlations," *Memorias do Instituto Oswaldo Cruz*, vol. 82, no. 1, pp. 59–66, 1987.

[31] F. Koberle, "The chronic Chagas cardiopathy," *Virchows Archiv Fur Pathologische Anatomie Und Physiologie Und Fur Klinische Medizin*, vol. 330, no. 3, pp. 267–295, 1957.

[32] A. Rassi Jr., A. Rassi, and J. Marcondes de Rezende, "American trypanosomiasis (Chagas disease)," *Infectious Disease Clinics of North America*, vol. 26, no. 2, pp. 275–291, 2012.

[33] J. P. Andrade, J. A. Marin-Neto, A. A. Paola et al., "I Latin American guidelines for the diagnosis and treatment of Chagas cardiomyopathy," *Arquivos Brasileiros de Cardiologia*, vol. 97, no. 2, supplement 3, pp. 1–48, 2011.

[34] J. A. Marin-Neto and Z. A. Andrade, "Why is there predominance of right heart failure in Chagas' disease?" *Arquivos Brasileiros de Cardiologia*, vol. 57, no. 3, pp. 181–183, 1991.

[35] A. C. Barreto, L. Higuchi Mde, P. L. Da Luz et al., "Comparison of histologic changes in Chagas'cardiomyopathy and dilated cardiomyopathy," *Arquivos Brasileiros de Cardiologia*, vol. 52, no. 2, 1989.

[36] C. Mady, A. C. Barretto, N. Stolf et al., "Endomyocardial biopsy in the indeterminate form of Chagas' disease," *Arquivos Brasileiros de Cardiologia*, vol. 36, no. 6, pp. 387–390, 1981.

[37] J. M. Hagar and S. H. Rahimtoola, "Chagas' heart disease," *Current Problems in Cardiology*, vol. 20, no. 12, pp. 825–924, 1995.

[38] Higuchi M. d. L., E. A. Lopes, A. C. Barretto et al., "Endomyocardial biopsy of the right ventricle. Significance of the ultrastructural changes in Chagas' cardiopathy," *Arquivos Brasileiros de Cardiologia*, vol. 44, no. 3, pp. 171–175, 1985.

[39] A. C. P. Barretto, C. Mady, E. Arteage-Fernandez et al., "Right ventricular endomyocardial biopsy in chronic Chagas' disease," *American Heart Journal*, vol. 111, no. 2, pp. 307–312, 1986.

[40] F.-X. Lescure, G. Le Loup, H. Freilij et al., "Chagas disease: Changes in knowledge and management," *The Lancet Infectious Diseases*, vol. 10, no. 8, pp. 556–570, 2010.

[41] H. F. G. Freitas, P. R. Chizzola, Â. T. Paes, A. C. P. Lima, and A. J. Mansur, "Risk stratification in a Brazilian hospital-based cohort of 1220 outpatients with heart failure: Role of Chagas' heart disease," *International Journal of Cardiology*, vol. 102, no. 2, pp. 239–247, 2005.

[42] M. D. C. P. Nunes, M. O. C. Rocha, A. L. P. Ribeiro et al., "Right ventricular dysfunction is an independent predictor of survival in patients with dilated chronic Chagas' cardiomyopathy," *International Journal of Cardiology*, vol. 127, no. 3, pp. 372–379, 2008.

[43] M. V. Simoes, A. Nonino, B. P. Simoes, O. C. Almeida-Filho, B. C. Maciel, and J. A. Marin-Neto, "Reagudization of Chagas myocarditis inducing exclusive right ventricular failure," *Arquivos Brasileiros de Cardiologia*, vol. 62, no. 6, pp. 435–437, 1994.

[44] M. V. Simões, F. A. Soares, and J. Marin-Neto, "Severe myocarditis and esophagitis during reversible long standing Chagas' disease recrudescence in immunocompromised host," *International Journal of Cardiology*, vol. 49, no. 3, pp. 271–273, 1995.

[45] F. F. Souza, O. Castro-e-Silva, J. A. Marin Neto et al., "Acute Chagasic Myocardiopathy After Orthotopic Liver Transplantation With Donor and Recipient Serologically Negative for Trypanosoma cruzi: A Case Report," *Transplantation Proceedings*, vol. 40, no. 3, pp. 875–878, 2008.

[46] H. A. Carrasco, M. Medina, G. Inglessis, A. Fuenmayor, C. Molina, and D. Davila, "Right ventricular function in Chagas disease," *International Journal of Cardiology*, vol. 2, no. 3-4, pp. 325–335, 1983.

[47] C. Mady, A. V. de Moraes, N. Galiano, and L. V. Decourt, "Hemodynamic study of the indeterminate form of Chagas' disease," *Arquivos Brasileiros de Cardiologia*, vol. 38, no. 4, pp. 271–275, 1982.

[48] M. D. C. P. Nunes, M. D. M. Barbosa, V. A. A. Brum, and M. O. D. C. Rocha, "Morphofunctional characteristics of the right ventricle in Chagas' dilated cardiomyopathy," *International Journal of Cardiology*, vol. 94, no. 1, pp. 79–85, 2004.

[49] R. G. Furtado, D. Do Carmo Rassi Frota, J. B. M. Silva et al., "Right ventricular doppler echocardiographic study of indeterminate form of chagas disease," *Arquivos Brasileiros de Cardiologia*, vol. 104, no. 3, pp. 209–217, 2015.

[50] M. M. Barbosa, M. O. C. Rocha, D. F. Vidigal et al., "Early detection of left ventricular contractility abnormalities by two-dimensional speckle tracking strain in Chagas' disease," *Echocardiography*, vol. 31, no. 5, pp. 623–630, 2014.

[51] H. T. Moreira, G. J. Volpe, J. A. Marin-Neto et al., "Evaluation of Right Ventricular Systolic Function in Chagas Disease Using Cardiac Magnetic Resonance Imaging," *Circulation: Cardiovascular Imaging*, vol. 10, no. 3, 2017.

[52] A. Rassi Jr., A. Rassi, W. C. Little et al., "Development and validation of a risk score for predicting death in Chagas' heart disease," *New England Journal of Medicine*, vol. 355, no. 8, pp. 799–808, 2006.

[53] A. Rassi Jr. and A. Rassi, "Predicting prognosis in patients with Chagas disease: why are the results of various studies so different?" *International Journal of Cardiology*, vol. 145, no. 1, pp. 64-65, 2010.

[54] M. Pavlicek, A. Wahl, T. Rutz et al., "Right ventricular systolic function assessment: Rank of echocardiographic methods vs. cardiac magnetic resonance imaging," *European Journal of Echocardiography*, vol. 12, no. 11, pp. 871–880, 2011.

[55] A. Pazin-Filho, M. M. D. Romano, R. Gomes Furtado et al., "Left Ventricular Global Performance and Diastolic Function in Indeterminate and Cardiac Forms of Chagas' Disease," *Journal of the American Society of Echocardiography*, vol. 20, no. 12, pp. 1338–1343, 2007.

[56] R. Cardoso, D. Garcia, G. Fernandes et al., "The Prevalence of Atrial Fibrillation and Conduction Abnormalities in Chagas' Disease: A Meta-Analysis," *Journal of Cardiovascular Electrophysiology*, vol. 27, no. 2, pp. 161–169, 2016.

[57] S. Williams-Blangero, T. Magalhaes, E. Rainwater, J. Blangero, R. Correa-Oliveira, and J. L. VandeBerg, "Electrocardiographic characteristics in a population with high rates of seropositivity for Trypanosoma cruzi infection," *American Journal of Tropical Medicine and Hygiene*, vol. 77, no. 3, pp. 495–499, 2007.

[58] J. Pimenta, N. Valente, and M. Miranda, "Long-term follow up of asymptomatic chagasic individuals with intraventricular conduction disturbances, correlating with non-chagasic patients," *Revista da Sociedade Brasileira de Medicina Tropical*, vol. 32, no. 6, pp. 621–631, 1999.

[59] J. H. Maguire, R. Hoff, I. Sherlock et al., "Cardiac morbidity and mortality due to Chagas' disease: Prospective electrocardiographic study of a Brazilian community," *Circulation*, vol. 75, no. 6, pp. 1140–1145, 1987.

[60] K. Vernooy, X. A. A. M. Verbeek, M. Peschar, and F. W. Prinzen, "Relation between Abnormal Ventricular Impulse Conduction and Heart Failure," *Journal of Interventional Cardiology*, vol. 16, no. 6, pp. 557–562, 2003.

[61] R. Marterer, Z. Hongchun, S. Tschauner, M. Koestenberger, and E. Sorantin, "Cardiac MRI assessment of right ventricular function: impact of right bundle branch block on the evaluation of cardiac performance parameters," *European Radiology*, vol. 25, no. 12, pp. 3528–3535, 2015.

[62] F. Sheehan and A. Redington, "The right ventricle: Anatomy, physiology and clinical imaging," *Heart*, vol. 94, no. 11, pp. 1510–1515, 2008.

[63] F. Haddad, S. A. Hunt, D. N. Rosenthal, and D. J. Murphy, "Right ventricular function in cardiovascular disease, part I: anatomy, physiology, aging, and functional assessment of the right ventricle," *Circulation*, vol. 117, no. 11, pp. 1436–1448, 2008.

[64] R. M. Lang, L. P. Badano, W. Tsang et al., "EAE/ASE recommendations for image acquisition and display using three-dimensional echocardiography," *European Heart Journal Cardiovascular Imaging*, vol. 13, no. 1, pp. 1–46, 2012.

[65] L. G. Rudski, W. W. Lai, J. Afilalo et al., "Guidelines for the echocardiographic assessment of the right heart in adults: a report from the American Society of Echocardiography endorsed by the European Association of Echocardiography, a registered branch of the European Society of Cardiology, and the Canadian Society of Echocardiography," *Journal of the American Society of Echocardiography*, vol. 23, no. 7, pp. 685–713, 786–788, 2010.

[66] R. M. Lang, L. P. Badano, V. Mor-Avi et al., "Recommendations for cardiac chamber quantification by echocardiography in adults: an update from the American Society of Echocardiography and the European Association of Cardiovascular Imaging," *European Heart Journal—Cardiovascular Imaging*, vol. 16, no. 3, pp. 233–271, 2015.

[67] C. Tei, L. H. Ling, D. O. Hodge et al., "New index of combined systolic and diastolic myocardial performance: a simple and reproducible measure of cardiac function—a study in normals and dilated cardiomyopathy," *Journal of Cardiology*, vol. 26, no. 6, pp. 357–366, 1995.

[68] H. Acquatella, "Echocardiography in Chagas heart disease," *Circulation*, vol. 115, no. 9, pp. 1124–1131, 2007.

[69] C. A. S. Nascimento, V. A. M. Gomes, S. K. Silva et al., "Left atrial and left ventricular diastolic function in chronic chagas disease," *Journal of the American Society of Echocardiography*, vol. 26, no. 12, pp. 1424–1433, 2013.

[70] M. V. L. Barros, F. S. Machado, A. L. P. Ribeiro, and M. O. Da Costa Rocha, "Detection of early right ventricular dysfunction in Chagas' disease using Doppler tissue imaging," *Journal of the American Society of Echocardiography*, vol. 15, no. 10, part 2, pp. 1197–1201, 2002.

[71] J.-U. Voigt, G. Pedrizzetti, P. Lysyansky et al., "Definitions for a common standard for 2D speckle tracking echocardiography: Consensus document of the EACVI/ASE/industry task force to standardize deformation imaging," *Journal of the American Society of Echocardiography*, vol. 28, no. 2, pp. 183–193, 2015.

[72] H. Blessberger and T. Binder, "Two dimensional speckle tracking echocardiography: Clinical applications," *Heart*, vol. 96, no. 24, pp. 2032–2040, 2010.

[73] H. Blessberger and T. Binder, "Two dimensional speckle tracking echocardiography: Basic principles," *Heart*, vol. 96, no. 9, pp. 716–722, 2010.

[74] D. Muraru, S. Onciul, D. Peluso et al., "Sex- and method-specific reference values for right ventricular strain by 2-dimensional speckle-tracking echocardiography," *Circulation: Cardiovascular Imaging*, vol. 9, no. 2, article e003866, 2016.

[75] V. A. M. Gomes, G. F. Alves, M. Hadlich et al., "Analysis of Regional Left Ventricular Strain in Patients with Chagas Disease and Normal Left Ventricular Systolic Function," *Journal of the American Society of Echocardiography*, vol. 29, no. 7, pp. 679–688, 2016.

[76] A. García-Álvarez, M. Sitges, A. Regueiro et al., "Myocardial deformation analysis in chagas heart disease with the use of speckle tracking echocardiography," *Journal of Cardiac Failure*, vol. 17, no. 12, pp. 1028–1034, 2011.

[77] M. S. M. Lima, H. R. Villarraga, M. C. D. Abduch et al., "Comprehensive left ventricular mechanics analysis by speckle tracking echocardiography in Chagas disease," *Cardiovascular Ultrasound*, vol. 14, no. 1, p. 20, 2016.

[78] W. G. Hundley, D. A. Bluemke, J. P. Finn et al., "ACCF/ACR/AHA/NASCI/SCMR 2010 expert consensus document on cardiovascular magnetic resonance: a report of the American College of Cardiology Foundation Task Force on Expert Consensus Documents," *Journal of the American College of Cardiology*, vol. 55, no. 23, pp. 2614–2662, 2010.

[79] C. E. Rochitte, P. F. Oliveira, J. M. Andrade et al., "Myocardial delayed enhancement by magnetic resonance imaging in patients with Chagas' disease: A marker of disease severity," *Journal of the American College of Cardiology*, vol. 46, no. 8, pp. 1553–1558, 2005.

[80] J. A. Torreão, B. M. Ianni, C. Mady et al., "Myocardial tissue characterization in Chagas' heart disease by cardiovascular magnetic resonance," *Journal of Cardiovascular Magnetic Resonance*, vol. 17, no. 1, p. 97, 2015.

[81] R. Kalil, E. A. Bocchi, B. M. Ferreira et al., "Magnetic resonance imaging in chronic Chagas cardiopathy. Correlation with endomyocardial biopsy findings," *Arquivos brasileiros de cardiologia*, vol. 65, no. 5, pp. 413–416, 1995.

[82] R. P. de Mello, G. Szarf, P. R. Schvartzman et al., "Delayed enhancement cardiac magnetic resonance imaging can identify the risk for ventricular tachycardia in chronic Chagas' heart disease," *Arquivos Brasileiros de Cardiologia*, vol. 98, no. 5, pp. 421–430, 2012.

[83] A. M. B. Bilate, V. M. C. Salemi, F. J. A. Ramires et al., "The Syrian hamster as a model for the dilated cardiomyopathy

of Chagas' disease: a quantitative echocardiographical and histopathological analysis," *Microbes and Infection*, vol. 5, no. 12, pp. 1116–1124, 2003.

[84] L. E. Ramirez, E. Lages-Silva, J. M. Soares Jr., and E. Chapadeiro, "The hamster (Mesocricetus auratus) as experimental model in Chagas' disease: parasitological and histopathological studies in acute and chronic phases of Trypanosoma cruzi infection," *Revista da Sociedade Brasileira de Medicina Tropical*, vol. 27, no. 3, pp. 163–169, 1994.

[85] L. F. L. De Oliveira, M. M. D. Romano, E. E. V. De Carvalho et al., "Histopathological correlates of global and segmental left ventricular systolic dysfunction in experimental chronic chagas cardiomyopathy," *Journal of the American Heart Association*, vol. 5, no. 1, article e002786, 2016.

[86] Y. Amano, M. Tachi, H. Tani, K. Mizuno, Y. Kobayashi, and S. Kumita, "T2-weighted cardiac magnetic resonance imaging of edema in myocardial diseases," *The Scientific World Journal*, vol. 2012, Article ID 194069, 7 pages, 2012.

[87] A. Schmidt, B. C. Maciel, and J. A. Marin-Neto, "Clinical Trial Report: Time is Resonant for Right Ventricular Evaluation," *Current Cardiovascular Imaging Reports*, vol. 4, no. 3, pp. 177–179, 2011.